Earth Syst. Sci. Data, 7, 349–396, 2015
www.earth-syst-sci-data.net/7/349/2015/
doi:10.5194/essd-7-349-2015

Open Access Earth System Science Data

Global Carbon Budget 2015

C. Le Quéré[1], R. Moriarty[1], R. M. Andrew[2], J. G. Canadell[3], S. Sitch[4], J. I. Korsbakken[2], P. Friedlingstein[5], G. P. Peters[2], R. J. Andres[6], T. A. Boden[6], R. A. Houghton[7], J. I. House[8], R. F. Keeling[9], P. Tans[10], A. Arneth[11], D. C. E. Bakker[12], L. Barbero[13,14], L. Bopp[15], J. Chang[15], F. Chevallier[15], L. P. Chini[16], P. Ciais[15], M. Fader[17], R. A. Feely[18], T. Gkritzalis[19], I. Harris[20], J. Hauck[21], T. Ilyina[22], A. K. Jain[23], E. Kato[24], V. Kitidis[25], K. Klein Goldewijk[26], C. Koven[27], P. Landschützer[28], S. K. Lauvset[29], N. Lefèvre[30], A. Lenton[31], I. D. Lima[32], N. Metzl[30], F. Millero[33], D. R. Munro[34], A. Murata[35], J. E. M. S. Nabel[22], S. Nakaoka[36], Y. Nojiri[36], K. O'Brien[37], A. Olsen[38,39], T. Ono[40], F. F. Pérez[41], B. Pfeil[38,39], D. Pierrot[13,14], B. Poulter[42], G. Rehder[43], C. Rödenbeck[44], S. Saito[45], U. Schuster[4], J. Schwinger[29], R. Séférian[46], T. Steinhoff[47], B. D. Stocker[48,49], A. J. Sutton[37,18], T. Takahashi[50], B. Tilbrook[51], I. T. van der Laan-Luijkx[52,53], G. R. van der Werf[54], S. van Heuven[55], D. Vandemark[56], N. Viovy[15], A. Wiltshire[57], S. Zaehle[44], and N. Zeng[58]

[1]Tyndall Centre for Climate Change Research, University of East Anglia, Norwich Research Park, Norwich NR4 7TJ, UK
[2]Center for International Climate and Environmental Research – Oslo (CICERO), Oslo, Norway
[3]Global Carbon Project, CSIRO Oceans and Atmosphere, GPO Box 3023, Canberra, ACT 2601, Australia
[4]College of Life and Environmental Sciences, University of Exeter, Exeter EX4 4QE, UK
[5]College of Engineering, Mathematics and Physical Sciences, University of Exeter, Exeter EX4 4QF, UK
[6]Carbon Dioxide Information Analysis Center (CDIAC), Oak Ridge National Laboratory, Oak Ridge, TN, USA
[7]Woods Hole Research Center (WHRC), Falmouth, MA 02540, USA
[8]Cabot Institute, Department of Geography, University of Bristol, Bristol BS8 1TH, UK
[9]University of California, San Diego, Scripps Institution of Oceanography, La Jolla, CA 92093-0244, USA
[10]National Oceanic & Atmospheric Administration, Earth System Research Laboratory (NOAA/ESRL), Boulder, CO 80305, USA
[11]Institute of Meteorology and Climate Research – Atmospheric Environmental Research (IMK-IFU), Karlsruhe Institute of Technology (KIT), 82467 Garmisch-Partenkirchen, Germany
[12]Centre for Ocean and Atmospheric Sciences, School of Environmental Sciences, University of East Anglia, Norwich NR4 7TJ, UK
[13]Cooperative Institute for Marine and Atmospheric Studies, Rosenstiel School for Marine and Atmospheric Science, University of Miami, Miami, FL 33149, USA
[14]National Oceanic & Atmospheric Administration/Atlantic Oceanographic & Meteorological Laboratory (NOAA/AOML), Miami, FL 33149, USA
[15]Laboratoire des Sciences du Climat et de l'Environnement, Institut Pierre-Simon Laplace, CEA-CNRS-UVSQ, CE Orme des Merisiers, 91191 Gif sur Yvette CEDEX, France
[16]Department of Geographical Sciences, University of Maryland, College Park, MD 20742, USA
[17]Institut Méditerranéen de Biodiversité et d'Ecologie marine et continentale, Aix-Marseille Université, CNRS, IRD, Avignon Université, Technopôle Arbois-Méditerranée, Bâtiment Villemin, BP 80, 13545 Aix-en-Provence CEDEX 04, France
[18]National Oceanic & Atmospheric Administration/Pacific Marine Environmental Laboratory (NOAA/PMEL), 7600 Sand Point Way NE, Seattle, WA 98115, USA
[19]Flanders Marine Institute, InnovOcean site, Wandelaarkaai 7, 8400 Ostend, Belgium
[20]Climatic Research Unit, University of East Anglia, Norwich Research Park, Norwich NR4 7TJ, UK
[21]Alfred-Wegener-Institut, Helmholtz Zentrum für Polar- und Meeresforschung, Am Handelshafen 12, 27570 Bremerhaven, Germany

Published by Copernicus Publications.

[22]Max Planck Institute for Meteorology, Bundesstr. 53, 20146 Hamburg, Germany
[23]Department of Atmospheric Sciences, University of Illinois, Urbana, IL 61821, USA
[24]Institute of Applied Energy (IAE), Minato-ku, Tokyo 105-0003, Japan
[25]Plymouth Marine Laboratory, Prospect Place, Plymouth PL1 3DH, UK
[26]PBL Netherlands Environmental Assessment Agency, The Hague/Bilthoven and Utrecht University, Utrecht, the Netherlands
[27]Earth Sciences Division, Lawrence Berkeley National Lab, 1 Cyclotron Road, Berkeley, CA 94720, USA
[28]Environmental Physics Group, Institute of Biogeochemistry and Pollutant Dynamics, ETH Zurich, Universitätstrasse 16, 8092 Zurich, Switzerland
[29]Uni Research Climate, Bjerknes Centre for Climate Research, Allegt. 55, 5007 Bergen, Norway
[30]Sorbonne Universités (UPMC, Univ Paris 06)-CNRS-IRD-MNHN, LOCEAN/IPSL Laboratory, 4 place Jussieu, 75005 Paris, France
[31]CSIRO Oceans and Atmosphere, P.O. Box 1538 Hobart, Tasmania, Australia
[32]Woods Hole Oceanographic Institution (WHOI), Woods Hole, MA 02543, USA
[33]Department of Ocean Sciences, RSMAS/MAC, University of Miami, 4600 Rickenbacker Causeway, Miami, FL 33149, USA
[34]Department of Atmospheric and Oceanic Sciences and Institute of Arctic and Alpine Research, University of Colorado Campus Box 450 Boulder, CO 80309-0450, USA
[35]Japan Agency for Marine-Earth Science and Technology (JAMSTEC), 2-15 Natsushimacho, Yokosuka, Kanagawa Prefecture 237-0061, Japan
[36]Center for Global Environmental Research, National Institute for Environmental Studies (NIES), 16-2 Onogawa, Tsukuba, Ibaraki 305-8506, Japan
[37]Joint Institute for the Study of the Atmosphere and Ocean, University of Washington, Seattle, WA 98115, USA
[38]Geophysical Institute, University of Bergen, Allégaten 70, 5007 Bergen, Norway
[39]Bjerknes Centre for Climate Research, Allégaten 70, 5007 Bergen, Norway
[40]National Research Institute for Fisheries Science, Fisheries Research Agency 2-12-4 Fukuura, Kanazawa-Ku, Yokohama 236-8648, Japan
[41]Instituto de Investigaciones Marinas (CSIC), C/Eduardo Cabello, 6. Vigo. Pontevedra, 36208, Spain
[42]Department of Ecology, Montana State University, Bozeman, MT 59717, USA
[43]Leibniz Institute for Baltic Sea Research Warnemünde, Seestr 15, 18119 Rostock, Germany
[44]Max Planck Institut für Biogeochemie, P.O. Box 600164, Hans-Knöll-Str. 10, 07745 Jena, Germany
[45]Marine Division, Global Environment and Marine Department, Japan Meteorological Agency, 1-3-4 Otemachi, Chiyoda-ku, Tokyo 100-8122, Japan
[46]Centre National de Recherche Météorologique–Groupe d'Etude de l'Atmosphère Météorologique (CNRM-GAME), Météo-France/CNRS, 42 Avenue Gaspard Coriolis, 31100 Toulouse, France
[47]GEOMAR Helmholtz Centre for Ocean Research Kiel, Düsternbrooker Weg 20, 24105 Kiel, Germany
[48]Climate and Environmental Physics, and Oeschger Centre for Climate Change Research, University of Bern, Bern, Switzerland
[49]Imperial College London, Life Science Department, Silwood Park, Ascot, Berkshire SL5 7PY, UK
[50]Lamont-Doherty Earth Observatory of Columbia University, Palisades, NY 10964, USA
[51]CSIRO Oceans and Atmosphere and Antarctic Climate and Ecosystems Co-operative Research Centre, Hobart, Australia
[52]Department of Meteorology and Air Quality, Wageningen University, P.O. Box 47, 6700AA Wageningen, the Netherlands
[53]ICOS-Carbon Portal, c/o Wageningen University, P.O. Box 47, 6700AA Wageningen, the Netherlands
[54]Faculty of Earth and Life Sciences, VU University Amsterdam, Amsterdam, the Netherlands
[55]Royal Netherlands Institute for Sea Research, Landsdiep 4, 1797 SZ 't Horntje (Texel), the Netherlands
[56]University of New Hampshire, Ocean Process Analysis Laboratory, 161 Morse Hall, 8 College Road, Durham, NH 03824, USA
[57]Met Office Hadley Centre, FitzRoy Road, Exeter EX1 3PB, UK
[58]Department of Atmospheric and Oceanic Science, University of Maryland, College Park, MD 20742, USA

Correspondence to: C. Le Quéré (c.lequere@uea.ac.uk)

Received: 2 November 2015 – Published in Earth Syst. Sci. Data Discuss.: 2 November 2015
Revised: 25 November 2015 – Accepted: 26 November 2015 – Published: 7 December 2015

Abstract. Accurate assessment of anthropogenic carbon dioxide (CO_2) emissions and their redistribution among the atmosphere, ocean, and terrestrial biosphere is important to better understand the global carbon cycle, support the development of climate policies, and project future climate change. Here we describe data sets and a methodology to quantify all major components of the global carbon budget, including their uncertainties, based on the combination of a range of data, algorithms, statistics, and model estimates and their interpretation by a broad scientific community. We discuss changes compared to previous estimates as well as consistency within and among components, alongside methodology and data limitations. CO_2 emissions from fossil fuels and industry (E_{FF}) are based on energy statistics and cement production data, while emissions from land-use change (E_{LUC}), mainly deforestation, are based on combined evidence from land-cover-change data, fire activity associated with deforestation, and models. The global atmospheric CO_2 concentration is measured directly and its rate of growth (G_{ATM}) is computed from the annual changes in concentration. The mean ocean CO_2 sink (S_{OCEAN}) is based on observations from the 1990s, while the annual anomalies and trends are estimated with ocean models. The variability in S_{OCEAN} is evaluated with data products based on surveys of ocean CO_2 measurements. The global residual terrestrial CO_2 sink (S_{LAND}) is estimated by the difference of the other terms of the global carbon budget and compared to results of independent dynamic global vegetation models forced by observed climate, CO_2, and land-cover change (some including nitrogen–carbon interactions). We compare the mean land and ocean fluxes and their variability to estimates from three atmospheric inverse methods for three broad latitude bands. All uncertainties are reported as $\pm 1\sigma$, reflecting the current capacity to characterise the annual estimates of each component of the global carbon budget. For the last decade available (2005–2014), E_{FF} was 9.0 ± 0.5 GtC yr^{-1}, E_{LUC} was 0.9 ± 0.5 GtC yr^{-1}, G_{ATM} was 4.4 ± 0.1 GtC yr^{-1}, S_{OCEAN} was 2.6 ± 0.5 GtC yr^{-1}, and S_{LAND} was 3.0 ± 0.8 GtC yr^{-1}. For the year 2014 alone, E_{FF} grew to 9.8 ± 0.5 GtC yr^{-1}, 0.6 % above 2013, continuing the growth trend in these emissions, albeit at a slower rate compared to the average growth of 2.2 % yr^{-1} that took place during 2005–2014. Also, for 2014, E_{LUC} was 1.1 ± 0.5 GtC yr^{-1}, G_{ATM} was 3.9 ± 0.2 GtC yr^{-1}, S_{OCEAN} was 2.9 ± 0.5 GtC yr^{-1}, and S_{LAND} was 4.1 ± 0.9 GtC yr^{-1}. G_{ATM} was lower in 2014 compared to the past decade (2005–2014), reflecting a larger S_{LAND} for that year. The global atmospheric CO_2 concentration reached 397.15 ± 0.10 ppm averaged over 2014. For 2015, preliminary data indicate that the growth in E_{FF} will be near or slightly below zero, with a projection of -0.6 [range of -1.6 to $+0.5$] %, based on national emissions projections for China and the USA, and projections of gross domestic product corrected for recent changes in the carbon intensity of the global economy for the rest of the world. From this projection of E_{FF} and assumed constant E_{LUC} for 2015, cumulative emissions of CO_2 will reach about 555 ± 55 GtC (2035 ± 205 GtCO$_2$) for 1870–2015, about 75 % from E_{FF} and 25 % from E_{LUC}. This living data update documents changes in the methods and data sets used in this new carbon budget compared with previous publications of this data set (Le Quéré et al., 2015, 2014, 2013). All observations presented here can be downloaded from the Carbon Dioxide Information Analysis Center (doi:10.3334/CDIAC/GCP_2015).

1 Introduction

The concentration of carbon dioxide (CO_2) in the atmosphere has increased from approximately 277 parts per million (ppm) in 1750 (Joos and Spahni, 2008), the beginning of the industrial era, to 397.15 ppm in 2014 (Dlugokencky and Tans, 2015). Daily averages went above 400 ppm for the first time at Mauna Loa station in May 2013 (Scripps, 2013). This station holds the longest running record of direct measurements of atmospheric CO_2 concentration (Tans and Keeling, 2014). The global monthly average concentration was above 400 ppm in March through May 2015 for the first time (Dlugokencky and Tans, 2015; Fig. 1), while at Mauna Loa the seasonally corrected monthly average concentration reached 400 ppm in March 2015 and continued to rise. The atmospheric CO_2 increase above pre-industrial levels was, initially, primarily caused by the release of carbon to the atmosphere from deforestation and other land-use-change activities (Ciais et al., 2013). While emissions from fossil fuels started before the industrial era, they only became the dominant source of anthropogenic emissions to the atmosphere from around 1920, and their relative share has continued to increase until present. Anthropogenic emissions occur on top of an active natural carbon cycle that circulates carbon between the atmosphere, ocean, and terrestrial biosphere reservoirs on timescales from days to millennia, while exchanges with geologic reservoirs occur at longer timescales (Archer et al., 2009).

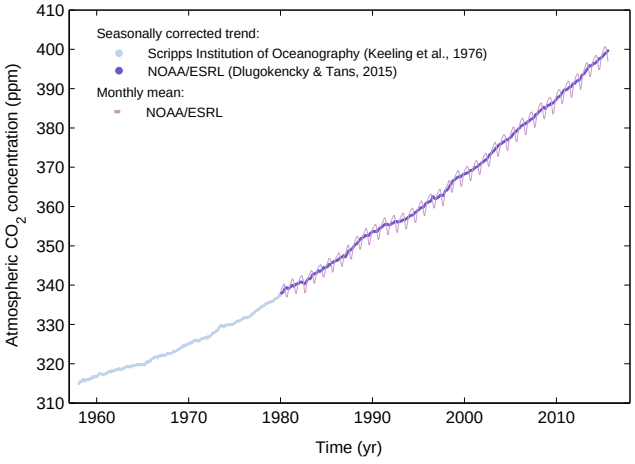

Figure 1. Surface average atmospheric CO_2 concentration, deseasonalised (ppm). The 1980–2015 monthly data are from NOAA/ESRL (Dlugokencky and Tans, 2015) and are based on an average of direct atmospheric CO_2 measurements from multiple stations in the marine boundary layer (Masarie and Tans, 1995). The 1958–1979 monthly data are from the Scripps Institution of Oceanography, based on an average of direct atmospheric CO_2 measurements from the Mauna Loa and South Pole stations (Keeling et al., 1976). To take into account the difference of mean CO_2 between the NOAA/ESRL and the Scripps station networks used here, the Scripps surface average (from two stations) was harmonised to match the NOAA/ESRL surface average (from multiple stations) by adding the mean difference of 0.542 ppm, calculated here from overlapping data during 1980–2012. The mean seasonal cycle is also shown from 1980.

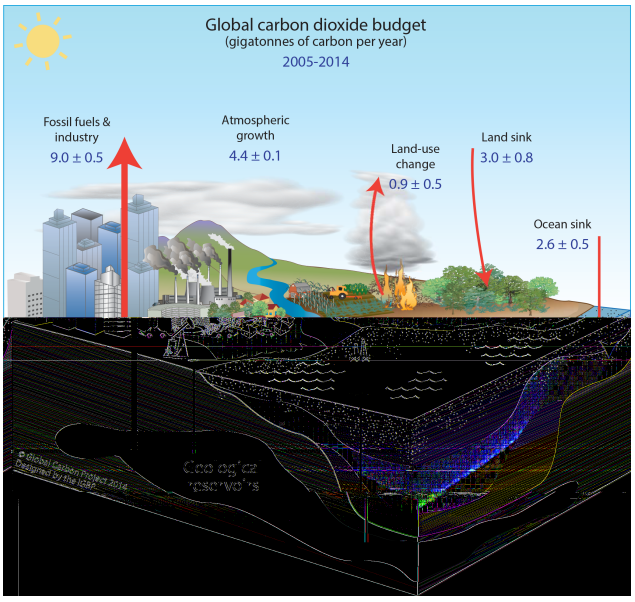

Figure 2. Schematic representation of the overall perturbation of the global carbon cycle caused by anthropogenic activities, averaged globally for the decade 2005–2014. The arrows represent emission from fossil fuels and industry (E_{FF}), emissions from deforestation and other land-use change (E_{LUC}), the growth of carbon in the atmosphere (G_{ATM}) and the uptake of carbon by the "sinks" in the ocean (S_{OCEAN}) and land (S_{LAND}) reservoirs. All fluxes are in units of GtC yr^{-1}, with uncertainties reported as $\pm 1\sigma$ (68 % confidence that the real value lies within the given interval) as described in the text. This figure is an update of one prepared by the International Geosphere-Biosphere Programme for the Global Carbon Project (GCP), first presented in Le Quéré (2009).

The global carbon budget presented here refers to the mean, variations, and trends in the perturbation of CO_2 in the atmosphere, referenced to the beginning of the industrial era. It quantifies the input of CO_2 to the atmosphere by emissions from human activities, the growth of CO_2 in the atmosphere, and the resulting changes in the storage of carbon in the land and ocean reservoirs in response to increasing atmospheric CO_2 levels, climate, and variability, and other anthropogenic and natural changes (Fig. 2). An understanding of this perturbation budget over time and the underlying variability and trends of the natural carbon cycle is necessary to understand the response of natural sinks to changes in climate, CO_2 and land-use-change drivers, and the permissible emissions for a given climate stabilisation target.

The components of the CO_2 budget that are reported annually in this paper include separate estimates for (1) the CO_2 emissions from fossil fuel combustion and oxidation and cement production (E_{FF}; GtC yr^{-1}), (2) the CO_2 emissions resulting from deliberate human activities on land leading to land-use change (E_{LUC}; GtC yr^{-1}), (3) the growth rate of CO_2 in the atmosphere (G_{ATM}; GtC yr^{-1}), and the uptake of CO_2 by the "CO_2 sinks" in (4) the ocean (S_{OCEAN}; GtC yr^{-1}) and (5) on land (S_{LAND}; GtC yr^{-1}). The CO_2 sinks as defined here include the response of the land and ocean to elevated CO_2 and changes in climate and other environmental conditions. The global emissions and their partitioning among the atmosphere, ocean, and land are in balance:

$$E_{FF} + E_{LUC} = G_{ATM} + S_{OCEAN} + S_{LAND}. \quad (1)$$

G_{ATM} is usually reported in ppm yr^{-1}, which we convert to units of carbon mass, GtC yr^{-1}, using 1 ppm = 2.12 GtC (Ballantyne et al., 2012; Prather et al., 2012; Table 1). We also include a quantification of E_{FF} by country, computed with both territorial- and consumption-based accounting (see Sect. 2.1.1).

Equation (1) partly omits two kinds of processes. The first is the net input of CO_2 to the atmosphere from the chemical oxidation of reactive carbon-containing gases from sources other than fossil fuels (e.g. fugitive anthropogenic CH_4 emissions, industrial processes, and changes in biogenic emissions from changes in vegetation, fires, wetlands), primarily methane (CH_4), carbon monoxide (CO), and volatile organic compounds such as isoprene and terpene. CO emissions are currently implicit in E_{FF} while anthropogenic CH_4 emissions are not and thus their inclusion would result in a small increase in E_{FF}. The second is the anthropogenic per-

Table 1. Factors used to convert carbon in various units (by convention, unit 1 = unit 2 · conversion).

Unit 1	Unit 2	Conversion	Source
GtC (gigatonnes of carbon)	ppm (parts per million)[a]	2.12[b]	Ballantyne et al. (2012)
GtC (gigatonnes of carbon)	PgC (petagrams of carbon)	1	SI unit conversion
$GtCO_2$ (gigatonnes of carbon dioxide)	GtC (gigatonnes of carbon)	3.664	44.01/12.011 in mass equivalent
GtC (gigatonnes of carbon)	MtC (megatonnes of carbon)	1000	SI unit conversion

[a] Measurements of atmospheric CO_2 concentration have units of dry-air mole fraction. "ppm" is an abbreviation for micromole per mole of dry air. [b] The use of a factor of 2.12 assumes that all the atmosphere is well mixed within one year. In reality, only the troposphere is well mixed and the growth rate of CO_2 in the less well-mixed stratosphere is not measured by sites from the NOAA network. Using a factor of 2.12 makes the approximation that the growth rate of CO_2 in the stratosphere equals that of the troposphere on a yearly basis and reflects the uncertainty in this value.

turbation to carbon cycling in terrestrial freshwaters, estuaries, and coastal areas, which modifies lateral fluxes from land ecosystems to the open ocean; the evasion CO_2 flux from rivers, lakes, and estuaries to the atmosphere; and the net air–sea anthropogenic CO_2 flux of coastal areas (Regnier et al., 2013). The inclusion of freshwater fluxes of anthropogenic CO_2 would affect the estimates of, and partitioning between, S_{LAND} and S_{OCEAN} in Eq. (1) in complementary ways, but would not affect the other terms. These flows are omitted in absence of annual information on the natural versus anthropogenic perturbation terms of these loops of the carbon cycle, and they are discussed in Sect. 2.7.

The CO_2 budget has been assessed by the Intergovernmental Panel on Climate Change (IPCC) in all assessment reports (Ciais et al., 2013; Denman et al., 2007; Prentice et al., 2001; Schimel et al., 1995; Watson et al., 1990), as well as by others (e.g. Ballantyne et al., 2012). These assessments included budget estimates for the decades of the 1980s, 1990s (Denman et al., 2007) and, most recently, the period 2002–2011 (Ciais et al., 2013). The IPCC methodology has been adapted and used by the Global Carbon Project (GCP, www.globalcarbonproject.org), which has coordinated a cooperative community effort for the annual publication of global carbon budgets up to the year 2005 (Raupach et al., 2007; including fossil emissions only), 2006 (Canadell et al., 2007), 2007 (published online; GCP, 2007), 2008 (Le Quéré et al., 2009), 2009 (Friedlingstein et al., 2010), 2010 (Peters et al., 2012b), 2012 (Le Quéré et al., 2013; Peters et al., 2013), 2013 (Le Quéré et al., 2014), and most recently 2014 (Friedlingstein et al., 2014; Le Quéré et al., 2015). The carbon budget year refers to the initial year of publication. Each of these papers updated previous estimates with the latest available information for the entire time series. From 2008, these publications projected fossil fuel emissions for one additional year using the projected world gross domestic product (GDP) and estimated trends in the carbon intensity of the global economy.

We adopt a range of ±1 standard deviation (σ) to report the uncertainties in our estimates, representing a likelihood of 68 % that the true value will be within the provided range if the errors have a Gaussian distribution. This choice reflects the difficulty of characterising the uncertainty in the CO_2 fluxes between the atmosphere and the ocean and land reservoirs individually, particularly on an annual basis, as well as the difficulty of updating the CO_2 emissions from land-use change. A likelihood of 68 % provides an indication of our current capability to quantify each term and its uncertainty given the available information. For comparison, the Fifth Assessment Report of the IPCC (AR5) generally reported a likelihood of 90 % for large data sets whose uncertainty is well characterised, or for long time intervals less affected by year-to-year variability. Our 68 % uncertainty value is near the 66 % which the IPCC characterises as "likely" for values falling into the $\pm 1\sigma$ interval. The uncertainties reported here combine statistical analysis of the underlying data and expert judgement of the likelihood of results lying outside this range. The limitations of current information are discussed in the paper and have been examined in detail elsewhere (Ballantyne et al., 2015).

All quantities are presented in units of gigatonnes of carbon (GtC, 10^{15} gC), which is the same as petagrams of carbon (PgC; Table 1). Units of gigatonnes of CO_2 (or billion tonnes of CO_2) used in policy are equal to 3.664 multiplied by the value in units of GtC.

This paper provides a detailed description of the data sets and methodology used to compute the global carbon budget estimates for the period pre-industrial (1750) to 2014 and in more detail for the period 1959 to 2014. We also provide decadal averages starting in 1960 and including the last decade (2005–2014), results for the year 2014, and a projection of E_{FF} for year 2015. Finally we provide cumulative emissions from fossil fuels and land-use change since year 1750, the pre-industrial period, and since year 1870, the reference year for the cumulative carbon estimate used by the IPCC (AR5) based on the availability of global temperature data (Stocker et al., 2013). This paper is intended to be updated every year using the format of "living data" to keep a record of budget versions and the changes in new data, revision of data, and changes in methodology that lead to changes in estimates of the carbon budget. Additional materials associated with the release of each new version will be posted on the GCP website (http://www.globalcarbonproject.org/carbonbudget). Data associated with this release are also available through the Global

Carbon Atlas (http://www.globalcarbonatlas.org). With this approach, we aim to provide the highest transparency and traceability in the reporting of CO_2, the key driver of climate change.

2 Methods

Multiple organisations and research groups around the world generated the original measurements and data used to complete the global carbon budget. The effort presented here is thus mainly one of synthesis, where results from individual groups are collated, analysed, and evaluated for consistency. We facilitate access to original data with the understanding that primary data sets will be referenced in future work (see Table 2 for how to cite the data sets). Descriptions of the measurements, models, and methodologies follow below and in-depth descriptions of each component are described elsewhere (e.g. Andres et al., 2012; Houghton et al., 2012).

This is the tenth version of the "global carbon budget" (see Introduction for details) and the fourth revised version of the "global carbon budget living data update". It is an update of Le Quéré et al. (2015), including data to year 2014 (inclusive) and a projection for fossil fuel emissions for year 2015. The main changes from Le Quéré et al. (2015) are (1) the use of national emissions for E_{FF} from the United Nations Framework Convention on Climate Change (UNFCCC) where available; (2) the projection of E_{FF} for 2015 is based on national emissions projections for China and USA, as well as GDP corrected for recent changes in the carbon intensity of the global economy for the rest of the world; and (3) that we apply minimum criteria of realism to select ocean data products and process models. The main methodological differences between annual carbon budgets are summarised in Table 3.

2.1 CO_2 emissions from fossil fuels and industry (E_{FF})

2.1.1 Emissions from fossil fuels and industry and their uncertainty

The calculation of global and national CO_2 emissions from fossil fuels, including gas flaring and cement production (E_{FF}), relies primarily on energy consumption data, specifically data on hydrocarbon fuels, collated and archived by several organisations (Andres et al., 2012). These include the Carbon Dioxide Information Analysis Center (CDIAC), the International Energy Agency (IEA), the United Nations (UN), the United States Department of Energy (DoE) Energy Information Administration (EIA), and more recently also the Planbureau voor de Leefomgeving (PBL) Netherlands Environmental Assessment Agency. Where available, we use national emissions estimated by the countries themselves and reported to the UNFCCC for the period 1990–2012 (42 countries). We assume that national emissions reported to the UNFCCC are the most accurate because national experts have access to additional and country-specific information, and because these emission estimates are periodically audited for each country through an established international methodology overseen by the UNFCCC. We also use global and national emissions estimated by CDIAC (Boden et al., 2013). The CDIAC emission estimates are the only data set that extends back in time to 1751 with consistent and well-documented emissions from fossil fuels, cement production, and gas flaring for all countries and their uncertainty (Andres et al., 2014, 2012, 1999); this makes the data set a unique resource for research of the carbon cycle during the fossil fuel era.

The global emissions presented here are from CDIAC's analysis, which provides an internally consistent global estimate including bunker fuels, minimising the effects of lower-quality energy trade data. Thus the comparison of global emissions with previous annual carbon budgets is not influenced by the use of data from UNFCCC national reports.

During the period 1959–2011, the emissions from fossil fuels estimated by CDIAC are based primarily on energy data provided by the UN Statistics Division (UN, 2014a, b; Table 4). When necessary, fuel masses/volumes are converted to fuel energy content using coefficients provided by the UN and then to CO_2 emissions using conversion factors that take into account the relationship between carbon content and energy (heat) content of the different fuel types (coal, oil, gas, gas flaring) and the combustion efficiency (to account, for example, for soot left in the combustor or fuel otherwise lost or discharged without oxidation). Most data on energy consumption and fuel quality (carbon content and heat content) are available at the country level (UN, 2014a). In general, CO_2 emissions for equivalent primary energy consumption are about 30 % higher for coal compared to oil, and 70 % higher for coal compared to natural gas (Marland et al., 2007). All estimated fossil fuel emissions are based on the mass flows of carbon and assume that the fossil carbon emitted as CO or CH_4 will soon be oxidised to CO_2 in the atmosphere and can be accounted for with CO_2 emissions (see Sect. 2.7).

Our emissions totals for the UNFCCC-reporting countries were recorded as in the UNFCCC submissions, which have a slightly larger system boundary than CDIAC. Additional emissions come from carbonates other than in cement manufacture, and thus UNFCCC totals will be slightly higher than CDIAC totals in general, although there are multiple sources for differences. We use the CDIAC method to report emissions by fuel type (e.g. all coal oxidation is reported under "coal", regardless of whether oxidation results from combustion as an energy source), which differs slightly from UNFCCC.

For the most recent 2–3 years when the UNFCCC estimates and UN statistics used by CDIAC are not yet available (or there was insufficient time to process and verify them), we generated preliminary estimates based on the BP annual energy review by applying the growth rates of en-

Table 2. How to cite the individual components of the global carbon budget presented here.

Component	Primary reference
Global emissions from fossil fuels and industry (E_{FF}), total and by fuel type	Boden et al. (2015; CDIAC: http://cdiac.ornl.gov/trends/emis/meth_reg.html)
National territorial emissions from fossil fuels and industry (E_{FF})	CDIAC source: Boden et al. (2015; CDIAC: http://cdiac.ornl.gov/trends/emis/meth_reg.html) UNFCCC source (2015; http://unfccc.int/national_reports/annex_i_ghg_inventories/national_inventories_submissions/items/8108.php; accessed May 2015)
National consumption-based emissions from fossil fuels and industry (E_{FF}) by country (consumption)	Peters et al. (2011b) updated as described in this paper
Land-use-change emissions (E_{LUC})	Houghton et al. (2012) combined with Giglio et al. (2013)
Atmospheric CO_2 growth rate (G_{ATM})	Dlugokencky and Tans (2015; NOAA/ESRL: http://www.esrl.noaa.gov/gmd/ccgg/trends/global.html; accessed 12 October 2015)
Ocean and land CO_2 sinks (S_{OCEAN} and S_{LAND})	This paper for S_{OCEAN} and S_{LAND} and references in Table 6 for individual models.

ergy consumption (coal, oil, gas) for 2013–2014 to the UNFCCC national emissions in 2012, and for 2012–2014 for the CDIAC national and global emissions in 2011 (BP, 2015). BP's sources for energy statistics overlap with those of the UN data, but are compiled more rapidly from about 70 countries covering about 96 % of global emissions. We use the BP values only for the year-to-year rate of change, because the rates of change are less uncertain than the absolute values and we wish to avoid discontinuities in the time series when linking the UN-based data with the BP data. These preliminary estimates are replaced by the more complete UNFCCC or CDIAC data based on UN statistics when they become available. Past experience and work by others (Andres et al., 2014; Myhre et al., 2009) show that projections based on the BP rate of change are within the uncertainty provided (see Sect. 3.2 and the Supplement from Peters et al., 2013).

Estimates of emissions from cement production by CDIAC are based on data on growth rates of cement production from the US Geological Survey up to year 2013 (van Oss, 2013), and up to 2014 for the top 18 countries (representing 85 % of global production; USGS, 2015). For countries without data in 2014 we use the 2013 values (zero growth). Some fraction of the CaO and MgO in cement is returned to the carbonate form during cement weathering, but this is generally regarded to be small and is ignored here.

Estimates of emissions from gas flaring by CDIAC are calculated in a similar manner to those from solid, liquid, and gaseous fuels, and rely on the UN Energy Statistics to supply the amount of flared or vented fuel. For emission years 2012–2014, flaring is assumed constant from 2011 (emission year) UN-based data. The basic data on gas flaring report atmospheric losses during petroleum production and processing that have large uncertainty and do not distinguish between gas that is flared as CO_2 or vented as CH_4. Fugitive emissions of CH_4 from the so-called upstream sector (e.g. coal mining and natural gas distribution) are not included in the accounts of CO_2 emissions except to the extent that they are captured in the UN energy data and counted as gas "flared or lost".

The published CDIAC data set includes 250 countries and regions. This expanded list includes countries that no longer exist, such as the USSR and East Pakistan. For the carbon budget, we reduce the list to 216 countries by reallocating emissions to the currently defined territories. This involved both aggregation and disaggregation, and does not change global emissions. Examples of aggregation include merging East and West Germany to the currently defined Germany. Examples of disaggregation include reallocating the emissions from former USSR to the resulting independent countries. For disaggregation, we use the emission shares when the current territory first appeared. The disaggregated estimates should be treated with care when examining countries' emissions trends prior to their disaggregation. For the most recent years, 2012–2014, the BP statistics are more aggregated, but we retain the detail of CDIAC by applying the growth rates of each aggregated region in the BP data set to its constituent individual countries in CDIAC.

Estimates of CO_2 emissions show that the global total of emissions is not equal to the sum of emissions from all countries. This is largely attributable to emissions that occur in international territory, in particular the combustion of fuels used in international shipping and aviation (bunker fuels), where the emissions are included in the global totals but are not attributed to individual countries. In practice, the emissions from international bunker fuels are calculated based on where the fuels were loaded, but they are not included with national emissions estimates. Other differences occur because globally the sum of imports in all countries is not equal to the sum of exports and because of differing treatment of oxidation of non-fuel uses of hydrocarbons (e.g. as

Table 3. Main methodological changes in the global carbon budget since first publication. Unless specified below, the methodology was identical to that described in the current paper. Furthermore, methodological changes introduced in one year are kept for the following years unless noted. Empty cells mean there were no methodological changes introduced that year.

Publication year[a]	Fossil fuel emissions			LUC emissions	Reservoirs			Uncertainty & other changes
	Global	Country (territorial)	Country (consumption)		Atmosphere	Ocean	Land	
2006 Raupach et al. (2007)		Split in regions						
2007 Canadell et al. (2007)				E_{LUC} based on FAO-FRA 2005; constant E_{LUC} for 2006	1959–1979 data from Mauna Loa; data after 1980 from global average	Based on one ocean model tuned to reproduced observed 1990s sink		$\pm 1\sigma$ provided for all components
2008 (online)				Constant E_{LUC} for 2007				
2009 Le Quéré et al. (2009)		Split between Annex B and non-Annex B	Results from an independent study discussed	Fire-based emission anomalies used for 2006–2008		Based on four ocean models normalised to observations with constant delta	First use of five DGVMs to compare with budget residual	
2010 Friedlingstein et al. (2010)	Projection for current year based on GDP	Emissions for top emitters		E_{LUC} updated with FAO-FRA 2010				
2011 Peters et al. (2012b)			Split between Annex B and non-Annex B					
2012 Le Quéré et al. (2013) Peters et al. (2013)		129 countries from 1959	129 countries and regions from 1990–2010 based on GTAP8.0	E_{LUC} for 1997–2011 includes interannual anomalies from fire-based emissions	All years from global average	Based on five ocean models normalised to observations with ratio	Ten DGVMs available for S_{LAND}; first use of four models to compare with E_{LUC}	
2013 Le Quéré et al. (2014)		250 countries[b]	134 countries and regions 1990–2011 based on GTAP8.1, with detailed estimates for years 1997, 2001, 2004, and 2007	E_{LUC} for 2012 estimated from 2001–2010 average		Based on six models compared with two data products to year 2011	Coordinated DGVM experiments for S_{LAND} and E_{LUC}	Confidence levels; cumulative emissions; budget from 1750
2014 Le Quéré et al. (2015)	Three years of BP data	Three years of BP data	Extended to 2012 with updated GDP data	E_{LUC} for 1997–2013 includes interannual anomalies from fire-based emissions		Based on seven models compared with three data products to year 2013	Based on 10 models	Inclusion of breakdown of the sinks in three latitude bands and comparison with three atmospheric inversions
2015 (this study)		National emissions from UNFCCC extended to 2014 also provided (along with CDIAC)	Detailed estimates introduced for 2011 based on GTAP9			Based on eight models compared with two data products to year 2014	Based on 10 models with assessment of minimum realism	The decadal uncertainty for the DGVM ensemble mean now uses $\pm 1\sigma$ of the decadal spread across models

[a] The naming convention of the budgets has changed. Up to and including 2010, the budget year (Carbon Budget 2010) represented the latest year of the data. From 2012, the budget year (Carbon Budget 2012) refers to the initial publication year. [b] The CDIAC database has about 250 countries, but we show data for about 216 countries since we aggregate and disaggregate some countries to be consistent with current country definitions (see Sect. 2.1.1 for more details).

solvents, lubricants, feedstocks), and changes in stock (Andres et al., 2012).

The uncertainty of the annual emissions from fossil fuels and industry for the globe has been estimated at ±5 % (scaled down from the published ±10 % at ±2σ to the use of ±1σ bounds reported here; Andres et al., 2012). This is consistent with a more detailed recent analysis of uncertainty of ±8.4 % at ±2σ (Andres et al., 2014) and at the high end of the range of ±5–10 % at ±2σ reported by Ballantyne et al. (2015). This includes an assessment of uncertainties in the amounts of fuel consumed, the carbon and heat contents of fuels, and the combustion efficiency. While in the budget we consider a fixed uncertainty of ±5 % for all years, in reality the uncertainty, as a percentage of the emissions, is growing with time because of the larger share of global emissions from non-Annex B countries (emerging economies and developing countries) with less precise statistical systems (Marland et al., 2009). For example, the uncertainty in Chinese emissions has been estimated at around ±10 % (for ±1σ; Gregg et al., 2008), and important potential biases have been identified that suggest China's emissions could be overestimated in published studies (Liu et al., 2015). Generally, emissions from mature economies with good statistical bases have an uncertainty of only a few percent (Marland, 2008). Further research is needed before we can quantify the time evolution of the uncertainty and its temporal error correlation structure. We note that, even if they are presented as 1σ estimates, uncertainties in emissions are likely to be mainly country-specific systematic errors related to underlying biases of energy statistics and to the accounting method used by each country. We assign a medium confidence to the results presented here because they are based on indirect estimates of emissions using energy data (Durant et al., 2010). There is only limited and indirect evidence for emissions, although there is a high agreement among the available estimates within the given uncertainty (Andres et al., 2014, 2012), and emission estimates are consistent with a range of other observations (Ciais et al., 2013), even though their regional and national partitioning is more uncertain (Francey et al., 2013).

2.1.2 Emissions embodied in goods and services

National emission inventories take a territorial (production) perspective and "include greenhouse gas emissions and removals taking place within national territory and offshore areas over which the country has jurisdiction" (Rypdal et al., 2006). That is, emissions are allocated to the country where and when the emissions actually occur. The territorial emission inventory of an individual country does not include the emissions from the production of goods and services produced in other countries (e.g. food and clothes) that are used for consumption. Consumption-based emission inventories for an individual country constitute another attribution point of view that allocates global emissions to products that are consumed within a country, and are conceptually calculated as the territorial emissions minus the "embedded" territorial emissions to produce exported products plus the emissions in other countries to produce imported products (consumption = territorial − exports + imports). The difference between the territorial- and consumption-based emission inventories is the net transfer (exports minus imports) of emissions from the production of internationally traded products. Consumption-based emission attribution results (e.g. Davis and Caldeira, 2010) provide additional information to territorial-based emissions that can be used to understand emission drivers (Hertwich and Peters, 2009), quantify emission (virtual) transfers by the trade of products between countries (Peters et al., 2011b), and potentially design more effective and efficient climate policy (Peters and Hertwich, 2008).

We estimate consumption-based emissions by enumerating the global supply chain using a global model of the economic relationships between economic sectors within and between every country (Andrew and Peters, 2013; Peters et al., 2011a). Due to availability of the input data, detailed estimates are made for the years 1997, 2001, 2004, 2007, and 2011 (using the methodology of Peters et al., 2011b) using economic and trade data from the Global Trade and Analysis Project version 9 (GTAP; Narayanan et al., 2015). The results cover 57 sectors and 140 countries and regions. The results are extended into an annual time series from 1990 to the latest year of the fossil fuel emissions or GDP data (2013 in this budget), using GDP data by expenditure in current exchange rate of US dollars (USD; from the UN National Accounts Main Aggregates Database; UN, 2014c) and time series of trade data from GTAP (based on the methodology in Peters et al., 2011b).

We estimate the sector-level CO_2 emissions using our own calculations based on the GTAP data and methodology, include flaring and cement emissions from CDIAC, and then scale the national totals (excluding bunker fuels) to match the CDIAC estimates from the most recent carbon budget. We do not include international transportation in our estimates of national totals, but we do include them in the global total. The time series of trade data provided by GTAP covers the period 1995–2011 and our methodology uses the trade shares as this data set. For the period 1990–1994 we assume the trade shares of 1995, while for 2012 and 2013 we assume the trade shares of 2011.

Comprehensive analysis of the uncertainty of consumption emissions accounts is still lacking in the literature, although several analyses of components of this uncertainty have been made (e.g. Dietzenbacher et al., 2012; Inomata and Owen, 2014; Karstensen et al., 2015; Moran and Wood, 2014). For this reason we do not provide an uncertainty estimate for these emissions, but based on model comparisons and sensitivity analysis, they are unlikely to be larger than for the territorial emission estimates (Peters et al., 2012a). Uncertainty is expected to increase for more detailed results, and

to decrease with aggregation (Peters et al., 2011b; e.g. the results for Annex B countries will be more accurate than the sector results for an individual country).

The consumption-based emissions attribution method considers the CO_2 emitted to the atmosphere in the production of products, but not the trade in fossil fuels (coal, oil, gas). It is also possible to account for the carbon trade in fossil fuels (Davis et al., 2011), but we do not present those data here. Peters et al. (2012a) additionally considered trade in biomass.

The consumption data do not modify the global average terms in Eq. (1) but are relevant to the anthropogenic carbon cycle as they reflect the trade-driven movement of emissions across the Earth's surface in response to human activities. Furthermore, if national and international climate policies continue to develop in an unharmonised way, then the trends reflected in these data will need to be accommodated by those developing policies.

2.1.3 Growth rate in emissions

We report the annual growth rate in emissions for adjacent years (in percent per year) by calculating the difference between the two years and then comparing to the emissions in the first year: $\left[\frac{E_{\mathrm{FF}}(t_{0+1})-E_{\mathrm{FF}}(t_0)}{E_{\mathrm{FF}}(t_0)}\right] \times 100\,\%\,\mathrm{yr}^{-1}$. This is the simplest method to characterise a 1-year growth compared to the previous year and is widely used. We apply a leap-year adjustment to ensure valid interpretations of annual growth rates. This would affect the growth rate by about $0.3\,\%\,\mathrm{yr}^{-1}$ (1/365) and causes growth rates to go up approximately 0.3 % if the first year is a leap year and down 0.3 % if the second year is a leap year.

The relative growth rate of E_{FF} over time periods of greater than 1 year can be re-written using its logarithm equivalent as follows:

$$\frac{1}{E_{\mathrm{FF}}}\frac{\mathrm{d}E_{\mathrm{FF}}}{\mathrm{d}t} = \frac{\mathrm{d}(\ln E_{\mathrm{FF}})}{\mathrm{d}t}. \quad (2)$$

Here we calculate relative growth rates in emissions for multi-year periods (e.g. a decade) by fitting a linear trend to $\ln(E_{\mathrm{FF}})$ in Eq. (2), reported in percent per year. We fit the logarithm of E_{FF} rather than E_{FF} directly because this method ensures that computed growth rates satisfy Eq. (6). This method differs from previous papers (Canadell et al., 2007; Le Quéré et al., 2009; Raupach et al., 2007) that computed the fit to E_{FF} and divided by average E_{FF} directly, but the difference is very small ($< 0.05\,\%$) in the case of E_{FF}.

2.1.4 Emissions projections

Energy statistics from BP are normally available around June for the previous year. To gain insight into emission trends for the current year (2015), we provide an assessment of global emissions for E_{FF} by combining individual assessments of emissions for China and the USA (the two biggest emitting countries), as well as the rest of the world.

We specifically estimate emissions in China because the evidence suggests a departure from the long-term trends in the carbon intensity of the economy used in emissions projections in previous global carbon budgets (e.g. Le Quéré et al., 2015), resulting from significant drops in industrial production against continued growth in economic output. This departure could be temporary (Jackson et al., 2015). Our 2015 estimate for China uses (1) apparent consumption of coal for January to August estimated using production data from the National Bureau of Statistics (2015b), imports and exports of coal from China Customs Statistics (General Administration of Customs of the People's Republic of China, 2015a, b), and from partial data on stock changes from industry sources (China Coal Industry Association, 2015; China Coal Resource, 2015); (2) apparent consumption of oil and gas for January to June from the National Energy Administration (2015); and (3) production of cement reported for January to August (National Bureau of Statistics of China, 2015b). Using these data, we estimate the change in emissions for the corresponding months in 2015 compared to 2014 assuming constant emission factors. We then assume that the relative changes during the first 6–8 months will persist throughout the year. The main sources of uncertainty are from the incomplete data on stock changes, the carbon content of coal, and the assumption of persistent behaviour for the rest of 2015. These are discussed further in Sect. 3.2.1. We tested our new method using data available in October 2014 to make a 2014 projection of coal consumption and cement production, both of which changed substantially in 2014. For the apparent consumption of coal we would have projected a change of $-3.2\,\%$ in coal use for 2014, compared to $-2.9\,\%$ reported by the National Bureau of Statistics of China in February 2015, while for the production of cement we would have projected a change of $+3.5\,\%$, compared to a realised change of $+2.3\,\%$. In both cases, the projection is consistent with the sign of the realised change. This new method should be more reliable as it is based on actual data, even if they are preliminary. Note that the growth rates we project for China are unaffected by recent upwards revisions of Chinese energy consumption statistics (National Bureau of Statistics of China, 2015a), as all data used here dates from after the revised period. The revisions do, however, affect the absolute value of the time series up to 2013, and hence the absolute value for 2015 extrapolated from that time series using projected growth rates. Further, because the revisions will increase China's share of total global emissions, the projected growth rate of global emissions will also be affected slightly. This effect is discussed in the Results section.

For the USA, we use the forecast of the US Energy Information Administration (EIA) "Short-term energy outlook" (October 2015) for emissions from fossil fuels. This is based on an energy forecasting model which is revised monthly, and takes into account heating-degree days, household ex-

penditures by fuel type, energy markets, policies, and other effects. We combine this with our estimate of emissions from cement production using the monthly US cement data from USGS for January–July, assuming changes in cement production over the first 7 months apply throughout the year. We estimate an uncertainty range using the revisions of historical October forecasts made by the EIA 1 year later. These revisions were less than 2 % during 2009–2014 (when a forecast was done), except for 2011, when it was −4.0 %. We thus use a conservative uncertainty range of −4.0 to +1.8 % around the central forecast.

For the rest of the world, we use the close relationship between the growth in GDP and the growth in emissions (Raupach et al., 2007) to project emissions for the current year. This is based on the so-called Kaya identity (also called IPAT identity, the acronym standing for human impact (I) on the environment, which is equal to the product of population (P), affluence (A), and technology (T)), whereby E_{FF} (GtC yr^{-1}) is decomposed by the product of GDP (USD yr^{-1}) and the fossil fuel carbon intensity of the economy (I_{FF}; GtC USD^{-1}) as follows:

$$E_{\mathrm{FF}} = \mathrm{GDP} \times I_{\mathrm{FF}}. \quad (3)$$

Such product-rule decomposition identities imply that the relative growth rates of the multiplied quantities are additive. Taking a time derivative of Eq. (3) gives

$$\frac{\mathrm{d}E_{\mathrm{FF}}}{\mathrm{d}t} = \frac{\mathrm{d}(\mathrm{GDP} \times I_{\mathrm{FF}})}{\mathrm{d}t} \quad (4)$$

and applying the rules of calculus

$$\frac{\mathrm{d}E_{\mathrm{FF}}}{\mathrm{d}t} = \frac{\mathrm{dGDP}}{\mathrm{d}t} \times I_{\mathrm{FF}} + \mathrm{GDP} \times \frac{\mathrm{d}I_{\mathrm{FF}}}{\mathrm{d}t}. \quad (5)$$

Finally, dividing Eq. (5) by (3) gives

$$\frac{1}{E_{\mathrm{FF}}}\frac{\mathrm{d}E_{\mathrm{FF}}}{\mathrm{d}t} = \frac{1}{\mathrm{GDP}}\frac{\mathrm{dGDP}}{\mathrm{d}t} + \frac{1}{I_{\mathrm{FF}}}\frac{\mathrm{d}I_{\mathrm{FF}}}{\mathrm{d}t}, \quad (6)$$

where the left-hand term is the relative growth rate of E_{FF} and the right-hand terms are the relative growth rates of GDP and I_{FF}, respectively, which can simply be added linearly to give overall growth rate. The growth rates are reported in percent by multiplying each term by 100 %. As preliminary estimates of annual change in GDP are made well before the end of a calendar year, making assumptions on the growth rate of I_{FF} allows us to make projections of the annual change in CO_2 emissions well before the end of a calendar year. The I_{FF} is based on GDP in constant PPP (purchasing power parity) from the IEA up to 2012 (IEA/OECD, 2014) and extended using the IMF growth rates for 2013 and 2014 (IMF, 2015). Experience of the past year has highlighted that the interannual variability in I_{FF} is the largest source of uncertainty in the GDP-based emissions projections. We thus use the standard deviation of the annual I_{FF} for the period 2005–2014 as a measure of uncertainty, reflecting $\pm 1\sigma$ as in the rest of the carbon budget. This is $\pm 1.4\,\%\,\mathrm{yr}^{-1}$ for the rest of the world (global emissions minus China and USA).

The 2015 projection for the world is made of the sum of the projections for China, the USA, and the rest of the world. The uncertainty is added quadratically among the three regions. The uncertainty here reflects the best of our expert opinion.

2.2 CO_2 emissions from land use, land-use change, and forestry (E_{LUC})

Land-use-change emissions reported here (E_{LUC}) include CO_2 fluxes from deforestation, afforestation, logging (forest degradation and harvest activity), shifting cultivation (cycle of cutting forest for agriculture and then abandoning), and regrowth of forests following wood harvest or abandonment of agriculture. Only some land management activities (Table 5) are included in our land-use-change emissions estimates (e.g. emissions or sinks related to management and management changes of established pasture and croplands are not included). Some of these activities lead to emissions of CO_2 to the atmosphere, while others lead to CO_2 sinks. E_{LUC} is the net sum of all anthropogenic activities considered. Our annual estimate for 1959–2010 is from a bookkeeping method (Sect. 2.2.1) primarily based on net forest area change and biomass data from the Forest Resource Assessment (FRA) of the Food and Agriculture Organization (FAO), which is only available at intervals of 5 years. We use the FAO FRA 2010 here (Houghton et al., 2012). Interannual variability in emissions due to deforestation and degradation has been coarsely estimated from satellite-based fire activity in tropical forest areas (Sect. 2.2.2; Giglio et al., 2013; van der Werf et al., 2010). The bookkeeping method is used to quantify the E_{LUC} over the time period of the available data, and the satellite-based deforestation fire information to incorporate interannual variability (E_{LUC} flux annual anomalies) from tropical deforestation fires. The satellite-based deforestation and degradation fire emissions estimates are available for years 1997–2014. We calculate the global annual anomaly in deforestation and degradation fire emissions in tropical forest regions for each year, compared to the 1997–2010 period, and add this annual flux anomaly to the E_{LUC} estimated using the bookkeeping method that is available up to 2010 only and assumed constant at the 2010 value during the period 2011–2014. We thus assume that all land management activities apart from deforestation and degradation do not vary significantly on a year-to-year basis. Other sources of interannual variability (e.g. the impact of climate variability on regrowth fluxes) are accounted for in S_{LAND}. In addition, we use results from dynamic global vegetation models (see Sect. 2.2.3 and Table 6) that calculate net land-use-change CO_2 emissions in response to land-cover-change reconstructions prescribed to each model in order to help quantify the uncertainty in E_{LUC} and to explore the consistency of

Table 4. Data sources used to compute each component of the global carbon budget. National emissions from UNFCCC are provided directly and thus no additional data sources need citing in this table.

Component	Process	Data source	Data reference
E_{FF} (global and CDIAC national)	Fossil fuel combustion and oxidation and gas flaring	UN Statistics Division to 2011	UN (2014a, b)
		BP for 2012–2014	BP (2015)
	Cement production	US Geological Survey	van Oss (2015) USGS (2015)
E_{LUC}	Land-cover change (deforestation, afforestation, and forest regrowth)	Forest Resource Assessment (FRA) of the Food and Agriculture Organization (FAO)	FAO (2010)
	Wood harvest Shifting agriculture	FAO Statistics Division FAO FRA and Statistics Division	FAOSTAT (2010) FAO (2010) FAOSTAT (2010)
	Interannual variability from peat fires and climate – land management interactions (1997–2013)	Global Fire Emissions Database (GFED4)	Giglio et al. (2013)
G_{ATM}	Change in atmospheric CO_2 concentration	1959–1980: CO_2 Program at Scripps Institution of Oceanography and other research groups	Keeling et al. (1976)
		1980–2015: US National Oceanic and Atmospheric Administration Earth System Research Laboratory	Dlugokencky and Tans (2015) Ballantyne et al. (2012)
S_{OCEAN}	Uptake of anthropogenic CO_2	1990–1999 average: indirect estimates based on CFCs, atmospheric O_2, and other tracer observations	Manning and Keeling (2006) Keeling et al. (2011) McNeil et al. (2003) Mikaloff Fletcher et al. (2006) as assessed by the IPCC in Denman et al. (2007)
	Impact of increasing atmospheric CO_2, climate, and variability	Ocean models	Table 6
S_{LAND}	Response of land vegetation to: Increasing atmospheric CO_2 concentration Climate and variability Other environmental changes	Budget residual	

our understanding. The three methods are described below, and differences are discussed in Sect. 3.2.

2.2.1 Bookkeeping method

Land-use-change CO_2 emissions are calculated by a bookkeeping method approach (Houghton, 2003) that keeps track of the carbon stored in vegetation and soils before deforestation or other land-use change, and the changes in forest age classes, or cohorts, of disturbed lands after land-use change, including possible forest regrowth after deforestation. The approach tracks the CO_2 emitted to the atmosphere immediately during deforestation, and over time due to the follow-up decay of soil and vegetation carbon in different pools, including wood product pools after logging and deforestation. It also tracks the regrowth of vegetation and associated build-up of soil carbon pools after land-use change. It considers transitions between forests, pastures, and cropland; shifting cultivation; degradation of forests where a fraction of the trees is removed; abandonment of agricultural land; and forest management such as wood harvest and, in the USA, fire management. In addition to tracking logging debris on the forest floor, the bookkeeping method tracks the fate of carbon contained in harvested wood products that is eventually emitted back to the atmosphere as CO_2, although a detailed treatment of the lifetime in each product pool is not performed (Earles et al., 2012). Harvested wood products are partitioned into three pools with different turnover times. All

Table 5. Comparison of the processes included in the E_{LUC} of the global carbon budget and the DGVMs. See Table 6 for model references. All models include deforestation and forest regrowth after abandonment of agriculture (or from afforestation activities on agricultural land).

	Bookkeeping	CLM4.5BGC	ISAM	JSBACH	JULES	LPJ-GUESS	LPJ	LPJmL	OCNv1.r240	ORCHIDEE	VISIT
Wood harvest and forest degradation[a]	yes	yes	yes	yes	no	no	no	no	yes	no	yes[b]
Shifting cultivation	yes	yes	no	yes	no	no	no	no	no	no	yes
Cropland harvest	yes	yes	yes	yes[c]	no	yes	no	yes	yes	yes	yes
Peat fires	no	yes	no	no	no	no	no	no	no	no	no
Fire simulation and/or suppression	for US only	yes	no	yes	no	yes	yes	yes	no	no	yes
Climate and variability	no	yes	yes	yes	yes	yes	yes	yes	yes	yes	yes
CO_2 fertilisation	no	yes	yes	yes	yes	yes	yes	yes	yes	yes	yes
Carbon–nitrogen interactions, including N deposition	no	yes	yes	no	no	no	no	no	yes	no	no

[a] Refers to the routine harvest of established managed forests rather than pools of harvested products. [b] Wood stems are harvested according to the land-use data. [c] Carbon from crop harvest is entirely transferred into the litter pools.

fuelwood is assumed burnt in the year of harvest ($1.0\,yr^{-1}$). Pulp and paper products are oxidised at a rate of $0.1\,yr^{-1}$, timber is assumed to be oxidised at a rate of $0.01\,yr^{-1}$, and elemental carbon decays at $0.001\,yr^{-1}$. The general assumptions about partitioning wood products among these pools are based on national harvest data (Houghton, 2003).

The primary land-cover-change and biomass data for the bookkeeping method analysis is the Forest Resource Assessment of the FAO, which provides statistics on forest-cover change and management at intervals of 5 years (FAO, 2010). The data are based on countries' self-reporting, some of which integrates satellite data in more recent assessments (Table 4). Changes in land cover other than forest are based on annual, national changes in cropland and pasture areas reported by the FAO Statistics Division (FAOSTAT, 2010). Land-use-change country data are aggregated by regions. The carbon stocks on land (biomass and soils), and their response functions subsequent to land-use change, are based on FAO data averages per land-cover type, per biome, and per region. Similar results were obtained using forest biomass carbon density based on satellite data (Baccini et al., 2012). The bookkeeping method does not include land ecosystems' transient response to changes in climate, atmospheric CO_2, and other environmental factors, but the growth/decay curves are based on contemporary data that will implicitly reflect the effects of CO_2 and climate at that time. Results from the bookkeeping method are available from 1850 to 2010.

2.2.2 Fire-based interannual variability in E_{LUC}

Land-use-change-associated CO_2 emissions calculated from satellite-based fire activity in tropical forest areas (van der Werf et al., 2010) provide information on emissions due to tropical deforestation and degradation that are complementary to the bookkeeping approach. They do not provide a direct estimate of E_{LUC} as they do not include non-combustion processes such as respiration, wood harvest, wood products, or forest regrowth. Legacy emissions such as decomposition from on-ground debris and soils are not included in this method either. However, fire estimates provide some insight into the year-to-year variations in the subcomponent of the total E_{LUC} flux that result from immediate CO_2 emissions during deforestation caused, for example, by the interactions between climate and human activity (e.g. there is more burning and clearing of forests in dry years) that are not represented by other methods. The "deforestation fire emissions" assume an important role of fire in removing biomass in the deforestation process, and thus can be used to infer gross instantaneous CO_2 emissions from deforestation using satellite-derived data on fire activity in regions with active deforestation. The method requires information on the fraction of total area burned associated with deforestation versus other types of fires, and this information can be merged with information on biomass stocks and the fraction of the biomass lost in a deforestation fire to estimate CO_2 emissions. The satellite-based deforestation fire emissions are limited to the tropics, where fires result mainly from human activities. Tropical deforestation is the largest and most variable single contributor to E_{LUC}.

Fire emissions associated with deforestation and tropical peat burning are based on the Global Fire Emissions Database (GFED4; accessed October 2015) described in van der Werf et al. (2010) but with updated burned area (Giglio et al., 2013) as well as burned area from relatively small fires that are detected by satellite as thermal anomalies but not mapped by the burned area approach (Randerson et al., 2012). The burned area information is used as input data in a modified version of the satellite-driven Carnegie–Ames–Stanford Approach (CASA) biogeochemical model to estimate carbon emissions associated with fires, keeping track of what fraction of fire emissions was due to deforestation (see van der Werf et al., 2010). The CASA model uses differ-

ent assumptions to compute decay functions compared to the bookkeeping method, and does not include historical emissions or regrowth from land-use change prior to the availability of satellite data. Comparing coincident CO emissions and their atmospheric fate with satellite-derived CO concentrations allows for some validation of this approach (e.g. van der Werf et al., 2008). Results from the fire-based method to estimate land-use-change emissions anomalies added to the bookkeeping mean E_{LUC} estimate are available from 1997 to 2014. Our combination of land-use-change CO_2 emissions where the variability in annual CO_2 deforestation emissions is diagnosed from fires assumes that year-to-year variability is dominated by variability in deforestation.

2.2.3 Dynamic global vegetation models (DGVMs)

Land-use-change CO_2 emissions have been estimated using an ensemble of 10 DGVMs. New model experiments up to year 2014 have been coordinated by the project "Trends and drivers of the regional-scale sources and sinks of carbon dioxide" (TRENDY; Sitch et al., 2015). We use only models that have estimated land-use-change CO_2 emissions and the terrestrial residual sink following the TRENDY protocol (see Sect. 2.5.2), thus providing better consistency in the assessment of the causes of carbon fluxes on land. Models use their latest configurations, summarised in Tables 5 and 6.

The DGVMs were forced with historical changes in land-cover distribution, climate, atmospheric CO_2 concentration, and N deposition. As further described below, each historical DGVM simulation was repeated with a time-invariant pre-industrial land-cover distribution, allowing for estimation of, by difference with the first simulation, the dynamic evolution of biomass and soil carbon pools in response to prescribed land-cover change. All DGVMs represent deforestation and (to some extent) regrowth, the most important components of E_{LUC}, but they do not represent all processes resulting directly from human activities on land (Table 5). DGVMs represent processes of vegetation growth and mortality, as well as decomposition of dead organic matter associated with natural cycles, and include the vegetation and soil carbon response to increasing atmospheric CO_2 levels and to climate variability and change. In addition, three models explicitly simulate the coupling of C and N cycles and account for atmospheric N deposition (Table 5). The DGVMs are independent of the other budget terms except for their use of atmospheric CO_2 concentration to calculate the fertilisation effect of CO_2 on primary production.

The DGVMs used a consistent land-use-change data set (Hurtt et al., 2011), which provided annual, half-degree, fractional data on cropland, pasture, primary vegetation, and secondary vegetation, as well as all underlying transitions between land-use states, including wood harvest and shifting cultivation. This data set used the HYDE (Klein Goldewijk et al., 2011) spatially gridded maps of cropland, pasture, and ice/water fractions of each grid cell as an input. The HYDE data are based on annual FAO statistics of change in agricultural area available to 2012 (FAOSTAT, 2010). For the years 2013 and 2014, the HYDE data were extrapolated by country for pastures and cropland separately based on the trend in agricultural area over the previous 5 years. The HYDE data are independent of the data set used in the bookkeeping method (Houghton, 2003, and updates), which is based primarily on forest area change statistics (FAO, 2010). Although the HYDE land-use-change data set indicates whether land-use changes occur on forested or non-forested land, typically only the changes in agricultural areas are used by the models and are implemented differently within each model (e.g. an increased cropland fraction in a grid cell can either be at the expense of grassland, or forest, the latter resulting in deforestation; land-cover fractions of the non-agricultural land differ between models). Thus the DGVM forest area and forest area change over time is not consistent with the Forest Resource Assessment of the FAO forest area data used for the bookkeeping model to calculate E_{LUC}. Similarly, model-specific assumptions are applied to convert deforested biomass or deforested area, and other forest product pools, into carbon in some models (Table 5).

The DGVM runs were forced by either 6-hourly CRU-NCEP or by monthly CRU temperature, precipitation, and cloud cover fields (transformed into incoming surface radiation) based on observations and provided on a $0.5° \times 0.5°$ grid and updated to 2014 (CRU TS3.23; Harris et al., 2015). The forcing data include both gridded observations of climate and global atmospheric CO_2, which change over time (Dlugokencky and Tans, 2015), and N deposition (as used in three models, Table 5; Lamarque et al., 2010). E_{LUC} is diagnosed in each model by the difference between a model simulation with prescribed historical land-cover change and a simulation with constant, pre-industrial land-cover distribution. Both simulations were driven by changing atmospheric CO_2, climate, and in some models N deposition over the period 1860–2014. Using the difference between these two DGVM simulations to diagnose E_{LUC} is not fully consistent with the definition of E_{LUC} in the bookkeeping method (Gasser and Ciais, 2013; Pongratz et al., 2014). The DGVM approach to diagnose land-use-change CO_2 emissions would be expected to produce systematically higher E_{LUC} emissions than the bookkeeping approach if all the parameters of the two approaches were the same, which is not the case (see Sect. 2.5.2).

2.2.4 Other published E_{LUC} methods

Other methods have been used to estimate CO_2 emissions from land-use change. We describe some of the most important methodological differences between the approach used here and other published methods, and for completion, we explain why they are not used in the budget.

Different definitions (e.g. the inclusion of fire management) for E_{LUC} can lead to significantly different estimates

Table 6. References for the process models and data products included in Figs. 6–8.

Model/data name	Reference	Change from Le Quéré et al. (2015)
Dynamic global vegetation models		
CLM4.5BGC[a]	Oleson et al. (2013)	No change
ISAM	Jain et al. (2013)[b]	We accounted for crop harvest for C3 and C4 crops based on Arora and Boer (2005) and agricultural soil carbon loss due to tillage (Jain et al., 2005)
JSBACH	Reick et al. (2013)[c]	Not applicable (first use of this model)
JULES[e]	Clark et al. (2011)[e]	Updated JULES version 4.3 compared to v3.2 for last year's budget. A number of small code changes, but no change in major science sections with the exception of an update in the way litter flux is calculated.
LPJ-GUESS	B. Smith et al. (2014)	Implementation of C / N interactions in soil and vegetation, including a complete update of the soil organic matter scheme
LPJ[f]	Sitch et al. (2003)	No change
LPJmL	Bondeau et al. (2007)[g]	Not applicable (first use of this model)
OCNv1.r240	Zaehle et al. (2011)[h]	Revised photosynthesis parameterisation allowing for temperature acclimation as well as cold and heat effects on canopy processes. Revised grassland phenology. Included wood harvest as a driver to simulate harvest and post-harvest regrowth. Using Hurtt land-use data set
ORCHIDEE	Krinner et al. (2005)	Revised parameters values for photosynthetic capacity for boreal forests (following assimilation of FLUXNET data), updated parameters values for stem allocation, maintenance respiration and biomass export for tropical forests (based on literature) and, CO_2 down-regulation process added to photosynthesis.
VISIT	Kato et al. (2013)[i]	No change
Data products for land-use-change emissions		
Bookkeeping	Houghton et al. (2012)	No change
Fire-based emissions	van der Werf et al. (2010)	No change
Ocean biogeochemistry models		
NEMO-PlankTOM5	Buitenhuis et al. (2010)[j]	No change
NEMO-PISCES (IPSL)[k]	Aumont and Bopp (2006)	No change
CCSM-BEC	Doney et al. (2009)	No change; small differences in the mean flux are caused by a change in how global and annual means were computed
MICOM-HAMOCC (NorESM-OC)	Assmann et al. (2010)[l,m]	Revised light penetration formulation and parameters for ecosystem module, revised salinity restoring scheme enforcing salt conservation, new scheme enforcing global freshwater balance, and model grid changed from displaced pole to tripolar
MPIOM-HAMOCC	Ilyina et al. (2013)	No change
NEMO-PISCES (CNRM)	Séférian et al. (2013)[n]	No change
CSIRO	Oke et al. (2013)	No change
MITgcm-REcoM2	Hauck et al. (2013)[o]	Not applicable (first use of this model)
Data products for ocean CO_2 flux		
Landschützer[p]	Landschützer et al. (2015)	No change
Jena CarboScope[p]	Rödenbeck et al. (2014)	Updated to version oc_1.2gcp2015
Atmospheric inversions for total CO_2 fluxes (land-use change + land + ocean CO_2 fluxes)		
CarbonTracker	Peters et al. (2010)	Updated to version CTE2015. Updates include using CO_2 observations from obspack_co2_1_GLOBALVIEWplus_v1.0_2015-07-30 (NOAA/ESRL, 2015b), prior SiBCASA biosphere and fire fluxes on 3-hourly resolution and fossil fuel emissions for 2010–2014 scaled to updated global totals.
Jena CarboScope	Rödenbeck et al. (2003)	Updated to version s81_v3.7
MACC[q]	Chevallier et al. (2005)	Updated to version 14.2. Updates include a change of the convection scheme and a revised data selection.

[a] Community Land Model 4.5. [b] See also El-Masri et al. (2013). [c] See also Goll et al. (2015). [d] Joint UK Land Environment Simulator. [e] See also Best et al. (2011). [f] Lund–Potsdam–Jena. [g] The LPJmL (Lund–Potsdam–Jena managed Land) version used also includes developments described in Rost et al. (2008; river routing and irrigation), Fader et al. (2010; agricultural management), Biemans et al. (2011; reservoir management), Schaphoff et al. (2013; permafrost and 5 layer hydrology), and Waha et al. (2012; sowing data) (sowing dates). [h] See also Zaehle et al. (2010) and Friend (2010). [i] See also Ito and Inatomi (2012). [j] With no nutrient restoring below the mixed layer depth. [k] Referred to as LSCE in previous carbon budgets. [l] With updates to the physical model as described in Tjiputra et al. (2013). [m] Further information (e.g. physical evaluation) for these models can be found in Danabasoglu et al. (2014). [n] Using winds from Atlas et al. (2011). [o] A few changes have been applied to the ecosystem model. (1) The constant Fe : C ratio was substituted by a constant Fe : N ratio. (2) A sedimentary iron source was implemented. (3) the following parameters were changed: CHL_N_max = 3.78, Fe2N = 0.033, deg_CHL_d = 0.1, Fe2N_d = 0.033, ligandStabConst = 200, constantIronSolubility = 0.02. [p] Updates using SOCATv3 plus new 2012–2014 data. [q] The MACCv14.2 CO_2 inversion system, initially described by Chevallier et al. (2005), relies on the global tracer transport model LMDZ (see also Supplement of Chevallier, 2015; Hourdin et al., 2006).

within models (Gasser and Ciais, 2013; Hansis et al., 2015; Pongratz et al., 2014) as well as between models and other approaches (Houghton et al., 2012; P. Smith et al., 2014). FAO uses the IPCC approach called "Tier 1" (e.g. Tubiello et al., 2015) to produce a "Land use – forest land" estimate from the Forest Resources Assessment data used in the bookkeeping method described in Sect. 2.2.1 (MacDicken, 2015). The Tier 1-type method applies a nationally reported mean forest carbon stock change (above and below ground living biomass) to nationally reported net forest area change, across all forest land combined (planted and natural forests). The methods implicitly assume instantaneous loss or gain of mean forest. Thus the Tier 1 approach provides an estimate of attributable emissions from the process of land-cover change, but it does not distribute these emissions through time. It also captures a fraction of what the global modelling approach considers residual carbon flux (S_{LAND}), it does not consider loss of soil carbon, and there are no legacy fluxes. Land-use fluxes estimated with this method were 0.47 GtC yr^{-1} in 2001–2010 and 0.22 GtC yr^{-1} in 2011–2015 (Federici et al., 2015). This estimate is not directly comparable with E_{LUC} used here because of the different boundary conditions.

Recent advances in satellite data leading to higher-resolution area change data (e.g. Hansen et al., 2013) and estimates of biomass in live vegetation (e.g. Baccini et al., 2012; Saatchi et al., 2011) have led to several satellite-based estimates of CO_2 emissions due to tropical deforestation (typically gross loss of forest area; Achard and House, 2015). These include estimates of 1.0 GtC yr^{-1} for 2000 to 2010 (Baccini et al., 2012), 0.8 GtC yr^{-1} for 2000 to 2005 (Harris et al., 2012), 0.9 GtC yr^{-1} for 2000 to 2010 for net area change (Achard et al., 2014), and 1.3 GtC yr^{-1} 2000 to 2010 (Tyukavina et al., 2015). These estimates include belowground carbon biomass using a scaling factor. Some estimate soil carbon loss, some assume instantaneous emissions, some do not account for regrowth fluxes, and none account for legacy fluxes from land-use change prior to the availability of satellite data. They are mostly estimates of tropical deforestation only, and do not capture regrowth flux after abandonment or planting (Achard and House, 2015). These estimates are also difficult to compare with E_{LUC} used here because they do not fully include legacy fluxes and forest regrowth.

2.2.5 Uncertainty assessment for E_{LUC}

Differences between the bookkeeping, the addition of fire-based interannual variability to the bookkeeping, and DGVM methods originate from three main sources: the land-cover-change data set, the different approaches used in models, and the different processes represented (Table 5). We examine the results from the 10 DGVMs and of the bookkeeping method to assess the uncertainty in E_{LUC}.

The uncertainties in annual E_{LUC} estimates are examined using the standard deviation across models, which averages 0.4 GtC yr^{-1} from 1959 to 2014 (Table 7). The mean of the multi-model E_{LUC} estimates is consistent with a combination of the bookkeeping method and fire-based emissions (Le Quéré et al., 2014), with the multi-model mean and bookkeeping method differing by less than 0.5 GtC yr^{-1} over 85 % of the time. Based on this comparison, we assess that an uncertainty of $\pm$0.5 GtC yr^{-1} provides a semi-quantitative measure of uncertainty for annual emissions, and reflects our best value judgment that there is at least 68 % chance ($\pm 1\sigma$) that the true land-use-change emission lies within the given range, for the range of processes considered here. This is consistent with the uncertainty analysis of Houghton et al. (2012), which partly reflects improvements in data on forest area change using data, and partly more complete understanding and representation of processes in models.

The uncertainties in the decadal E_{LUC} estimates are also examined using the DGVM ensemble, although they are likely correlated between decades. The correlations between decades come from (1) common biases in system boundaries (e.g. not counting forest degradation in some models); (2) common definition for the calculation of E_{LUC} from the difference of simulations with and without land-use change (a source of bias vs. the unknown truth); (3) common and uncertain land-cover-change input data which also cause a bias, though if a different input data set is used each decade, decadal fluxes from DGVMs may be partly decorrelated; and (4) model structural errors (e.g. systematic errors in biomass stocks). In addition, errors arising from uncertain DGVM parameter values would be random, but they are not accounted for in this study, since no DGVM provided an ensemble of runs with perturbed parameters.

Prior to 1959, the uncertainty in E_{LUC} is taken as $\pm$33 %, which is the ratio of uncertainty to mean from the 1960s (Table 7), the first decade available. This ratio is consistent with the mean standard deviation of DGMVs' land-use-change emissions over 1870–1958 (0.38 GtC) over the multi-model mean (1.1 GtC).

2.3 Atmospheric CO_2 growth rate (G_{ATM})

Global atmospheric CO_2 growth rate estimates

The atmospheric CO_2 growth rate is provided by the US National Oceanic and Atmospheric Administration Earth System Research Laboratory (NOAA/ESRL; Dlugokencky and Tans, 2015), which is updated from Ballantyne et al. (2012). For the 1959–1980 period, the global growth rate is based on measurements of atmospheric CO_2 concentration averaged from the Mauna Loa and South Pole stations, as observed by the CO_2 Program at Scripps Institution of Oceanography (Keeling et al., 1976). For the 1980–2014 time period, the global growth rate is based on the average of multiple stations selected from the marine boundary layer sites with well-mixed background air (Ballantyne et al., 2012), after fitting each station with a smoothed curve as a func-

Table 7. Comparison of results from the bookkeeping method and budget residuals with results from the DGVMs and inverse estimates for the periods 1960–1969, 1970–1979, 1980–1989, 1990–1999, 2000–2009, the last decade, and the last year available. All values are in GtC yr^{-1}. The DGVM uncertainties represents $\pm 1\sigma$ of the decadal or annual (for 2014 only) estimates from the 10 individual models; for the inverse models all three results are given where available.

	Mean (GtC yr^{-1})						
	1960–1969	1970–1979	1980–1989	1990–1999	2000–2009	2005–2014	2014
Land-use-change emissions (E_{LUC})							
Bookkeeping method	1.5 ± 0.5	1.3 ± 0.5	1.4 ± 0.5	1.6 ± 0.5	1.0 ± 0.5	0.9 ± 0.5	1.1 ± 0.5
DGVMs[a]	1.2 ± 0.4	1.2 ± 0.4	1.3 ± 0.4	1.2 ± 0.4	1.2 ± 0.4	1.4 ± 0.4	1.4 ± 0.5
Residual terrestrial sink (S_{LAND})							
Budget residual	1.7 ± 0.7	1.7 ± 0.8	1.6 ± 0.8	2.6 ± 0.8	2.4 ± 0.8	3.0 ± 0.8	4.1 ± 0.9
DGVMs[a]	1.1 ± 0.6	2.1 ± 0.3	1.7 ± 0.4	2.3 ± 0.3	2.7 ± 0.4	3.0 ± 0.5	3.6 ± 0.9
Total land fluxes ($S_{LAND} - E_{LUC}$)							
Budget ($E_{FF} - G_{ATM} - S_{OCEAN}$)	0.2 ± 0.5	0.4 ± 0.6	0.2 ± 0.6	1.0 ± 0.6	1.5 ± 0.6	2.1 ± 0.7	3.0 ± 0.7
DGVMs[a]	-0.1 ± 0.6	0.9 ± 0.4	0.5 ± 0.5	1.1 ± 0.5	1.5 ± 0.4	1.6 ± 0.4	2.3 ± 0.9
Inversions (CTE2015/Jena CarboScope/MACC)[b]	–/–/–	–/–/–	–/0.3[b]/0.8[b]	–/1.1[b]/1.8[b]	–/1.6[b]/2.4[b]	2.0[b]/2.0[b]/3.3[b]	2.8[b]/2.6[b]/4.2[b]

[a] Note that the decadal uncertainty calculation for the DGVMs is smaller here compared to previous global carbon budgets because it uses $\pm 1\sigma$ of the decadal estimates for the DGVMs, compared to the average of the annual $\pm 1\sigma$ estimates in previous years. It thus represents the true model range for their decadal estimates. This change was introduced to be consistent with the decadal uncertainty calculations in Table 8. [b] Estimates are not corrected for the influence of river fluxes, which would reduce the fluxes by 0.45 GtC yr^{-1} when neglecting the anthropogenic influence on land (Sect. 7.2.2). CTE2015 refers to Peters et al. (2010), Jena CarboScope to Rödenbeck et al. (2014), and MACC to Chevallier et al. (2005); see Table 6.

tion of time, and averaging by latitude band (Masarie and Tans, 1995). The annual growth rate is estimated by Dlugokencky and Tans (2015) from atmospheric CO_2 concentration by taking the average of the most recent December–January months corrected for the average seasonal cycle and subtracting this same average 1 year earlier. The growth rate in units of ppm yr^{-1} is converted to units of GtC yr^{-1} by multiplying by a factor of 2.12 GtC ppm^{-1} (Ballantyne et al., 2012) for consistency with the other components.

The uncertainty around the annual growth rate based on the multiple stations data set ranges between 0.11 and 0.72 GtC yr^{-1}, with a mean of 0.61 GtC yr^{-1} for 1959–1979 and 0.19 GtC yr^{-1} for 1980–2014, when a larger set of stations were available (Dlugokencky and Tans, 2015). It is based on the number of available stations, and thus takes into account both the measurement errors and data gaps at each station. This uncertainty is larger than the uncertainty of ± 0.1 GtC yr^{-1} reported for decadal mean growth rate by the IPCC because errors in annual growth rate are strongly anti-correlated in consecutive years leading to smaller errors for longer timescales. The decadal change is computed from the difference in concentration 10 years apart based on a measurement error of 0.35 ppm. This error is based on offsets between NOAA/ESRL measurements and those of the World Meteorological Organization World Data Centre for Greenhouse Gases (NOAA/ESRL, 2015a) for the start and end points (the decadal change uncertainty is $\sqrt{(2(0.35\,\text{ppm})^2)}(10\,\text{yr})^{-1}$ assuming that each yearly measurement error is independent). This uncertainty is also used in Table 8.

The contribution of anthropogenic CO and CH_4 is neglected from the global carbon budget (see Sect. 2.7.1). We assign a high confidence to the annual estimates of G_{ATM} because they are based on direct measurements from multiple and consistent instruments and stations distributed around the world (Ballantyne et al., 2012).

In order to estimate the total carbon accumulated in the atmosphere since 1750 or 1870, we use an atmospheric CO_2 concentration of 277 ± 3 or 288 ± 3 ppm, respectively, based on a cubic spline fit to ice core data (Joos and Spahni, 2008). The uncertainty of ± 3 ppm (converted to $\pm 1\sigma$) is taken directly from the IPCC's assessment (Ciais et al., 2013). Typical uncertainties in the atmospheric growth rate from ice core data are ± 1–1.5 GtC per decade as evaluated from the Law Dome data (Etheridge et al., 1996) for individual 20-year intervals over the period from 1870 to 1960 (Bruno and Joos, 1997).

2.4 Ocean CO_2 sink

Estimates of the global ocean CO_2 sink are based on a combination of a mean CO_2 sink estimate for the 1990s from observations, and a trend and variability in the ocean CO_2 sink for 1959–2014 from eight global ocean biogeochemistry models. We use two observation-based estimates of S_{OCEAN} available for recent decades to provide a qualitative assessment of confidence in the reported results.

Table 8. Decadal mean in the five components of the anthropogenic CO_2 budget for the periods 1960–1969, 1970–1979, 1980–1989, 1990–1999, 2000–2009, the last decade, and the last year available. All values are in GtC yr^{-1}. All uncertainties are reported as $\pm 1\sigma$. A data set containing data for each year during 1959–2014 is available at http://cdiac.ornl.gov/GCP/carbonbudget/2015/. Please follow the terms of use and cite the original data sources as specified on the data set.

	Mean (GtC yr^{-1})						
	1960–1969	1970–1979	1980–1989	1990–1999	2000–2009	2005–2014	2014
Emissions							
Fossil fuels and industry (E_{FF})	3.1 ± 0.2	4.7 ± 0.2	5.5 ± 0.3	6.4 ± 0.3	7.8 ± 0.4	9.0 ± 0.5	9.8 ± 0.5
Land-use-change emissions (E_{LUC})	1.5 ± 0.5	1.3 ± 0.5	1.4 ± 0.5	1.6 ± 0.5	1.0 ± 0.5	0.9 ± 0.5	1.1 ± 0.5
Partitioning							
Atmospheric growth rate (G_{ATM})	1.7 ± 0.1	2.8 ± 0.1	3.4 ± 0.1	3.1 ± 0.1	4.0 ± 0.1	4.4 ± 0.1	3.9 ± 0.2
Ocean sink (S_{OCEAN})*	1.1 ± 0.5	1.5 ± 0.5	2.0 ± 0.5	2.2 ± 0.5	2.3 ± 0.5	2.6 ± 0.5	2.9 ± 0.5
Residual terrestrial sink (S_{LAND})	1.7 ± 0.7	1.7 ± 0.8	1.6 ± 0.8	2.6 ± 0.8	2.4 ± 0.8	3.0 ± 0.8	4.1 ± 0.9

* The uncertainty in S_{OCEAN} for the 1990s is directly based on observations, while that for other decades combines the uncertainty from observations with the model spread (Sect. 2.4.3).

2.4.1 Observation-based estimates

A mean ocean CO_2 sink of 2.2 ± 0.4 GtC yr^{-1} for the 1990s was estimated by the IPCC (Denman et al., 2007) based on indirect observations and their spread: ocean/land CO_2 sink partitioning from observed atmospheric O_2 / N_2 concentration trends (Manning and Keeling, 2006), an oceanic inversion method constrained by ocean biogeochemistry data (Mikaloff Fletcher et al., 2006), and a method based on penetration timescale for CFCs (McNeil et al., 2003). This is comparable with the sink of 2.0 ± 0.5 GtC yr^{-1} estimated by Khatiwala et al. (2013) for the 1990s, and with the sink of 1.9 to 2.5 GtC yr^{-1} estimated from a range of methods for the period 1990–2009 (Wanninkhof et al., 2013), with uncertainties ranging from ± 0.3 to ± 0.7 GtC yr^{-1}. The most direct way for estimating the observation-based ocean sink is from the product of (sea–air pCO_2 difference) × (gas transfer coefficient). Estimates based on sea–air pCO_2 are fully consistent with indirect observations (Wanninkhof et al., 2013), but their uncertainty is larger mainly due to difficulty in capturing complex turbulent processes in the gas transfer coefficient (Sweeney et al., 2007) and because of uncertainties in the pre-industrial river-induced outgassing of CO_2 (Jacobson et al., 2007).

Both observation-based estimates compute the ocean CO_2 sink and its variability using interpolated measurements of surface ocean fugacity of CO_2 (pCO_2 corrected for the non-ideal behaviour of the gas; Pfeil et al., 2013). The measurements were from the Surface Ocean CO_2 Atlas (SOCAT v3; Bakker et al., 2014, 2015), which contains 14.5 million data to the end of 2014. This was extended with 1.4 million additional measurements over years 2013–2014 (see data attribution Table A1 in Appendix A), submitted to SOCAT but not yet fully quality controlled following standard SOCAT procedures. Revisions and corrections to previously reported measurements were also included where they were available. All new data were subjected to an automated quality control system to detect and remove the most obvious errors (e.g. incorrect reporting of metadata such as position, wrong units, clearly unrealistic data). The combined SOCAT v3 and preliminary new 2013–2014 measurements were mapped using a data-driven diagnostic method (Rödenbeck et al., 2013) and a combined self-organising map and feed-forward neural network (Landschützer et al., 2014). The global observation-based estimates were adjusted to remove a background (not part of the anthropogenic ocean flux) ocean source of CO_2 to the atmosphere of 0.45 GtC yr^{-1} from river input to the ocean (Jacobson et al., 2007) in order to make them comparable to S_{OCEAN}, which only represents the annual uptake of anthropogenic CO_2 by the ocean. Several other data-based products are available, but they partly show large discrepancies with observed variability that need to be resolved. Here we used the two data products that had the best fit to observations, distinctly better than most in their representation of tropical and global variability (Rödenbeck et al., 2015).

We use the data-based product of Khatiwala et al. (2009) updated by Khatiwala et al. (2013) to estimate the anthropogenic carbon accumulated in the ocean during 1765–1958 (60.2 GtC) and 1870–1958 (47.5 GtC), and assume an oceanic uptake of 0.4 GtC for 1750–1765 (for which time no data are available) based on the mean uptake during 1765–1770. The estimate of Khatiwala et al. (2009) is based on regional disequilibrium between surface pCO_2 and atmospheric CO_2, and a Green's function utilising transient ocean tracers like CFCs and ^{14}C to ascribe changes through time.

It does not include changes associated with changes in ocean circulation, temperature, and climate, but these are thought to be small over the time period considered here (Ciais et al., 2013). The uncertainty in cumulative uptake of ± 20 GtC (converted to $\pm 1\sigma$) is taken directly from the IPCC's review of the literature (Rhein et al., 2013), or about ± 30 % for the annual values (Khatiwala et al., 2009).

2.4.2 Global ocean biogeochemistry models

The trend in the ocean CO_2 sink for 1959–2014 is computed using a combination of eight global ocean biogeochemistry models (Table 6). The models represent the physical, chemical, and biological processes that influence the surface ocean concentration of CO_2 and thus the air–sea CO_2 flux. The models are forced by meteorological reanalysis and atmospheric CO_2 concentration data available for the entire time period. Models do not include the effects of anthropogenic changes in nutrient supply. They compute the air–sea flux of CO_2 over grid boxes of 1 to 4° in latitude and longitude. The ocean CO_2 sink for each model is normalised to the observations by dividing the annual model values by their average over 1990–1999 and multiplying this with the observation-based estimate of 2.2 GtC yr^{-1} (obtained from Manning and Keeling, 2006; McNeil et al., 2003; Mikaloff Fletcher et al., 2006). The ocean CO_2 sink for each year (t) in GtC yr^{-1} is therefore

$$S_{\mathrm{OCEAN}}(t) = \frac{1}{n}\sum_{m=1}^{m=n} \frac{S^m_{\mathrm{OCEAN}}(t)}{S^m_{\mathrm{OCEAN}}(1990\text{–}1999)} \times 2.2\,\mathrm{GtC\,yr^{-1}}, \quad (7)$$

where n is the number of models. This normalisation ensures that the ocean CO_2 sink for the global carbon budget is based on observations, whereas the trends and annual values in CO_2 sinks are from model estimates. The normalisation based on a ratio assumes that if models over- or underestimate the sink in the 1990s, it is primarily due to the process of diffusion, which depends on the gradient of CO_2. Thus a ratio is more appropriate than an offset as it takes into account the time dependence of CO_2 gradients in the ocean. The mean uncorrected ocean CO_2 sink from the eight models for 1990–1999 ranges between 1.6 and 2.4 GtC yr^{-1}, with a multi-model mean of 1.9 GtC yr^{-1}.

2.4.3 Uncertainty assessment for S_{OCEAN}

The uncertainty around the mean ocean sink of anthropogenic CO_2 was quantified by Denman et al. (2007) for the 1990s (see Sect. 2.4.1). To quantify the uncertainty around annual values, we examine the standard deviation of the normalised model ensemble. We use further information from the two data-based products to assess the confidence level. The average standard deviation of the normalised ocean model ensemble is 0.13 GtC yr^{-1} during 1980–2010 (with a maximum of 0.27), but it increases as the model ensemble goes back in time, with a standard deviation of 0.22 GtC yr^{-1} across models in the 1960s. We estimate that the uncertainty in the annual ocean CO_2 sink is about ± 0.5 GtC yr^{-1} from the fractional uncertainty of the data uncertainty of ± 0.4 GtC yr^{-1} and standard deviation across models of up to ± 0.27 GtC yr^{-1}, reflecting both the uncertainty in the mean sink from observations during the 1990s (Denman et al., 2007; Sect. 2.4.1) and in the interannual variability as assessed by models.

We examine the consistency between the variability in the model-based and the data-based products to assess confidence in S_{OCEAN}. The interannual variability in the ocean fluxes (quantified as the standard deviation) of the two data-based estimates for 1986–2014 (where they overlap) is ± 0.38 GtC yr^{-1} (Rödenbeck et al., 2014) and ± 0.40 GtC yr^{-1} (Landschützer et al., 2015), compared to ± 0.27 GtC yr^{-1} for the normalised model ensemble. The standard deviation includes a component of trend and decadal variability in addition to interannual variability, and their relative influence differs across estimates. The phase is generally consistent between estimates, with a higher ocean CO_2 sink during El Niño events. The annual data-based estimates correlate with the ocean CO_2 sink estimated here with a correlation of $r = 0.51$ (0.34 to 0.58 for individual models), and $r = 0.71$ (0.54 to 0.72) for the data-based estimates of Rödenbeck et al. (2014) and Landschützer et al. (2015), respectively (simple linear regression), but their mutual correlation is only 0.55. The use of annual data for the correlation may reduce the strength of the relationship because the dominant source of variability associated with El Niño events is less than 1 year. We assess a medium confidence level to the annual ocean CO_2 sink and its uncertainty because they are based on multiple lines of evidence, and the results are consistent in that the interannual variability in the model and data-based estimates are all generally small compared to the variability in atmospheric CO_2 growth rate. Nevertheless the various results do not show agreement in interannual variability on the global scale or for the relative roles of the annual and decadal variability compared to the trend.

2.5 Terrestrial CO_2 sink

The difference between, on the one hand, fossil fuel (E_{FF}) and land-use-change emissions (E_{LUC}) and, on the other hand, the growth rate in atmospheric CO_2 concentration (G_{ATM}) and the ocean CO_2 sink (S_{OCEAN}) is attributable to the net sink of CO_2 in terrestrial vegetation and soils (S_{LAND}), within the given uncertainties (Eq. 1). Thus, this sink can be estimated as the residual of the other terms in the mass balance budget, as well as directly calculated using DGVMs. The residual land sink (S_{LAND}) is thought to be in part because of the fertilising effect of rising atmospheric CO_2 on plant growth, N deposition, and effects of climate change such as the lengthening of the growing season in

northern temperate and boreal areas. S_{LAND} does not include gross land sinks directly resulting from land-use change (e.g. regrowth of vegetation) as these are estimated as part of the net land-use flux (E_{LUC}). System boundaries make it difficult to attribute exactly CO_2 fluxes on land between S_{LAND} and E_{LUC} (Erb et al., 2013), and by design most of the uncertainties in our method are allocated to S_{LAND} for those processes that are poorly known or represented in models.

2.5.1 Residual of the budget

For 1959–2014, the terrestrial carbon sink was estimated from the residual of the other budget terms by rearranging Eq. (1):

$$S_{LAND} = E_{FF} + E_{LUC} - (G_{ATM} + S_{OCEAN}). \quad (8)$$

The uncertainty in S_{LAND} is estimated annually from the root sum of squares of the uncertainty in the right-hand terms assuming the errors are not correlated. The uncertainty averages to $\pm 0.8\,GtC\,yr^{-1}$ over 1959–2014 (Table 7). S_{LAND} estimated from the residual of the budget includes, by definition, all the missing processes and potential biases in the other components of Eq. (8).

2.5.2 DGVMs

A comparison of the residual calculation of S_{LAND} in Eq. (8) with estimates from DGVMs as used to estimate E_{LUC} in Sect. 2.2.3, but here excluding the effects of changes in land cover (using a constant pre-industrial land-cover distribution), provides an independent estimate of the consistency of S_{LAND} with our understanding of the functioning of the terrestrial vegetation in response to CO_2 and climate variability (Table 7). As described in Sect. 2.2.3, the DGVM runs that exclude the effects of changes in land cover include all climate variability and CO_2 effects over land, but they do not include reductions in CO_2 sink capacity associated with human activity directly affecting changes in vegetation cover and management, which by design is allocated to E_{LUC}. This effect has been estimated to have led to a reduction in the terrestrial sink by $0.5\,GtC\,yr^{-1}$ since 1750 (Gitz and Ciais, 2003). The models in this configuration estimate the mean and variability in S_{LAND} based on atmospheric CO_2 and climate, and thus both terms can be compared to the budget residual. We apply three criteria for minimum model realism by including only those models with (1) steady state after spin-up, (2) net land fluxes ($S_{LAND} - E_{LUC}$) that are a carbon sink over the 1990s as constrained by global atmospheric and oceanic observations (McNeil et al., 2003; Manning and Keeling, 2006; Mikaloff Fletcher et al., 2006), and (3) global E_{LUC} that is a carbon source over the 1990s. Ten models met these three criteria.

The annual standard deviation of the CO_2 sink across the 10 DGVMs averages to $\pm 0.7\,GtC\,yr^{-1}$ for the period 1959 to 2014. The model mean, over different decades, correlates with the budget residual with $r = 0.71$ (0.52 to $r = 0.71$ for individual models). The standard deviation is similar to that of the five model ensembles presented in Le Quéré et al. (2009), but the correlation is improved compared to $r = 0.54$ obtained in the earlier study. The DGVM results suggest that the sum of our knowledge on annual CO_2 emissions and their partitioning is plausible (see Discussion), and provide insight into the underlying processes and regional breakdown. However as the standard deviation across the DGVMs (e.g. $\pm 0.9\,GtC\,yr^{-1}$ for year 2014) is of the same magnitude as the combined uncertainty due to the other components (E_{FF}, E_{LUC}, G_{ATM}, S_{OCEAN}; Table 7), the DGVMs do not provide further reduction of uncertainty on the annual terrestrial CO_2 sink compared to the residual of the budget (Eq. 8). Yet, DGVM results are largely independent of the residual of the budget, and it is worth noting that the residual method and ensemble mean DGVM results are consistent within their respective uncertainties. We attach a medium confidence level to the annual land CO_2 sink and its uncertainty because the estimates from the residual budget and averaged DGVMs match well within their respective uncertainties, and the estimates based on the residual budget are primarily dependent on E_{FF} and G_{ATM}, both of which are well constrained.

2.6 The atmospheric perspective

The worldwide network of atmospheric measurements can be used with atmospheric inversion methods to constrain the location of the combined total surface CO_2 fluxes from all sources, including fossil and land-use-change emissions and land and ocean CO_2 fluxes. The inversions assume E_{FF} to be well known, and they solve for the spatial and temporal distribution of land and ocean fluxes from the residual gradients of CO_2 between stations that are not explained by emissions. Inversions used atmospheric CO_2 data to the end of 2014 (including preliminary values in some cases), as well as three atmospheric CO_2 inversions (Table 6) to infer the total CO_2 flux over land regions and the distribution of the total land and ocean CO_2 fluxes for the mid–high-latitude Northern Hemisphere (30–90° N), tropics (30° S–30° N) and mid–high-latitude region of the Southern Hemisphere (30–90° S). We focus here on the largest and most consistent sources of information and use these estimates to comment on the consistency across various data streams and process-based estimates.

Atmospheric inversions

The three inversion systems used in this release are the CarbonTracker (Peters et al., 2010), the Jena CarboScope (Rödenbeck, 2005), and MACC (Chevallier et al., 2005). They are based on the same Bayesian inversion principles that interpret the same, for the most part, observed time series (or

subsets thereof) but use different methodologies that represent some of the many approaches used in the field. This mainly concerns the time resolution of the estimates (i.e. weekly or monthly), spatial breakdown (i.e. grid size), assumed correlation structures, and mathematical approach. The details of these approaches are documented extensively in the references provided. Each system uses a different transport model, which was demonstrated to be a driving factor behind differences in atmospheric-based flux estimates, and specifically their global distribution (Stephens et al., 2007).

The three inversions use atmospheric CO_2 observations from various flask and in situ networks. They prescribe spatial and global E_{FF} that can vary from that presented here. The CarbonTracker and MACC inversions prescribed the same global E_{FF} as in Sect. 2.1.1, during 2010–2014 for CarbonTracker and during 1979–2014 in MACC. The Jena-s81_v3.7 inversion uses E_{FF} from EDGAR4.2. Different spatial and temporal distributions of E_{FF} were prescribed in each inversion.

Given their prescribed map of E_{FF}, each inversion estimates natural fluxes from a similar set of surface CO_2 measurement stations, and CarbonTracker additionally uses two sites of aircraft CO_2 vertical profiles over the Amazon and Siberia, regions where surface observations are sparse. The atmospheric transport models of each inversion are TM5 for CarbonTracker, TM3 for Jena-s81_v3.7, and LMDZ for MACC. These three models are based on the same ECMWF wind fields. The three inversions use different prior natural fluxes, which partly influences their optimised fluxes. MACC assumes that the prior land flux is zero on the annual mean in each grid cell of the transport model, so that any sink or source on land is entirely reflecting the information brought by atmospheric measurements. CarbonTracker simulates a small prior sink on land from the SIBCASA model that results from regrowth following fire disturbances of an otherwise net zero biosphere. Jena s81_v3.7 assumes a prior on the long-term mean land sink pattern, using the time-averaged net ecosystem exchange of the LPJ model. Inversion results for the sum of natural ocean and land fluxes (Fig. 8) are better constrained in the Northern Hemisphere (NH) than in the tropics, because of the higher measurement stations density in the NH.

Finally, results from atmospheric inversions include the natural CO_2 fluxes from rivers (which need to be taken into account to allow comparison to other sources) and chemical oxidation of reactive carbon-containing gases (which are neglected here). These inverse estimates are not truly independent of the other estimates presented here as the atmospheric observations include a set of observations used to estimate the global atmospheric growth rate (Sect. 2.3). However they provide new information on the regional distribution of fluxes.

We focus the analysis on two known strengths of the inverse approach: the derivation of the year-to-year changes in total land fluxes ($S_{LAND} - E_{LUC}$) consistent with the whole network of atmospheric observations, and the spatial breakdown of combined land and ocean fluxes ($S_{OCEAN} + S_{LAND} - E_{LUC}$) across large regions of the globe. The total land flux correlates well with that estimated from the budget residual (Eq. 1) with correlations for the annual time series ranging from $r = 0.89$ to 0.93, and with the DGVM multi-model mean with correlations for the annual time series ranging from $r = 0.71$ to 0.80 ($r = 0.49$ to 0.81 for individual DGVMs and inversions). The spatial breakdown is discussed in Sect. 3.1.3.

2.7 Processes not included in the global carbon budget

2.7.1 Contribution of anthropogenic CO and CH_4 to the global carbon budget

Anthropogenic emissions of CO and CH_4 to the atmosphere are eventually oxidised to CO_2 and thus are part of the global carbon budget. These contributions are omitted in Eq. (1), but an attempt is made in this section to estimate their magnitude and identify the sources of uncertainty. Anthropogenic CO emissions are from incomplete fossil fuel and biofuel burning and deforestation fires. The main anthropogenic emissions of fossil CH_4 that matter for the global carbon budget are the fugitive emissions of coal, oil, and gas upstream sectors (see below). These emissions of CO and CH_4 contribute a net addition of fossil carbon to the atmosphere.

In our estimate of E_{FF} we assumed (Sect. 2.1.1) that all the fuel burned is emitted as CO_2; thus CO anthropogenic emissions and their atmospheric oxidation into CO_2 within a few months are already counted implicitly in E_{FF} and should not be counted twice (same for E_{LUC} and anthropogenic CO emissions by deforestation fires). Anthropogenic emissions of fossil CH_4 are not included in E_{FF}, because these fugitive emissions are not included in the fuel inventories. Yet they contribute to the annual CO_2 growth rate after CH_4 gets oxidised into CO_2. Anthropogenic emissions of fossil CH_4 represent 15 % of total CH_4 emissions (Kirschke et al., 2013) that is 0.061 GtC yr^{-1} for the past decade. Assuming steady state, these emissions are all converted to CO_2 by OH oxidation and thus explain 0.06 GtC yr^{-1} of the global CO_2 growth rate in the past decade.

Other anthropogenic changes in the sources of CO and CH_4 from wildfires, biomass, wetlands, ruminants, or permafrost changes are similarly assumed to have a small effect on the CO_2 growth rate.

2.7.2 Anthropogenic carbon fluxes in the land to ocean aquatic continuum

The approach used to determine the global carbon budget considers only anthropogenic CO_2 emissions and their partitioning among the atmosphere, ocean, and land. In this analysis, the land and ocean reservoirs that take up anthropogenic

CO_2 from the atmosphere are conceived as independent carbon storage repositories. This approach thus omits that carbon is continuously displaced along the land–ocean aquatic continuum (LOAC) comprising freshwaters, estuaries, and coastal areas (Bauer et al., 2013; Regnier et al., 2013). A significant fraction of this lateral carbon flux is entirely "natural" and is thus a steady-state component of the pre-industrial carbon cycle. The remaining fraction is anthropogenic carbon entrained into the lateral transport loop of the LOAC, a perturbation that is relevant for the global carbon budget presented here.

The results of the analysis of Regnier et al. (2013) can be summarised in three points of relevance to the anthropogenic CO_2 budget. First, the anthropogenic carbon input from land to hydrosphere, F_{LH}, estimated at $1 \pm 0.5\,GtC\,yr^{-1}$ is significant compared to the other terms of Eq. (1) (Table 8), and implies that only a portion of the anthropogenic CO_2 taken up by land ecosystems remains sequestered in soil and biomass pools. Second, some of the exported anthropogenic carbon is stored in the LOAC (ΔC_{LOAC}, $0.55 \pm 0.3\,GtC\,yr^{-1}$) and some is released back to the atmosphere as CO_2 (E_{LOAC}, $0.35 \pm 0.2\,GtC\,yr^{-1}$), the magnitude of these fluxes resulting from the combined effects of freshwaters, estuaries, and coastal seas. Third, a small fraction of anthropogenic carbon displaced by the LOAC is transferred to the open ocean, where it accumulates (F_{HO}, $0.1 \pm > 0.05\,GtC\,yr^{-1}$). The anthropogenic perturbation of the carbon fluxes from land to ocean does not contradict the method used in Sect. 2.5 to define the ocean sink and residual terrestrial sink. However, it does point to the need to account for the fate of anthropogenic carbon once it is removed from the atmosphere by land ecosystems (summarised in Fig. 2). In theory, direct estimates of changes of the ocean inorganic carbon inventory over time would see the land flux of anthropogenic carbon and would thus have a bias relative to air–sea flux estimates and tracer-based reconstructions. However, currently the value is small enough to be not noticeable relative to the errors in the individual techniques.

The residual terrestrial sink in a budget that accounts for the LOAC will be larger than S_{LAND}, as the flux is partially offset by the net source of CO_2 to the atmosphere, i.e. E_{LOAC}, of $0.35 \pm 0.3\,GtC\,yr^{-1}$ from rivers, estuaries, and coastal seas:

$$S_{LAND+LOAC} = E_{FF} + E_{LUC} - (G_{ATM} + S_{OCEAN}) + E_{LOAC}. \quad (9)$$

The residual terrestrial sink (S_{LAND}) is $3.0 \pm 0.8\,GtC\,yr^{-1}$ for 2005–2014 as calculated according to Eq. (8; Table 7), while $S_{LAND+LOAC}$ is $3.3 \pm 0.9\,GtC\,yr^{-1}$ over the same time period. A fraction of anthropogenic CO_2 taken up by land ecosystems is exported to the LOAC (F_{LH}). With the LOAC included, we now have

$$\Delta C_{TE} = S_{LAND+LOAC} - E_{LUC} - F_{LH}, \quad (10)$$

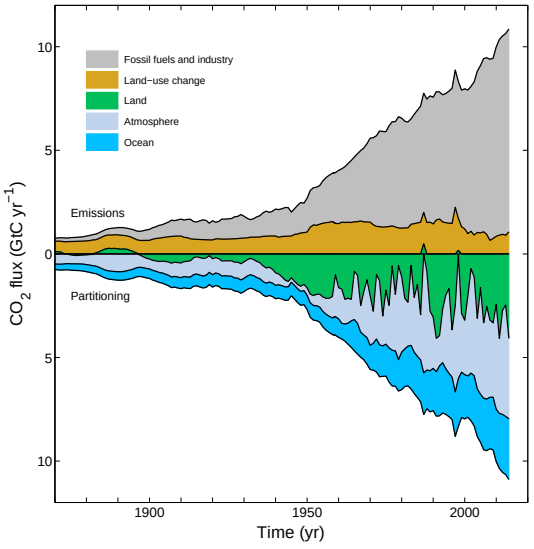

Figure 3. Combined components of the global carbon budget illustrated in Fig. 2 as a function of time, for emissions from fossil fuels and industry (E_{FF}; grey) and emissions from land-use change (E_{LUC}; brown), as well as their partitioning among the atmosphere (G_{ATM}; light blue), land (S_{LAND}; green), and oceans (S_{OCEAN}; dark blue). All time series are in $GtC\,yr^{-1}$. G_{ATM} and S_{OCEAN} (and by construction also S_{LAND}) prior to 1959 are based on different methods. The primary data sources for fossil fuels and industry are from Boden et al. (2013), with uncertainty of about ±5 % (±1σ); land-use-change emissions are from Houghton et al. (2012) with uncertainties of about ±30 %; atmospheric growth rate prior to 1959 is from Joos and Spahni (2008) with uncertainties of about ±1–1.5 $GtC\,decade^{-1}$ or ±0.1–0.15 $GtC\,yr^{-1}$ (Bruno and Joos, 1997), and from Dlugokencky and Tans (2015) from 1959 with uncertainties of about $\pm 0.2\,GtC\,yr^{-1}$; the ocean sink prior to 1959 is from Khatiwala et al. (2013) with uncertainty of about ±30 %, and from this study from 1959 with uncertainties of about $\pm 0.5\,GtC\,yr^{-1}$; and the residual land sink is obtained by difference (Eq. 8), resulting in uncertainties of about ±50 % prior to 1959 and $\pm 0.8\,GtC\,yr^{-1}$ after that. See the text for more details of each component and their uncertainties.

where ΔC_{TE} is the change in annual terrestrial ecosystems carbon storage, including land vegetation, litter, and soil. ΔC_{TE} is $1.4\,GtC\,yr^{-1}$ for the period 2005–2014. It is notably smaller than what would be calculated in a traditional budget that ignores the LOAC. In this case, the change in carbon storage is estimated as $2.1\,Gt\,C\,yr^{-1}$ from the difference between S_{LAND} ($3.0\,Gt\,C\,yr^{-1}$) and E_{LUC} ($0.9\,Gt\,C\,yr^{-1}$; Table 8). All estimates of LOAC are given with low confidence, because they originate from a single source. The carbon budget presented here implicitly incorporates the fluxes from the LOAC into S_{LAND}. We do not attempt to separate these fluxes because the uncertainties in either estimate are too large, and there is insufficient information available to estimate the LOAC fluxes on an annual basis.

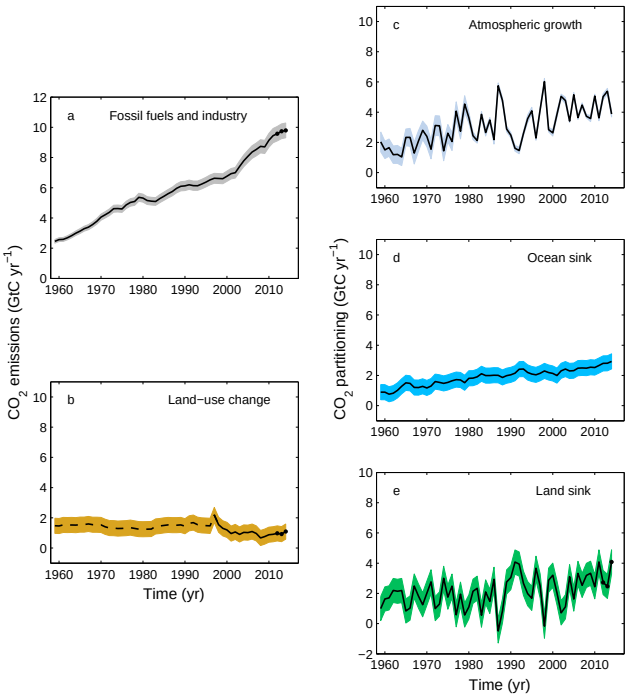

Figure 4. Components of the global carbon budget and their uncertainties as a function of time, presented individually for **(a)** emissions from fossil fuels and industry (E_{FF}), **(b)** emissions from land-use change (E_{LUC}), **(c)** atmospheric CO_2 growth rate (G_{ATM}), **(d)** the ocean CO_2 sink (S_{OCEAN}; positive indicates a flux from the atmosphere to the ocean), and **(e)** the land CO_2 sink (S_{LAND}; positive indicates a flux from the atmosphere to the land). All time series are in GtC yr^{-1} with the uncertainty bounds representing $\pm 1\sigma$ in shaded colour. Data sources are as in Fig. 3. The black dots in panels **(a)**, **(b)**, and **(e)** show preliminary values for 2012, 2013, and 2014 that originate from a different data set to the remainder of the data, as explained in the text.

3 Results

3.1 Global carbon budget averaged over decades and its variability

The global carbon budget averaged over the last decade (2005–2014) is shown in Fig. 2. For this time period, 91 % of the total emissions ($E_{FF} + E_{LUC}$) were caused by fossil fuels and industry, and 9 % by land-use change. The total emissions were partitioned among the atmosphere (44 %), ocean (26 %), and land (30 %). All components except land-use-change emissions have grown since 1959 (Figs. 3 and 4), with important interannual variability in the atmospheric growth rate and in the land CO_2 sink (Fig. 4), as well as some decadal variability in all terms (Table 8).

3.1.1 CO_2 emissions

Global CO_2 emissions from fossil fuels and industry have increased every decade from an average of 3.1 ± 0.2 GtC yr^{-1} in the 1960s to an average of 9.0 ± 0.5 GtC yr^{-1} during 2005–2014 (Table 8 and Fig. 5). The growth rate in these emissions decreased between the 1960s and the 1990s, from 4.5 % yr^{-1} in the 1960s (1960–1969), 2.9 % yr^{-1} in the 1970s (1970–1979), 1.9 % yr^{-1} in the 1980s (1980–1989), and finally to 1.0 % yr^{-1} in the 1990s (1990–1999), before it began increasing again in the 2000s at an average growth rate of 3.2 % yr^{-1}, decreasing to 2.2 % yr^{-1} for the last decade (2005–2014). In contrast, CO_2 emissions from land-use change have remained constant, in our analysis at around 1.5 ± 0.5 GtC yr^{-1} between 1960 and 1999 and 1.0 ± 0.5 GtC yr^{-1} during 2000–2014. The decrease in emissions from land-use change between the 1990s and 2000s is highly uncertain. It is not found in the current ensemble of the DGVMs (Fig. 6), which are otherwise consistent with the bookkeeping method within their respective uncertainty (Table 7). It is also not found in the study of tropical deforestation of Achard et al. (2014), where the fluxes in the 1990s were similar to those of the 2000s and outside our uncertainty range. A new study based on FAO data to 2015 (Federici et al., 2015) suggests that E_{LUC} decreased during 2011–2015 compared to 2001–2010.

3.1.2 Partitioning

The growth rate in atmospheric CO_2 increased from 1.7 ± 0.1 GtC yr^{-1} in the 1960s to 4.4 ± 0.1 GtC yr^{-1} during 2005–2014 with important decadal variations (Table 8). Both ocean and land CO_2 sinks increased roughly in line with the atmospheric increase, but with significant decadal variability on land (Table 8). The ocean CO_2 sink increased from 1.1 ± 0.5 GtC yr^{-1} in the 1960s to 2.6 ± 0.5 GtC yr^{-1} during 2005–2014, with interannual variations of the order of a few tenths of GtC yr^{-1} generally showing an increased ocean sink during El Niño (i.e. 1982–1983, 1991–1993, 1997–1998) events (Fig. 7; Rödenbeck et al., 2014). Although there is some coherence between the ocean models and data products and among data products, their mutual correlation is weak and highlights disagreement on the exact amplitude of the interannual variability, as well as on the relative importance of the trend versus the variability (Sect. 2.4.3 and Fig. 7). As shown in Fig. 7, the two data products and most model estimates produce a mean CO_2 sink for the 1990s that is below the mean assessed by the IPCC from indirect (but arguably more reliable) observations (Denman et al., 2007; Sect. 2.4.1). This discrepancy suggests we may need to reassess estimates of the mean ocean carbon sinks.

The land CO_2 sink increased from 1.7 ± 0.7 GtC yr^{-1} in the 1960s to 3.0 ± 0.8 GtC yr^{-1} during 2005–2014, with important interannual variations of up to 2 GtC yr^{-1} generally showing a decreased land sink during El Niño events, overcompensating for the increase in ocean sink and accounting for the enhanced atmospheric growth rate during El Niño events. The high uptake anomaly around year 1991 is thought to be caused by the effect of the volcanic eruption of Mount

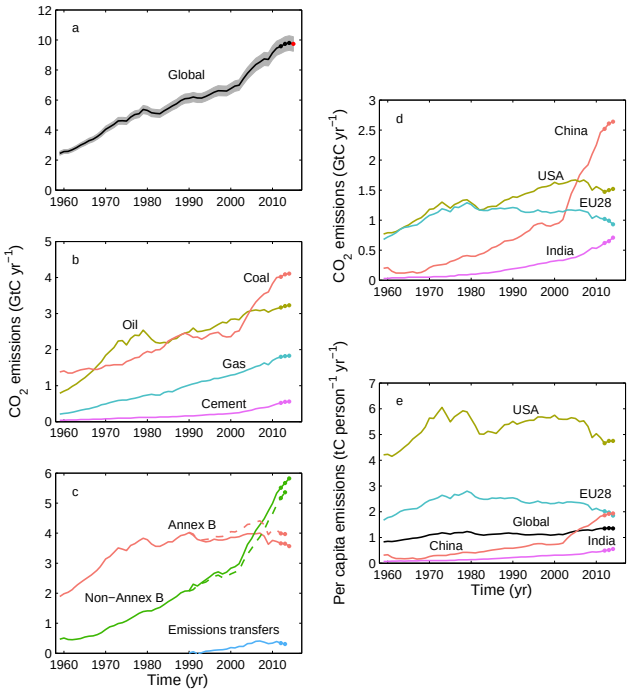

Figure 5. CO_2 emissions from fossil fuels and industry for **(a)** the globe, including an uncertainty of ±5 % (grey shading), the emissions extrapolated using BP energy statistics (black dots), and the emissions projection for year 2015 based on GDP projection (red dot); **(b)** global emissions by fuel type, including coal (salmon), oil (olive), gas (turquoise), and cement (purple), and excluding gas flaring, which is small (0.6 % in 2013); **(c)** territorial (full line) and consumption (dashed line) emissions for the countries listed in the Annex B of the Kyoto Protocol (salmon lines; mostly advanced economies with emissions limitations) versus non-Annex B countries (green lines) – also shown are the emissions transfers from non-Annex B to Annex B countries (light-blue line); **(d)** territorial CO_2 emissions for the top three country emitters (USA – olive; China – salmon; India – purple) and for the European Union (EU28, the 28 member states of the EU in 2012 – turquoise), and **(e)** per-capita emissions for the top three country emitters and the EU (all colours as in panel **d**) and the world (black). In panels **(b)** to **(e)**, the dots show the preliminary data that were extrapolated from BP energy statistics for 2012, 2013, and 2014. All time series are in GtC yr^{-1} except the per-capita emissions (panel **e**), which are in tonnes of carbon per person per year (tC $person^{-1}$ yr^{-1}). All territorial emissions are primarily from Boden et al. (2013) except national data for the USA and EU28 for 1990–2012, which are reported by the countries to the UNFCCC as detailed in the text; consumption-based emissions are updated from Peters et al. (2011a).

Pinatubo on climate and is not generally reproduced by the DGVMs, but it is assigned to the land by the two inverse systems that include this period (Fig. 6). The larger land CO_2 sink during 2005–2014 compared to the 1960s is reproduced by all the DGVMs in response to combined atmospheric CO_2 increase, climate, and variability (3.0 ± 0.5 GtC yr^{-1} for the period 2005–2014 and average change of 1.9 GtC yr^{-1} relative to the 1960s), consistent with the budget residual and reflecting a common knowledge of the processes (Table 7). The DGVM ensemble mean of 3.0 ± 0.5 GtC yr^{-1} also reproduces the observed mean for the period 2005–2014 calculated from the budget residual (Table 7).

The total CO_2 fluxes on land ($S_{LAND} - E_{LUC}$) constrained by the atmospheric inversions show in general very good agreement with the global budget estimate, as expected given the strong constraints of G_{ATM} and the small relative uncertainty typically assumed on S_{OCEAN} and E_{FF} by inversions. The total land flux is of similar magnitude for the decadal average, with estimates for 2005–2014 from the three inversions of 2.0, 2.0, and 3.3 GtC yr^{-1} compared to 2.1 ± 0.7 GtC yr^{-1} for the total flux computed with the carbon budget from other terms in Eq. (1) (Table 7). The three inversions' total land sink would be 1.6, 1.6, and 2.9 GtC yr^{-1} when including a mean river flux adjustment of 0.45 GtC yr^{-1}, though the exact adjustment would be smaller when taking into account the anthropogenic contribution to river fluxes (Sect. 2.7.2). The interannual variability in the inversions also matched the residual-based S_{LAND} closely (Fig. 6). The total land flux from the DGVM multi-model mean also compares well with the estimate from the carbon budget and atmospheric inversions, with a decadal mean of 1.6 ± 0.4 GtC yr^{-1} (Table 7; 2005–2014), although individual models differ by several GtC for some years (Fig. 6).

3.1.3 Distribution

Figure 8 shows the partitioning of the total surface fluxes excluding emissions from fossil fuels and industry ($S_{OCEAN} + S_{LAND} - E_{LUC}$) according to the process models in the ocean and on land, and to the three atmospheric inversions. The total surface fluxes provide information on the regional distribution of those fluxes by latitude band (Fig. 8). The global mean CO_2 fluxes from process models for 2005–2014 is 4.2 ± 0.5 GtC yr^{-1}. This is comparable to the fluxes of 4.7 ± 0.5 GtC yr^{-1} inferred from the remainder of the carbon budget ($E_{FF} - G_{ATM}$ in Eq. 1; Table 8) within their respective uncertainties. The total CO_2 fluxes from the three inversions range between 4.4 and 4.9 GtC yr^{-1}, consistent with the carbon budget as expected from the constraints on the inversions.

In the south (south of 30° S), the atmospheric inversions and process models all suggest a CO_2 sink for 2005–2014 of between 1.2 and 1.5 GtC yr^{-1} (Fig. 8), although the details of the interannual variability are not fully consistent across methods. The interannual variability in the south is low because of the dominance of ocean area with low variability compared to land areas.

In the tropics (30° S–30° N), both the atmospheric inversions and process models suggest the carbon balance in this region is close to neutral over the past decade, with fluxes for 2005–2014 ranging between −0.6 and +0.6 GtC yr^{-1}. The three inversions consistently allocate more year-to-year vari-

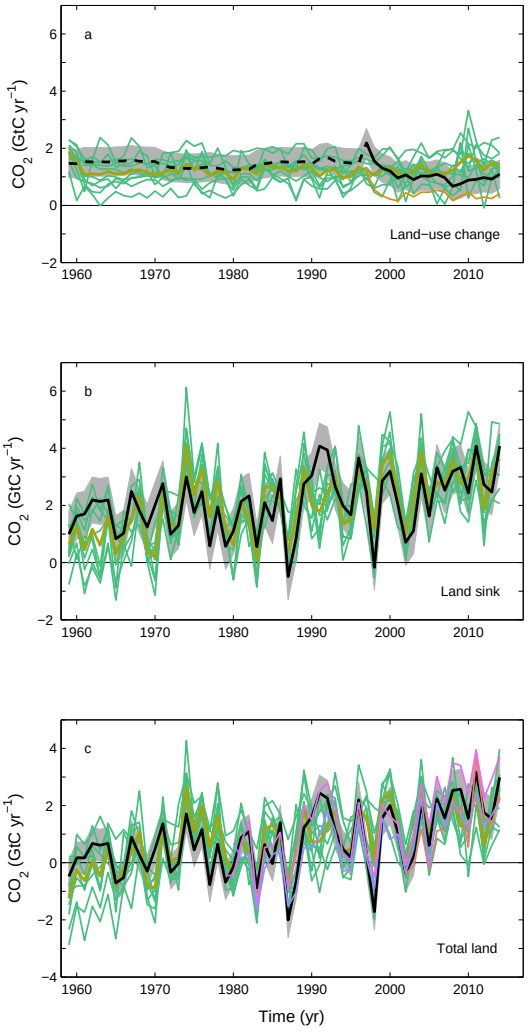

Figure 6. **(a)** Comparison of the atmosphere–land CO_2 flux showing budget values of E_{LUC} (black). CO_2 emissions from land-use change showing individual DGVM results (green) and the multi-model mean (olive), as well as fire-based results (orange); land-use-change data prior to 1997 (dashed black) highlight the start of satellite data from that year. **(b)** Land CO_2 sink (S_{LAND}; black) showing individual DGVM results (green) and multi-model mean (olive). **(c)** Total land CO_2 fluxes **(b–a)** from DGVM results (green) and the multi-model mean (olive); atmospheric inversions of Chevallier et al. (2005; MACC, v14.2) (purple), Rödenbeck et al. (2003; Jena CarboScope, s81_v3.7) (violet), and Peters et al. (2010; Carbon Tracker, vCTE2015) (salmon) (see Table 6); and the carbon balance from Eq. (1) (black). In **(c)** the inversions were adjusted for the pre-industrial land sink of CO_2 from river input, by adding a sink of 0.45 GtC yr^{-1} (Jacobson et al., 2007). This adjustment does not take into account the anthropogenic contribution to river fluxes (see Sect. 2.7.2).

ability in CO_2 fluxes to the tropics compared to the north (north of 30° N; Fig. 8). This variability is dominated by land fluxes. Inversions are consistent with each other and with the mean of process models.

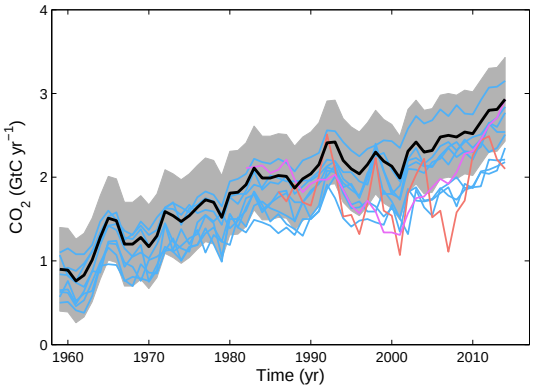

Figure 7. Comparison of the anthropogenic atmosphere–ocean CO_2 flux shows the budget values of S_{OCEAN} (black), individual ocean models before normalisation (blue), and the two ocean-data-based products (Rödenbeck et al., 2014, in salmon and Landschützer et al., 2015, in purple; see Table 6). Both data-based products were adjusted for the pre-industrial ocean source of CO_2 from river input to the ocean, which is not present in the models, by adding a sink of 0.45 GtC yr^{-1} (Jacobson et al., 2007) so as to make them comparable to S_{OCEAN}. This adjustment does not take into account the anthropogenic contribution to river fluxes (see Sect. 2.7.2).

In the north (north of 30° N), the inversions and process models are not in full agreement on the magnitude of the CO_2 sink, with the ensemble mean of the process models suggesting a total Northern Hemisphere sink for 2005–2014 of 2.3 ± 0.4 GtC yr^{-1}, while the three inversions estimate a sink of 2.5, 3.4, and 3.6 GtC yr^{-1}. The mean difference can only partly be explained by the influence of river fluxes, as this flux in the Northern Hemisphere would be less than 0.45 GtC yr^{-1}, particularly when the anthropogenic contribution to river fluxes are accounted for. The CarbonTracker inversion is within 1 standard deviation of the process models for the mean sink during their overlap period. MACC and Jena-s81_v3.7 give a higher sink in the north than the process models, and a correspondingly higher source in the tropics. Differences between CarbonTracker and MACC, Jena-s81_v3.7 may be related to differences in inter-hemispheric mixing time of their transport models, and other inversion settings. Differences also result from different fossil fuel emissions assumed in the inversions, as the inversions primarily constrain the sum of fossil fuel and land fluxes. Differences between the mean fluxes of MACC, Jena-s81_v3.7 and the ensemble of process models cannot be simply explained. They could reflect either a bias in these two inversions or missing processes or biases in the process models, such as the lack of adequate parameterisations for forest management in the north and for forest degradation emissions in tropics for the DGVMs.

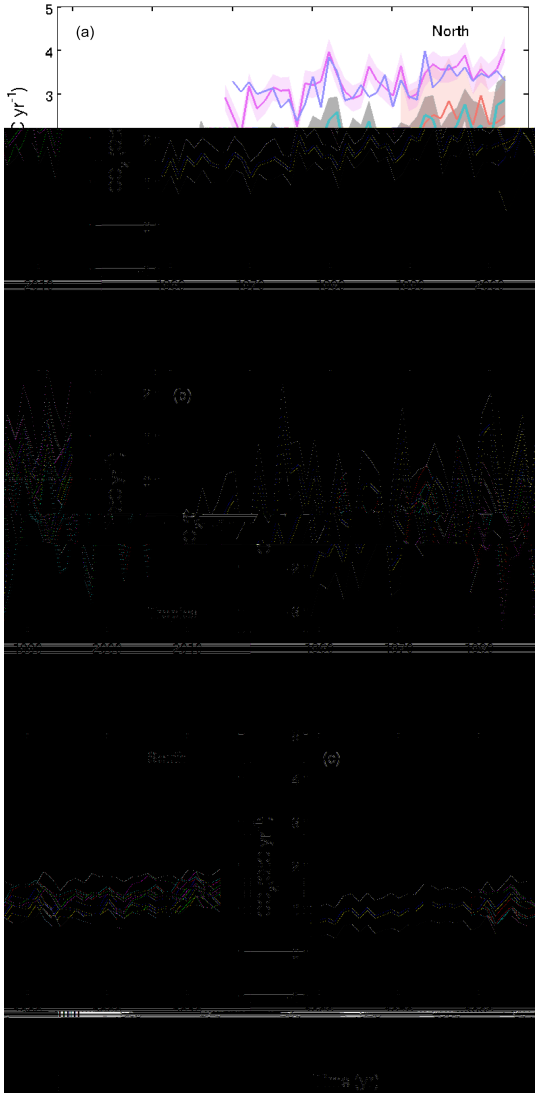

Figure 8. Atmosphere-to-surface CO_2 flux ($S_{OCEAN} + S_{LAND} - E_{LUC}$) by latitude bands for the **(a)** north (north of 30° N), **(b)** tropics (30° S–30° N), and **(c)** south (south of 30° S). Estimates from the combination of the multi-model means for the land and oceans are shown (turquoise) with $\pm 1\sigma$ of the model ensemble (in grey). Results from the three atmospheric inversions are shown in purple (Chevallier et al., 2005; MACC, v14.2), violet (Rödenbeck et al., 2003; Jena CarboScope, s81_v3.7), and salmon (Peters et al., 2010; Carbon Tracker, vCTE2015); see Table 6.

The estimated contribution of the north from process models is sensitive both to the ensemble of process models used and to the specifics of each inversion. Indeed, the process model results from Le Quéré et al. (2015) included a slightly different model ensemble (see Table 6) with no assessment of minimum model realism. The model ensemble from Le Quéré et al. (2015) showed a larger model spread and smaller sink (2.0 ± 0.8 GtC yr^{-1} for the latest decade), with also different trend in the 1960s. All three inversions show substantial differences in variability and/or trend, and one inversion substantial difference in the mean northern sink.

3.2 Global carbon budget for year 2014 and emissions projection for 2015

3.2.1 CO_2 emissions

Global CO_2 emissions from fossil fuels and industry reached 9.8 ± 0.5 GtC in 2014 (Fig. 5), distributed among coal (42 %), oil (33 %), gas (19 %), cement (5.7 %), and gas flaring (0.6 %). The first four categories increased by 0.4, 0.8, 0.4, and 2.5 % respectively over the previous year. Due to lack of data, gas flaring in 2012–2014 is assumed the same as 2011.

Emissions in 2014 were 0.6 % higher than in 2013, an increase well below the decadal average of 2.2 % yr^{-1} (2005–2014). Growth in 2014 is lower than our projection of 2.5 % yr^{-1} made last year (Le Quéré et al., 2015) based on an estimated GDP growth of 3.3 % yr^{-1} and a decrease in I_{FF} of -0.7 % yr^{-1} (Table 9), and is also outside the provided likely range of 1.3–3.5 %. The latest estimate of GDP growth for 2014 was 3.4 % yr^{-1} (IMF, 2015) and hence I_{FF} improved by 2.8 % yr^{-1}. This I_{FF} is low compared to recent years (Table 9), but not outside the range of variability observed in recent decades, suggesting that our uncertainty range may have been underestimated. Almost half of the lower growth compared to expectations can be attributed to a lower growth in emissions than anticipated in China (1.1 % compared to 4.5 % in our projection; Friedlingstein et al., 2014), which primarily reflects structural changes in China's economy (Green and Stern, 2015). Similar structural change occurred following the global financial crisis of 2008–2009 that particularly affected Western economies, which also made the emissions projections based on GDP temporarily problematic and outside of the steady behaviour assumed by the GDP/intensity approach (Peters et al., 2012b). For this reason we provide an emissions projection with explicit projection for China based on energy and cement data during January–August 2015 (see Sect. 2.1.4). Climatic variability could also have contributed to the lower emissions in China (from reported high rainfall possibly leading to higher hydropower capacity utilisation), and in Europe and the USA, where the combined emissions changes account for 37 % of the lower growth compared to expectations (Friedlingstein et al., 2014).

Using separate projections for China, the USA, and the rest of the world as described in Sect. 2.1.4, we project that the growth in global CO_2 emissions from fossil fuels and cement production will be near or slightly below zero in 2015, with a change of -0.6 % (range of -1.6 % to $+0.5$ %) from 2014 levels. Our method is imprecise and contains several assumptions that could influence the results beyond the given range, and as such is indicative only.

Table 9. Actual CO_2 emissions from fossil fuels and industry (E_{FF}) compared to projections made the previous year based on world GDP (IMF October 2015) and the fossil fuel intensity of GDP (I_{FF}) based on subtracting the CO_2 and GDP growth rates. The "Actual" values are the latest estimate available, and the "Projected" value for 2015 refers to those presented in this paper. A correction for leap years is applied (Sect. 2.1.3).

	E_{FF}		GDP		I_{FF}	
	Projected	Actual	Projected	Actual	Projected	Actual
2009[a]	−2.8 %	−0.5 %	−1.1 %	0.0 %	−1.7 %	−0.5 %
2010[b]	> 3 %	5.1 %	4.8 %	5.4 %	> −1.7 %	−0.3 %
2011[c]	3.1 ± 1.5 %	3.4 %	4.0 %	4.2 %	−0.9 ± 1.5 %	−0.8 %
2012[d]	2.6 % (1.9 to 3.5)	1.3 %	3.3 %	3.4 %	−0.7 %	−2.1 %
2013[e]	2.1 % (1.1 to 3.1)	1.7 %	2.9 %	3.3 %	−0.8 %	−1.6 %
2014[f]	2.5 % (1.3 to 3.5)	0.6 %	3.3 %	3.4 %	−0.7 %	−2.8 %
2015[g]	−0.6 % (−1.6 to 0.5)	–	3.1 %	–	−3.7 %	–

[a] Le Quéré et al. (2009). [b] Friedlingstein et al. (2010). [c] Peters et al. (2013). [d] Le Quéré et al. (2013). [e] Le Quéré et al. (2014). [f] Friedlingstein et al. (2014) and Le Quéré et al. (2015). [g] This study.

Within the given assumptions, global emissions decrease to 9.7 ± 0.5 GtC (35.7 ± 1.8 $GtCO_2$) in 2015, but are still 59 % above emissions in 1990.

For China, the expected change based largely on available data during January to August (see Sect. 2.1.4) is for a decrease in emissions of −3.9 % (range of −4.6 to −1.1 %) in 2015 compared to 2014. This uncertainty includes a range of −4.6 to −3.2 % considering different adjustments for stocks and no changes in the carbon content of coal, and is based on estimated decreases in apparent coal consumption (−5.3 %) and cement production (−5.0 %) and estimated growth in apparent oil (+3.2 %) and natural gas (+1.4 %) consumption. However, there are additional uncertainties from the carbon content of coal. While China's Energy Statistical Yearbooks indicate declining carbon content over recent years, preliminary data suggest an increase of up to 3 % in 2014. The Chinese government has introduced measures expressly to address the declining quality of coal (which also leads to lower carbon content) by closing lower-quality mines and placing restrictions on the quality of imported coal. Allowing for a similar increase in 2015 (0 to 3 %), we expand the uncertainty range of China's emissions growth to −4.6 to −1.1 %. Finally, China revised its emissions statistics upwards recently, which would affect the absolute value of emissions for China (but not the trend). With a slightly higher global contribution for China, our projection of global emissions "growth" for 2015 would decline further from −0.6 to −0.8 %, a small difference that falls within our uncertainty range.

For the USA, the EIA emissions projection for 2015 combined with cement data from USGS gives a decrease of −1.5 % (range of −5.5 to +0.3 %) compared to 2014. For the rest of the world, the expected growth for 2015 of +1.2 % (range of −0.2 to +2.6 %) is computed using the GDP projection for the world excluding China and the USA of 2.3 % made by the IMF (2015) and a decrease in I_{FF} of −1.1 % yr^{-1}, which is the average from 2005 to 2014. The uncertainty range is based on the standard deviation of the interannual variability in I_{FF} during 2005–2014 of ±1.4 %.

In 2014, the largest contributions to global CO_2 emissions were from China (27 %), the USA (15 %), the EU (28 member states; 10 %), and India (7 %), with the percentages compared to the global total including bunker fuels (3.0 %). These four regions account for 59 % of global emissions. Growth rates for these countries from 2013 to 2014 were 1.2 % (China), 0.8 % (USA), −5.8 % (EU28), and 8.6 % (India). The per-capita CO_2 emissions in 2014 were 1.3 tC $person^{-1}$ yr^{-1} for the globe, and were 4.8 (USA), 1.9 (China), 1.8 (EU28), and 0.5 tC $person^{-1}$ yr^{-1} (India) for the four highest emitting countries (Fig. 5e).

Territorial emissions in Annex B countries have decreased slightly by 0.1 % yr^{-1} on average from 1990 to 2013, while consumption emissions grew at 0.8 % yr^{-1} to 2007, after which they have declined at 1.5 % yr^{-1} (Fig. 5c). In non-Annex B countries, territorial emissions have grown at 4.4 % yr^{-1}, while consumption emissions have grown at 4.1 % yr^{-1}. In 1990, 66 % of global territorial emissions were emitted in Annex B countries (34 % in non-Annex B, and 2 % in bunker fuels used for international shipping and aviation), while in 2013 this had reduced to 38 % (58 % in non-Annex B and 3 % in bunker fuels). In terms of consumption emissions this split was 64 % in 1990 and 39 % in 2013 (34 to 55 % in non-Annex B). The difference between territorial and consumption emissions (the net emission transfer via international trade) from non-Annex B to Annex B countries has increased from near zero in 1990 to 0.3 GtC yr^{-1} around 2005 and remained relatively stable between 2006 and 2013 (Fig. 5). The increase in net emission transfers of 0.30 GtC yr^{-1} between 1990 and 2013 compares with the emission reduction of 0.37 GtC yr^{-1} in Annex B countries. These results show the importance of net emission transfer via international trade from non-Annex B to Annex B coun-

tries, and the stabilisation of emissions transfer when averaged over Annex B countries during the past decade. In 2013, the biggest emitters from a consumption perspective were China (23 % of the global total), USA (16 %), EU28 (12 %), and India (6 %).

Based on fire activity, the global CO_2 emissions from land-use change are estimated as 1.1 ± 0.5 GtC in 2014, similar to the 2005–2014 average of 0.9 ± 0.5 GtC yr^{-1} and the DGVM estimate for 2014 of 1.4 ± 0.5 GtC yr^{-1}. However, the estimated annual variability is not generally consistent between methods, except that all methods estimate that variability in E_{LUC} is small relative to the variability from S_{LAND} (Fig. 6a). This could be partly due to the design of the DGVM experiments, which use flux differences between simulations with and without land-cover change, and thus may overestimate variability, e.g. due to fires in forest regions where the contemporary forest cover is smaller than pre-industrial cover used in the "without land-cover-change" runs. The extrapolated land-cover input data for 2013–2014 in the DGVM may also explain part of the discrepancy.

3.2.2 Partitioning

The atmospheric CO_2 growth rate was 3.9 ± 0.2 GtC in 2014 (1.83 ± 0.09 ppm; Fig. 4; Dlugokencky and Tans, 2015). This is below the 2005–2014 average of 4.4 ± 0.1 GtC yr^{-1}, though the interannual variability in atmospheric growth rate is large.

The ocean CO_2 sink was 2.9 ± 0.5 GtC yr^{-1} in 2014, an increase of 0.1 GtC yr^{-1} over 2013 according to ocean models. Seven of the eight ocean models produce an increase in the ocean CO_2 sink in 2014 compared to 2013, with the last model producing a very small reduction. However, of the two data products available over that period, Rödenbeck et al. (2014) produce a decrease of -0.1 GtC yr^{-1}, while Landschützer et al. (2015) produce an increase of 0.2 GtC yr^{-1}. Thus there is no overall consistency in the annual change in the ocean CO_2 sink, although there is an indication of increasing convergence among products for the assessment of multi-year changes, as suggested by the time-series correlations reported in Sect. 2.4.3 (see also Landschützer et al., 2015). A small increase in the ocean CO_2 sink in 2014 would be consistent with the observed El Niño neutral conditions and continued rising atmospheric CO_2. All estimates suggest an ocean CO_2 sink for 2014 that is larger than the 2005–2014 average of 2.6 ± 0.5 GtC yr^{-1}.

The terrestrial CO_2 sink calculated as the residual from the carbon budget was 4.1 ± 0.9 GtC in 2014, 1.1 GtC higher than the 3.0 ± 0.8 GtC yr^{-1} averaged over 2005–2014 (Fig. 4). This is among the largest S_{LAND} calculated since 1959, equal to year 2011 (Poulter et al., 2014) and 2011. In contrast to 2011, when La Niña conditions prevailed, and 1991, when the Pinatubo eruption occurred, the large S_{LAND} in 2014 occurred under neutral El Niño conditions. The DGVM mean produced a sink of 3.6 ± 0.9 GtC in 2014, 0.7 GtC yr^{-1} over the 2005–2014 average (Table 7), smaller but still consistent with observations (Poulter et al., 2014). In the DGVM ensemble, 2014 is the fifth largest S_{LAND}, after 1974, 2011, 2004, and 2000. There is no agreement between models and inversions on the regional origin of the 2014 flux anomaly (Fig. 8).

Cumulative emissions for 1870–2014 were 400 ± 20 GtC for E_{FF}, and 145 ± 50 GtC for E_{LUC} based on the bookkeeping method of Houghton et al. (2012) for 1870–1996 and a combination with fire-based emissions for 1997–2014 as described in Sect. 2.2 (Table 10). The cumulative emissions are rounded to the nearest 5 GtC. The total cumulative emissions for 1870–2014 are 545 ± 55 GtC. These emissions were partitioned among the atmosphere (230 ± 5 GtC based on atmospheric measurements in ice cores of 288 ppm (Sect. "Global atmospheric CO_2 growth rate estimates"; Joos and Spahni, 2008) and recent direct measurements of 397.2 ppm; Dlugokencky and Tans, 2014), ocean (155 ± 20 GtC using Khatiwala et al., 2013, prior to 1959 and Table 8 otherwise), and land (160 ± 60 GtC by the difference).

Cumulative emissions for the early period 1750–1869 were 3 GtC for E_{FF}, and about 45 GtC for E_{LUC} (rounded to nearest 5), of which 10 GtC were emitted in the period 1850–1870 (Houghton et al., 2012) and 30 GtC were emitted in the period 1750–1850 based on the average of four publications (22 GtC by Pongratz et al., 2009; 15 GtC by van Minnen et al., 2009; 64 GtC by Shevliakova et al., 2009; and 24 GtC by Zaehle et al., 2011). The growth in atmospheric CO_2 during that time was about 25 GtC, and the ocean uptake about 20 GtC, implying a land uptake of 5 GtC. These numbers have large relative uncertainties but balance within the limits of our understanding.

Cumulative emissions for 1750–2014 based on the sum of the two periods above (before rounding to the nearest 5 GtC) were 405 ± 20 GtC for E_{FF}, and 190 ± 65 GtC for E_{LUC}, for a total of 590 ± 70 GtC, partitioned among the atmosphere (255 ± 5 GtC), ocean (170 ± 20 GtC), and land (165 ± 70 GtC).

Cumulative emissions through to year 2015 can be estimated based on the 2015 projections of E_{FF} (Sect. 3.2), the largest contributor, and assuming a constant E_{LUC} of 0.9 GtC. For 1870–2015, these are 555 ± 55 GtC (2040 ± 200 GtCO$_2$) for total emissions, with about 75 % contribution from E_{FF} (410 ± 20 GtC) and about 25 % contribution from E_{LUC} (145 ± 50 GtC). Cumulative emissions since year 1870 are higher than the emissions of 515 [445 to 585] GtC reported by the IPCC (Stocker et al., 2013) because they include an additional 43 GtC from emissions in 2012–2015 (mostly from E_{FF}). The uncertainty presented here ($\pm 1\sigma$) is smaller than the range of 90 % used by IPCC, but both estimates overlap within their uncertainty ranges.

Table 10. Cumulative CO_2 emissions for the periods 1750–2014, 1870–2014, and 1870–2015 in gigatonnes of carbon (GtC). We also provide the 1850–2005 time period used in a number of model evaluation publications. All uncertainties are reported as $\pm 1\sigma$. All values are rounded to the nearest 5 GtC as in Stocker et al. (2013), reflecting the limits of our capacity to constrain cumulative estimates. Thus some columns will not exactly balance because of rounding errors.

Units of GtC	1750–2014	1850–2005	1870–2014	1870–2015
Emissions				
Fossil fuels and industry (E_{FF})	405 ± 20	320 ± 15	400 ± 20	$410 \pm 20^*$
Land-use-change emissions (E_{LUC})	190 ± 65	150 ± 55	145 ± 50	$145 \pm 50^*$
Total emissions	590 ± 70	470 ± 55	545 ± 55	$555 \pm 55^*$
Partitioning				
Atmospheric growth rate (G_{ATM})	255 ± 5	195 ± 5	230 ± 5	
Ocean sink (S_{OCEAN})	170 ± 20	160 ± 20	155 ± 20	
Residual terrestrial sink (S_{LAND})	165 ± 70	115 ± 60	160 ± 60	

* The extension to year 2015 uses the emissions projections for fossil fuels and industry for 2015 of 9.7 GtC (Sect. 3.2) and assumes a constant E_{LUC} flux (Sect. 2.2).

4 Discussion

Each year when the global carbon budget is published, each component for all previous years is updated to take into account corrections that are the result of further scrutiny and verification of the underlying data in the primary input data sets. The updates have generally been relatively small and focused on the most recent years, except for land-use change, where they are more significant but still generally within the provided uncertainty range (Fig. 9). The difficulty in accessing land-cover-change data to estimate E_{LUC} is the key problem to providing continuous records of emissions in this sector. Current FAO estimates are based on statistics reported at the country level and are not spatially explicit. Advances in satellite recovery of land-cover change could help to keep track of land-use change through time (Achard et al., 2014; Harris et al., 2012). Revisions in E_{LUC} for the 2008/2009 budget were the result of the release of FAO (2010), which contained a major update to forest-cover change for the period 2000–2005 and provided the data for the following 5 years to 2010 (Fig. 9b). The differences this year could be attributable to both the different data and the different methods. Updates to values for any given year in each component of the global carbon budget were highest at $0.82\,GtC\,yr^{-1}$ for the atmospheric growth rate (from a correction to year 1979), $0.24\,GtC\,yr^{-1}$ for fossil fuels and industry, and $0.52\,GtC\,yr^{-1}$ for the ocean CO_2 sink (from a change from one to multiple models; Fig. 9). The update for the residual land CO_2 sink was also large (Fig. 9e), with a maximum value of $0.83\,GtC\,yr^{-1}$, directly reflecting revisions in other terms of the budget.

Our capacity to separate the carbon budget components can be evaluated by comparing the land CO_2 sink estimated through two approaches: (1) the budget residual (S_{LAND}), which includes errors and biases from all components, and (2) the land CO_2 sink estimate by the DGVM ensemble, which is based on our understanding of processes of how the land responds to increasing CO_2, climate, and variability. Furthermore, the inverse model estimates which formally merge observational constraints with process-based models to close the global budget can provide constraints on the total land flux. These estimates are generally close (Fig. 6), both for the mean and for the interannual variability. The annual estimates from the DGVM over 1959 to 2014 correlate with the annual budget residual with $r = 0.71$ (Sect. 2.5.2; Fig. 6). The DGVMs produce a decadal mean and standard deviation across models of $3.0 \pm 0.4\,GtC\,yr^{-1}$ for the period 2005–2014, fully consistent with the estimate of $3.0 \pm 0.8\,GtC\,yr^{-1}$ produced with the budget residual (Table 7). New insights into total surface fluxes arise from the comparison with the atmospheric inversions, and their regional breakdown already provides a semi-independent way to validate the results. The comparison shows a first-order consistency between inversions and process models but with a lot of discrepancies, particularly for the allocation of the mean land sink between the tropics and the Northern Hemisphere. Understanding these discrepancies and further analysis of regional carbon budgets would provide additional information to quantify and improve our estimates, as has been undertaken by the project REgional Carbon Cycle Assessment and Processes (RECCAP; Canadell et al., 2012–2013).

Annual estimates of each component of the global carbon budgets have their limitations, some of which could be improved with better data and/or better understanding of carbon dynamics. The primary limitations involve resolving fluxes on annual timescales and providing updated estimates for recent years for which data-based estimates are not yet available or only beginning to emerge. Of the various terms in the global budget, only the burning of fossil fuels and atmospheric growth rate terms are based primarily on empirical inputs supporting annual estimates in this carbon budget. The data on fossil fuels and industry are based on sur-

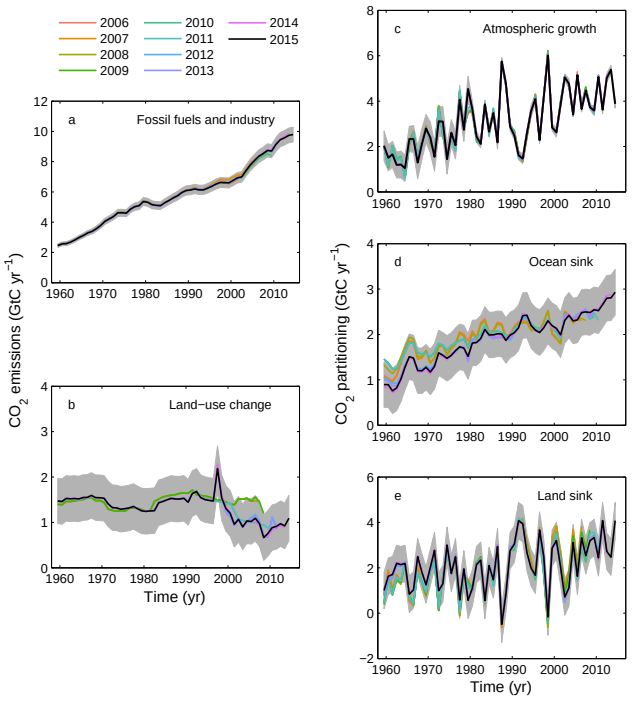

Figure 9. Comparison of global carbon budget components released annually by GCP since 2006. CO_2 emissions from both **(a)** fossil fuels and industry (E_{FF}) and **(b)** land-use change (E_{LUC}), as well as their partitioning among **(c)** the atmosphere (G_{ATM}), **(d)** the ocean (S_{OCEAN}), and **(e)** the land (S_{LAND}). See legend for the corresponding years, with the 2006 carbon budget from Raupach et al. (2007), 2007 from Canadell et al. (2007), 2008 released online only, 2009 from Le Quéré et al. (2009), 2010 from Friedlingstein et al. (2010), 2011 from Peters et al. (2012b), 2012 from Le Quéré et al. (2013), 2013 from Le Quéré et al. (2014), and 2014 from Le Quéré et al. (2015) and this year's budget (2015; this study). The budget year generally corresponds to the year when the budget was first released. All values are in GtC yr^{-1}.

vey data in all countries. The other terms can be provided on an annual basis only through the use of models. While these models represent the current state of the art, they provide only simulated changes in primary carbon budget components. For example, the decadal trends in global ocean uptake and the interannual variations associated with El Niño–Southern Oscillation (i.e. ENSO) are not directly constrained by observations, although many of the processes controlling these trends are sufficiently well known that the model-based trends still have value as benchmarks for further validation. Data-based products for the ocean CO_2 sink provide new ways to evaluate the model results, and could be used directly as data become more rapidly available and methods for creating such products improve. However, there are still large discrepancies among data-based estimates, in large part due to the lack of routine data sampling, that preclude their direct use for now (see Rödenbeck et al., 2015). Estimates of land-use-change emissions and their year-to-year variability have even larger uncertainty, and many of the underlying data are not available as an annual update. Efforts are underway to work with annually available satellite area change data or FAO-reported data in combination with fire data and modelling to provide annual updates for future budgets. The best resolved changes are in atmospheric growth (G_{ATM}), fossil fuel emissions (E_{FF}), and, by difference, the change in the sum of the remaining terms ($S_{OCEAN} + S_{LAND} - E_{LUC}$). The variations from year-to-year in these remaining terms are largely model-based at this time. Further efforts to increase the availability and use of annual data for estimating the remaining terms with annual to decadal resolution are especially needed.

Our approach also depends on the reliability of the energy and land-cover-change statistics provided at the country level, and are thus potentially subject to biases. Thus it is critical to develop multiple ways to estimate the carbon balance at the global and regional level, including estimates from the inversion of atmospheric CO_2 concentration, the use of other oceanic and atmospheric tracers, and the compilation of emissions using alternative statistics (e.g. sectors). It is also important to challenge the consistency of information across observational streams, for example to contrast the coherence of temperature trends with those of CO_2 sink trends. Multiple approaches ranging from global to regional scale would greatly help increase confidence and reduce uncertainty in CO_2 emissions and their fate.

5 Conclusions

The estimation of global CO_2 emissions and sinks is a major effort by the carbon cycle research community that requires a combination of measurements and compilation of statistical estimates and results from models. The delivery of an annual carbon budget serves two purposes. First, there is a large demand for up-to-date information on the state of the anthropogenic perturbation of the climate system and its underpinning causes. A broad stakeholder community relies on the data sets associated with the annual carbon budget including scientists, policy makers, businesses, journalists, and the broader society increasingly engaged in adapting to and mitigating human-driven climate change. Second, over the last decade we have seen unprecedented changes in the human and biophysical environments (e.g. increase in the growth of fossil fuel emissions, ocean temperatures, and strength of the land sink), which call for more frequent assessments of the state of the planet, and by implications a better understanding of the future evolution of the carbon cycle, as well as the requirements for climate change mitigation and adaptation. Both the ocean and the land surface presently remove a large fraction of anthropogenic emissions. Any significant change in the function of carbon sinks is of great importance to climate policymaking, as they affect the excess carbon dioxide remaining in the atmosphere and therefore the compati-

ble emissions for any climate stabilisation target. Better constraints of carbon cycle models against contemporary data sets raise the capacity for the models to become more accurate at future projections.

This all requires more frequent, robust, and transparent data sets and methods that can be scrutinised and replicated. After 10 annual releases from the GCP, the effort is growing and the traceability of the methods has become increasingly complex. Here, we have documented in detail the data sets and methods used to compile the annual updates of the global carbon budget, explained the rationale for the choices made, the limitations of the information, and finally highlighted the need for additional information where gaps exist.

This paper will help, via "living data", to keep track of new budget updates. The evolution over time of the carbon budget is now a key indicator of the anthropogenic perturbation of the climate system, and its annual delivery joins a set of other climate indicators to monitor the evolution of human-induced climate change, such as the annual updates on the global surface temperature, sea level rise, and minimum Arctic sea ice extent.

Appendix A

Table A1. Attribution of fCO_2 measurements for years 2013–2014 used in addition to SOCAT v3 (Bakker et al., 2014, 2015) to inform ocean data products.

Vessel	Start date yyyy-mm-dd	End date yyyy-mm-dd	Regions	No. of samples	Principal Investigators	DOI (if available)/comment
Atlantic Companion	2014-02-21	2014-02-26	North Atlantic	2462	Steinhoff, T., M. Becker and A. Körtzinger	
Atlantic Companion	2014-04-26	2014-05-02	North Atlantic	3036	Steinhoff, T., M. Becker and A. Körtzinger	
Atlantic Companion	2014-05-31	2014-06-04	North Atlantic	2365	Steinhoff, T., M. Becker and A. Körtzinger	
Atlantic Companion	2014-06-16	2014-06-22	North Atlantic	6124	Steinhoff, T., M. Becker and A. Körtzinger	
Atlantic Companion	2014-08-27	2014-08-30	North Atlantic	3963	Steinhoff, T., M. Becker and A. Körtzinger	
Atlantic Companion	2014-09-28	2014-10-04	North Atlantic	7239	Steinhoff, T., M. Becker and A. Körtzinger	
Benguela Stream	2014-07-15	2014-07-20	North Atlantic	4523	Schuster, U.	
Benguela Stream	2013-12-28	2014-01-05	North Atlantic, Tropical Atlantic	6241	Schuster, U.	
Benguela Stream	2014-01-08	2014-01-13	North Atlantic, Tropical Atlantic	4400	Schuster, U.	
Benguela Stream	2014-02-23	2014-03-02	North Atlantic, Tropical Atlantic	6014	Schuster, U.	
Benguela Stream	2014-02-23	2014-03-02	North Atlantic, Tropical Atlantic	5612	Schuster, U.	
Benguela Stream	2014-04-18	2014-04-27	North Atlantic, Tropical Atlantic	7376	Schuster, U.	
Benguela Stream	2014-04-30	2014-05-08	North Atlantic, Tropical Atlantic	6819	Schuster, U.	
Benguela Stream	2014-05-17	2014-05-25	North Atlantic, Tropical Atlantic	6390	Schuster, U.	
Benguela Stream	2014-06-14	2014-06-21	North Atlantic, Tropical Atlantic	3397	Schuster, U.	
Benguela Stream	2014-06-25	2014-07-03	North Atlantic, Tropical Atlantic	6624	Schuster, U.	
Benguela Stream	2014-07-23	2014-07-31	North Atlantic, Tropical Atlantic	6952	Schuster, U.	
Benguela Stream	2014-11-12	2014-11-20	North Atlantic, Tropical Atlantic	5043	Schuster, U.	
Benguela Stream	2014-12-10	2014-12-19	North Atlantic, Tropical Atlantic	7046	Schuster, U.	
Benguela Stream	2014-12-10	2014-12-19	North Atlantic, Tropical Atlantic	7046	Schuster, U.	
Cap Blanche	2014-02-01	2014-02-13	Tropical Pacific, Southern Ocean	6148	Feely, R., C. Cosca, S. Alin and G. Lebon	
Cap Blanche	2014-03-27	2014-04-10	Tropical Pacific, Southern Ocean	6428	Feely, R., C. Cosca, S. Alin and G. Lebon	
Cap Blanche	2014-05-23	2014-06-05	Tropical Pacific, Southern Ocean	6016	Feely, R., C. Cosca, S. Alin and G. Lebon	
Cap Blanche	2014-07-18	2014-07-30	Tropical Pacific, Southern Ocean	5394	Feely, R., C. Cosca, S. Alin and G. Lebon	
Cap Blanche	2014-09-12	2014-09-25	Tropical Pacific, Southern Ocean	6083	Feely, R., C. Cosca, S. Alin and G. Lebon	
Cap Blanche	2014-11-13	2014-11-26	Tropical Pacific, Southern Ocean	5876	Feely, R., C. Cosca, S. Alin and G. Lebon	
Cap Vilano	2013-02-01	2013-02-13	Tropical Pacific, Southern Ocean	4709	Cosca, C., R. Feely, S. Alin and G. Lebon	
Cap Vilano	2013-03-28	2013-04-11	Tropical Pacific, Southern Ocean	5390	Cosca, C., R. Feely, S. Alin and G. Lebon	
Cap Vilano	2013-05-24	2013-06-06	Tropical Pacific, Southern Ocean	5096	Cosca, C., R. Feely, S. Alin and G. Lebon	
Colibri	2014-07-04	2014-07-15	North Atlantic, Tropical Atlantic	4853	Lefèvre, N. and D. Diverrès	
Colibri	2014-08-27	2014-09-03	North Atlantic, Tropical Atlantic	3881	Lefèvre, N.. and D. Diverrès	
Colibri	2014-09-12	2014-09-23	North Atlantic, Tropical Atlantic	5940	Lefèvre, N.. and D. Diverrès	
Colibri	2014-10-25	2014-11-04	North Atlantic, Tropical Atlantic	5725	Lefèvre, N. and D. Diverrès	
Colibri	2014-07-18	2014-07-19	Tropical Atlantic	313	Lefèvre, N. and D. Diverrès	
Explorer of the Seas	2013-06-25	2013-06-27	North Atlantic	672	Wanninkhof, R., D. Pierrot and L. Barbero	doi:10.3334/CDIAC/OTG.VOS_EXP2014
Explorer of the Seas	2013-07-06	2013-07-11	North Atlantic	1496	Wanninkhof, R., D. Pierrot and L. Barbero	doi:10.3334/CDIAC/OTG.VOS_EXP2014
Explorer of the Seas	2013-07-20	2013-07-25	North Atlantic	1375	Wanninkhof, R., D. Pierrot and L. Barbero	doi:10.3334/CDIAC/OTG.VOS_EXP2014

Table A1. Continued.

Vessel	Start date yyyy-mm-dd	End date yyyy-mm-dd	Regions	No. of samples	Principal Investigators	DOI (if available)/comment
Explorer of the Seas	2013-08-03	2013-08-08	North Atlantic	1436	Wanninkhof, R., D. Pierrot and L. Barbero	doi:10.3334/CDIAC/OTG.VOS_EXP2014
Explorer of the Seas	2013-08-17	2013-08-22	North Atlantic	1138	Wanninkhof, R., D. Pierrot and L. Barbero	doi:10.3334/CDIAC/OTG.VOS_EXP2014
Explorer of the Seas	2014-04-08	2014-04-09	North Atlantic	209	Wanninkhof, R., D. Pierrot and L. Barbero	doi:10.3334/CDIAC/OTG.VOS_EXP2014
Explorer of the Seas	2014-04-19	2014-04-24	North Atlantic	1424	Wanninkhof, R., D. Pierrot and L. Barbero	doi:10.3334/CDIAC/OTG.VOS_EXP2014
Explorer of the Seas	2014-05-03	2014-05-08	North Atlantic	1512	Wanninkhof, R., D. Pierrot and L. Barbero	doi:10.3334/CDIAC/OTG.VOS_EXP2014
Explorer of the Seas	2014-05-17	2014-05-22	North Atlantic	1349	Wanninkhof, R., D. Pierrot and L. Barbero	doi:10.3334/CDIAC/OTG.VOS_EXP2014
Explorer of the Seas	2014-05-31	2014-06-05	North Atlantic	1194	Wanninkhof, R., D. Pierrot and L. Barbero	doi:10.3334/CDIAC/OTG.VOS_EXP2014
Explorer of the Seas	2014-06-14	2014-06-19	North Atlantic	1142	Wanninkhof, R., D. Pierrot and L. Barbero	doi:10.3334/CDIAC/OTG.VOS_EXP2014
Explorer of the Seas	2014-06-28	2014-07-03	North Atlantic	1479	Wanninkhof, R., D. Pierrot and L. Barbero	doi:10.3334/CDIAC/OTG.VOS_EXP2014
Explorer of the Seas	2014-07-12	2014-07-17	North Atlantic	1489	Wanninkhof, R., D. Pierrot and L. Barbero	doi:10.3334/CDIAC/OTG.VOS_EXP2014
Explorer of the Seas	2014-07-26	2014-07-31	North Atlantic	1474	Wanninkhof, R., D. Pierrot and L. Barbero	doi:10.3334/CDIAC/OTG.VOS_EXP2014
Explorer of the Seas	2014-08-09	2014-08-14	North Atlantic	1468	Wanninkhof, R., D. Pierrot and L. Barbero	doi:10.3334/CDIAC/OTG.VOS_EXP2014
Explorer of the Seas	2014-08-23	2014-08-28	North Atlantic	1277	Wanninkhof, R., D. Pierrot and L. Barbero	doi:10.3334/CDIAC/OTG.VOS_EXP2014
Explorer of the Seas	2014-08-29	2014-09-06	North Atlantic	2846	Wanninkhof, R., D. Pierrot and L. Barbero	doi:10.3334/CDIAC/OTG.VOS_EXP2014
Explorer of the Seas	2014-09-06	2014-09-11	North Atlantic	1479	Wanninkhof, R., D. Pierrot and L. Barbero	doi:10.3334/CDIAC/OTG.VOS_EXP2014
Explorer of the Seas	2014-09-11	2014-09-20	North Atlantic	2956	Wanninkhof, R., D. Pierrot and L. Barbero	doi:10.3334/CDIAC/OTG.VOS_EXP2014
Explorer of the Seas	2014-09-20	2014-09-22	North Atlantic	728	Wanninkhof, R., D. Pierrot and L. Barbero	doi:10.3334/CDIAC/OTG.VOS_EXP2014
Explorer of the Seas	2014-10-04	2014-10-09	North Atlantic	1444	Wanninkhof, R., D. Pierrot and L. Barbero	doi:10.3334/CDIAC/OTG.VOS_EXP2014
Explorer of the Seas	2014-10-18	2014-10-23	North Atlantic	1504	Wanninkhof, R., D. Pierrot and L. Barbero	doi:10.3334/CDIAC/OTG.VOS_EXP2014
Explorer of the Seas	2013-04-02	2013-04-07	North Atlantic, Tropical Atlantic	1301	Wanninkhof, R., D. Pierrot and L. Barbero	doi:10.3334/CDIAC/OTG.VOS_EXP2014
Explorer of the Seas	2013-06-27	2013-07-06	North Atlantic, Tropical Atlantic	3329	Wanninkhof, R., D. Pierrot and L. Barbero	doi:10.3334/CDIAC/OTG.VOS_EXP2014
Explorer of the Seas	2013-07-11	2013-07-20	North Atlantic, Tropical Atlantic	3372	Wanninkhof, R., D. Pierrot and L. Barbero	doi:10.3334/CDIAC/OTG.VOS_EXP2014
Explorer of the Seas	2013-07-25	2013-08-03	North Atlantic, Tropical Atlantic	3350	Wanninkhof, R., D. Pierrot and L. Barbero	doi:10.3334/CDIAC/OTG.VOS_EXP2014
Explorer of the Seas	2013-08-08	2013-08-17	North Atlantic, Tropical Atlantic	3393	Wanninkhof, R., D. Pierrot and L. Barbero	doi:10.3334/CDIAC/OTG.VOS_EXP2014
Explorer of the Seas	2014-04-01	2014-04-05	North Atlantic, Tropical Atlantic	1189	Wanninkhof, R., D. Pierrot and L. Barbero	doi:10.3334/CDIAC/OTG.VOS_EXP2014
Explorer of the Seas	2014-04-10	2014-04-19	North Atlantic, Tropical Atlantic	3297	Wanninkhof, R., D. Pierrot and L. Barbero	doi:10.3334/CDIAC/OTG.VOS_EXP2014
Explorer of the Seas	2014-04-24	2014-05-03	North Atlantic, Tropical Atlantic	2968	Wanninkhof, R., D. Pierrot and L. Barbero	doi:10.3334/CDIAC/OTG.VOS_EXP2014
Explorer of the Seas	2014-05-08	2014-05-17	North Atlantic, Tropical Atlantic	3324	Wanninkhof, R., D. Pierrot and L. Barbero	doi:10.3334/CDIAC/OTG.VOS_EXP2014
Explorer of the Seas	2014-05-22	2014-05-31	North Atlantic, Tropical Atlantic	2850	Wanninkhof, R., D. Pierrot and L. Barbero	doi:10.3334/CDIAC/OTG.VOS_EXP2014
Explorer of the Seas	2014-06-05	2014-06-14	North Atlantic, Tropical Atlantic	3374	Wanninkhof, R., D. Pierrot and L. Barbero	doi:10.3334/CDIAC/OTG.VOS_EXP2014
Explorer of the Seas	2014-06-19	2014-06-28	North Atlantic, Tropical Atlantic	3386	Wanninkhof, R., D. Pierrot and L. Barbero	doi:10.3334/CDIAC/OTG.VOS_EXP2014
Explorer of the Seas	2014-07-03	2014-07-12	North Atlantic, Tropical Atlantic	3397	Wanninkhof, R., D. Pierrot and L. Barbero	doi:10.3334/CDIAC/OTG.VOS_EXP2014
Explorer of the Seas	2014-07-17	2014-07-26	North Atlantic, Tropical Atlantic	3404	Wanninkhof, R., D. Pierrot and L. Barbero	doi:10.3334/CDIAC/OTG.VOS_EXP2014
Explorer of the Seas	2014-07-31	2014-08-09	North Atlantic, Tropical Atlantic	3392	Wanninkhof, R., D. Pierrot and L. Barbero	doi:10.3334/CDIAC/OTG.VOS_EXP2014
Explorer of the Seas	2014-08-14	2014-08-23	North Atlantic, Tropical Atlantic	3307	Wanninkhof, R., D. Pierrot and L. Barbero	doi:10.3334/CDIAC/OTG.VOS_EXP2014
Explorer of the Seas	2014-09-25	2014-10-04	North Atlantic, Tropical Atlantic	2967	Wanninkhof, R., D. Pierrot and L. Barbero	doi:10.3334/CDIAC/OTG.VOS_EXP2014
Explorer of the Seas	2014-10-09	2014-10-18	North Atlantic, Tropical Atlantic	3069	Wanninkhof, R., D. Pierrot and L. Barbero	doi:10.3334/CDIAC/OTG.VOS_EXP2014

Table A1. Continued.

Vessel	Start date yyyy-mm-dd	End date yyyy-mm-dd	Regions	No. of samples	Principal Investigators	DOI (if available)/comment
Explorer of the Seas	2014-10-23	2014-11-01	North Atlantic, Tropical Atlantic	3074	Wanninkhof, R., D. Pierrot and L. Barbero	doi:10.3334/CDIAC/OTG.VOS_EXP2014
Explorer of the Seas	2014-11-01	2014-11-11	North Atlantic, Tropical Atlantic	1809	Wanninkhof, R., D. Pierrot and L. Barbero	doi:10.3334/CDIAC/OTG.VOS_EXP2014
Explorer of the Seas	2014-11-21	2014-11-24	North Atlantic, Tropical Atlantic	567	Wanninkhof, R., D. Pierrot and L. Barbero	doi:10.3334/CDIAC/OTG.VOS_EXP2014
Explorer of the Seas	2014-12-04	2014-12-13	North Atlantic, Tropical Atlantic	3773	Wanninkhof, R., D. Pierrot and L. Barbero	doi:10.3334/CDIAC/OTG.VOS_EXP2014
Explorer of the Seas	2014-12-23	2014-12-27	North Atlantic, Tropical Atlantic	1516	Wanninkhof, R., D. Pierrot and L. Barbero	doi:10.3334/CDIAC/OTG.VOS_EXP2014
Explorer of the Seas	2014-12-27	2015-01-04	North Atlantic, Tropical Atlantic	1315	Wanninkhof, R., D. Pierrot and L. Barbero	doi:10.3334/CDIAC/OTG.VOS_EXP2014
Explorer of the Seas	2014-11-25	2014-11-29	Tropical Atlantic	1653	Wanninkhof, R., D. Pierrot and L. Barbero	doi:10.3334/CDIAC/OTG.VOS_EXP2014
Explorer of the Seas	2014-11-29	2014-12-04	Tropical Atlantic	1680	Wanninkhof, R., D. Pierrot and L. Barbero	doi:10.3334/CDIAC/OTG.VOS_EXP2014
Explorer of the Seas	2014-12-14	2014-12-18	Tropical Atlantic	899	Wanninkhof, R., D. Pierrot and L. Barbero	doi:10.3334/CDIAC/OTG.VOS_EXP2014
Explorer of the Seas	2014-12-18	2014-12-23	Tropical Atlantic	1787	Wanninkhof, R., D. Pierrot and L. Barbero	doi:10.3334/CDIAC/OTG.VOS_EXP2014
Finnmaid	2012-01-13	2014-12-31	North Atlantic	22 000	Rehder, G. and M. Glockzin	
G.O. Sars	2014-07-08	2014-11-16	Arctic, North Atlantic	24 405	Lauvset, S.K. and I. Skjelvan	
Gordon Gunter	2014-02-20	2014-02-26	North Atlantic	22 000	Wanninkhof, R., D. Pierrot and L. Barbero	doi:10.3334/CDIAC/OTG.AOML_BIGELOW_ECOAST_2014
Gordon Gunter	2014-03-01	2014-03-09	North Atlantic	3742	Wanninkhof, R., D. Pierrot and L. Barbero	doi:10.3334/CDIAC/OTG.AOML_BIGELOW_ECOAST_2014
Gordon Gunter	2014-03-11	2014-04-03	North Atlantic	8189	Wanninkhof, R., D. Pierrot and L. Barbero	doi:10.3334/CDIAC/OTG.AOML_BIGELOW_ECOAST_2014
Gordon Gunter	2014-04-08	2014-04-28	North Atlantic	7753	Wanninkhof, R., D. Pierrot and L. Barbero	doi:10.3334/CDIAC/OTG.AOML_BIGELOW_ECOAST_2014
Gordon Gunter	2014-06-06	2014-06-13	North Atlantic, Tropical Atlantic	3338	Wanninkhof, R., D. Pierrot and L. Barbero	doi:10.3334/CDIAC/OTG.AOML_BIGELOW_ECOAST_2014
Gordon Gunter	2014-07-04	2014-07-16	Tropical Atlantic	5399	Wanninkhof, R., D. Pierrot and L. Barbero	doi:10.3334/CDIAC/OTG.AOML_BIGELOW_ECOAST_2014
Gordon Gunter	2014-07-21	2014-07-30	Tropical Atlantic	4074	Wanninkhof, R., D. Pierrot and L. Barbero	doi:10.3334/CDIAC/OTG.AOML_BIGELOW_ECOAST_2014
Henry B. Bigelow	2014-03-29	2014-04-04	North Atlantic	2196	Wanninkhof, R., D. Pierrot and L. Barbero	doi:10.3334/CDIAC/OTG.AOML_BIGELOW_ECOAST_2014
Henry B. Bigelow	2014-04-11	2014-04-25	North Atlantic	6651	Wanninkhof, R., D. Pierrot and L. Barbero	doi:10.3334/CDIAC/OTG.AOML_BIGELOW_ECOAST_2014
Henry B. Bigelow	2014-05-06	2014-05-16	North Atlantic	4302	Wanninkhof, R., D. Pierrot and L. Barbero	doi:10.3334/CDIAC/OTG.AOML_BIGELOW_ECOAST_2014
Henry B. Bigelow	2014-05-16	2014-05-23	North Atlantic	3233	Wanninkhof, R., D. Pierrot and L. Barbero	doi:10.3334/CDIAC/OTG.AOML_BIGELOW_ECOAST_2014
Henry B. Bigelow	2014-05-27	2014-06-01	North Atlantic	2085	Wanninkhof, R., D. Pierrot and L. Barbero	doi:10.3334/CDIAC/OTG.AOML_BIGELOW_ECOAST_2014
Henry B. Bigelow	2014-06-18	2014-07-01	North Atlantic	5458	Wanninkhof, R., D. Pierrot and L. Barbero	doi:10.3334/CDIAC/OTG.AOML_BIGELOW_ECOAST_2014
Henry B. Bigelow	2014-07-25	2014-07-30	North Atlantic	2226	Wanninkhof, R., D. Pierrot and L. Barbero	doi:10.3334/CDIAC/OTG.AOML_BIGELOW_ECOAST_2014
Henry B. Bigelow	2014-08-05	2014-08-16	North Atlantic	5231	Wanninkhof, R., D. Pierrot and L. Barbero	doi:10.3334/CDIAC/OTG.AOML_BIGELOW_ECOAST_2014
Henry B. Bigelow	2014-09-08	2014-09-19	North Atlantic	4847	Wanninkhof, R., D. Pierrot and L. Barbero	doi:10.3334/CDIAC/OTG.AOML_BIGELOW_ECOAST_2014
Henry B. Bigelow	2014-09-23	2014-10-03	North Atlantic	4620	Wanninkhof, R., D. Pierrot and L. Barbero	doi:10.3334/CDIAC/OTG.AOML_BIGELOW_ECOAST_2014
Henry B. Bigelow	2014-10-07	2014-10-23	North Atlantic	7736	Wanninkhof, R., D. Pierrot and L. Barbero	doi:10.3334/CDIAC/OTG.AOML_BIGELOW_ECOAST_2014
Henry B. Bigelow	2014-10-28	2014-11-13	North Atlantic	6615	Wanninkhof, R., D. Pierrot and L. Barbero	doi:10.3334/CDIAC/OTG.AOML_BIGELOW_ECOAST_2014
James Clark Ross	2014-03-20	2014-04-12	North Atlantic	2113	Kitidis, V. and I. Brown	
Laurence M. Gould	2012-12-31	2013-02-06	Southern Ocean	10 816	Sweeney, C., T. Takahashi, T. Newberger and D.R. Munro	accessed from CDIAC on 08/06/2015
Laurence M. Gould	2013-02-13	2013-02-24	Southern Ocean	2030	Sweeney, C., T. Takahashi, T. Newberger and D.R. Munro	accessed from CDIAC on 08/06/2015
Laurence M. Gould	2013-03-11	2013-04-07	Southern Ocean	4110	Sweeney, C., T. Takahashi, T. Newberger and D.R. Munro	accessed from CDIAC on 08/06/2015
Laurence M. Gould	2013-04-13	2013-05-05	Southern Ocean	4099	Sweeney, C., T. Takahashi, T. Newberger and D.R. Munro	accessed from CDIAC on 08/06/2015
Laurence M. Gould	2013-05-12	2013-05-24	Southern Ocean	3171	Sweeney, C., T. Takahashi, T. Newberger and D.R. Munro	accessed from CDIAC on 08/06/2015
Laurence M. Gould	2013-06-01	2013-07-05	Southern Ocean	3808	Sweeney, C., T. Takahashi, T. Newberger and D.R. Munro	accessed from CDIAC on 08/06/2015
Laurence M. Gould	2013-09-14	2013-09-26	Southern Ocean	3410	Sweeney, C., T. Takahashi, T. Newberger and D.R. Munro	accessed from CDIAC on 08/06/2015
Laurence M. Gould	2013-10-05	2013-10-22	Southern Ocean	2284	Sweeney, C., T. Takahashi, T. Newberger and D.R. Munro	accessed from CDIAC on 08/06/2015

Table A1. Continued.

Vessel	Start date yyyy-mm-dd	End date yyyy-mm-dd	Regions	No. of samples	Principal Investigators	DOI (if available)/comment
Laurence M. Gould	2013-10-28	2013-11-15	Southern Ocean	3788	Sweeney, C., T. Takahashi, T. Newberger and D.R. Munro	accessed from CDIAC on 08/06/2015
Laurence M. Gould	2013-11-23	2013-12-19	Southern Ocean	7535	Sweeney, C., T. Takahashi, T. Newberger and D.R. Munro	accessed from CDIAC on 08/06/2015
Laurence M. Gould	2014-01-01	2014-02-07	Southern Ocean	11 783	Sweeney, C., T. Takahashi, T. Newberger and D.R. Munro	
Laurence M. Gould	2014-02-14	2014-03-16	Southern Ocean	5805	Sweeney, C., T. Takahashi, T. Newberger and D.R. Munro	
Laurence M. Gould	2014-03-22	2014-04-03	Southern Ocean	1109	Sweeney, C., T. Takahashi, T. Newberger and D.R. Munro	
Laurence M. Gould	2014-04-09	2014-05-10	Southern Ocean	3170	Sweeney, C., T. Takahashi, T. Newberger and D.R. Munro	
Laurence M. Gould	2014-06-23	2014-08-21	Southern Ocean	3615	Sweeney, C., T. Takahashi, T. Newberger and D.R. Munro	
Laurence M. Gould	2014-09-14	2014-09-26	Southern Ocean	2058	Sweeney, C., T. Takahashi, T. Newberger and D.R. Munro	
Laurence M. Gould	2014-10-08	2014-10-20	Southern Ocean	1642	Sweeney, C., T. Takahashi, T. Newberger and D.R. Munro	
Laurence M. Gould	2014-10-28	2014-11-22	Southern Ocean	6921	Sweeney, C., T. Takahashi, T. Newberger and D.R. Munro	
Laurence M. Gould	2014-11-28	2014-12-20	Southern Ocean	6476	Sweeney, C., T. Takahashi, T. Newberger and D.R. Munro	
Marion Dufresne	2014-01-09	2014-02-16	Indian Ocean, Southern Ocean	7524	Metzl, N. and C. Lo Monaco	
Mirai	2012-11-28	2013-02-13	Southern Ocean	4832	Murata, A.	
Mooring	2012-08-22	2013-07-09	North Atlantic	1507	Sutton, A.	doi:10.3334/CDIAC/OTG.TSM_NH_70W_43N
Mooring	2013-10-04	2014-04-29	North Pacific	1651	Sutton, A.	doi:10.3334/CDIAC/otg.TSM_LaPush_125W_48N
Mooring	2012-11-02	2013-06-06	Tropical Pacific	1257	Sutton, A.	
Mooring	2013-06-06	2013-11-28	Tropical Pacific	1415	Sutton, A.	
New Century 2	2014-08-11	2014-09-08	North Atlantic, Tropical Atlantic, North Pacific, Tropical Pacific	2698	Nakaoka, S.	
New Century 2	2014-12-12	2015-01-12	North Atlantic, Tropical Atlantic, North Pacific, Tropical Pacific	1811	Nakaoka, S.	
New Century 2	2014-04-11	2014-04-26	North Pacific	1608	Nakaoka, S.	
New Century 2	2014-04-27	2014-05-10	North Pacific	1442	Nakaoka, S.	
New Century 2	2014-05-13	2014-05-27	North Pacific	1408	Nakaoka, S.	
New Century 2	2014-05-28	2014-06-09	North Pacific	1392	Nakaoka, S.	
New Century 2	2014-06-12	2014-06-25	North Pacific	1220	Nakaoka, S.	
New Century 2	2014-06-25	2014-07-05	North Pacific	1174	Nakaoka, S.	
New Century 2	2014-09-10	2014-09-24	North Pacific	1108	Nakaoka, S.	
New Century 2	2014-09-25	2014-10-07	North Pacific	1004	Nakaoka, S.	
New Century 2	2014-10-11	2014-10-27	North Pacific	1001	Nakaoka, S.	
New Century 2	2014-10-28	2014-11-09	North Pacific	1174	Nakaoka, S.	
New Century 2	2014-07-14	2014-08-10	North Pacific, Tropical Pacific	2167	Nakaoka, S.	
New Century 2	2014-11-14	2014-12-12	North Pacific, Tropical Pacific	2391	Nakaoka, S.	
Nuka Arctica	2014-07-07	2014-07-15	Arctic, North Atlantic	2333	Omar, A., A. Olsen and T. Johannessen	
Nuka Arctica	2014-08-27	2014-09-05	Arctic, North Atlantic	2607	Omar, A., A. Olsen and T. Johannessen	
Nuka Arctica	2014-09-08	2014-09-18	Arctic, North Atlantic	2398	Omar, A., A. Olsen and T. Johannessen	
Nuka Arctica	2014-01-06	2014-01-12	Arctic, North Atlantic	2369	Omar, A., A. Olsen and T. Johannessen	
Nuka Arctica	2014-01-14	2014-01-24	Arctic, North Atlantic	2728	Omar, A., A. Olsen and T. Johannessen	
Nuka Arctica	2014-01-24	2014-02-01	Arctic, North Atlantic	1990	Omar, A., A. Olsen and T. Johannessen	
Nuka Arctica	2014-02-04	2014-02-14	Arctic, North Atlantic	2661	Omar, A., A. Olsen and T. Johannessen	
Nuka Arctica	2014-02-15	2014-02-22	Arctic, North Atlantic	2030	Omar, A., A. Olsen and T. Johannessen	
Nuka Arctica	2014-02-26	2014-03-05	Arctic, North Atlantic	2179	Omar, A., A. Olsen and T. Johannessen	
Nuka Arctica	2014-03-07	2014-03-13	Arctic, North Atlantic	2311	Omar, A., A. Olsen and T. Johannessen	
Nuka Arctica	2014-03-18	2014-03-27	Arctic, North Atlantic	3262	Omar, A., A. Olsen and T. Johannessen	
Nuka Arctica	2014-03-29	2014-04-05	Arctic, North Atlantic	2799	Omar, A., A. Olsen and T. Johannessen	
Nuka Arctica	2014-04-09	2014-04-17	Arctic, North Atlantic	3136	Omar, A., A. Olsen and T. Johannessen	

Table A1. Continued.

Vessel	Start date yyyy-mm-dd	End date yyyy-mm-dd	Regions	No. of samples	Principal Investigators	DOI (if available)/comment
Nuka Arctica	2014-04-18	2014-04-25	Arctic, North Atlantic	2429	Omar, A., A. Olsen and T. Johannessen	
Nuka Arctica	2014-05-13	2014-05-18	Arctic, North Atlantic	1420	Omar, A., A. Olsen and T. Johannessen	
Nuka Arctica	2014-05-23	2014-05-31	Arctic, North Atlantic	1191	Omar, A., A. Olsen and T. Johannessen	
Nuka Arctica	2014-06-11	2014-06-12	Arctic, North Atlantic	274	Omar, A., A. Olsen and T. Johannessen	
Nuka Arctica	2014-06-13	2014-06-22	Arctic, North Atlantic	3077	Omar, A., A. Olsen and T. Johannessen	
Nuka Arctica	2014-07-26	2014-08-05	Arctic, North Atlantic	3362	Omar, A., A. Olsen and T. Johannessen	
Nuka Arctica	2014-08-08	2014-08-14	Arctic, North Atlantic	2266	Omar, A., A. Olsen and T. Johannessen	
Nuka Arctica	2014-08-15	2014-08-23	Arctic, North Atlantic	2483	Omar, A., A. Olsen and T. Johannessen	
Nuka Arctica	2014-09-20	2014-09-28	Arctic, North Atlantic	1931	Omar, A., A. Olsen and T. Johannessen	
Nuka Arctica	2014-09-28	2014-10-06	Arctic, North Atlantic	769	Omar, A., A. Olsen and T. Johannessen	
Nuka Arctica	2014-10-08	2014-10-16	Arctic, North Atlantic	1029	Omar, A., A. Olsen and T. Johannessen	
Nuka Arctica	2014-10-17	2014-10-24	Arctic, North Atlantic	1540	Omar, A., A. Olsen and T. Johannessen	
Nuka Arctica	2014-10-28	2014-11-06	Arctic, North Atlantic	648	Omar, A., A. Olsen and T. Johannessen	
Nuka Arctica	2014-11-20	2014-11-28	Arctic, North Atlantic	1451	Omar, A., A. Olsen and T. Johannessen	
Polarstern	2014-07-07	2014-08-02	Arctic	25 088	van Heuven, S. and M. Hoppema	
Polarstern	2014-08-05	2014-10-04	Arctic	55 349	van Heuven, S. and M. Hoppema	
Polarstern	2014-06-08	2014-06-30	Arctic, North Atlantic	20 871	van Heuven, S. and M. Hoppema	
Polarstern	2014-03-09	2014-04-12	North Atlantic, Tropical Atlantic, Southern Ocean	32 939	van Heuven, S. and M. Hoppema	
Polarstern	2014-10-26	2014-11-28	North Atlantic, Tropical Atlantic, Southern Ocean	30 655	van Heuven, S. and M. Hoppema	
Polarstern	2013-12-21	2014-03-04	Southern Ocean	69 740	van Heuven, S. and M. Hoppema	
Polarstern	2014-12-03	2015-01-31	Southern Ocean	28 299	van Heuven, S. and M. Hoppema	
Pourquoi Pas?	2014-05-17	2014-06-28	North Atlantic	2835	Padin, X.A. and F.F. Pérez	
Reykjafoss	2013-09-06	2013-09-17	North Atlantic	3481	Wanninkhof, R., D. Pierrot and L. Barbero	
Reykjafoss	2013-09-19	2013-09-30	North Atlantic	3991	Wanninkhof, R., D. Pierrot and L. Barbero	
Reykjafoss	2013-10-17	2013-10-25	North Atlantic	2291	Wanninkhof, R., D. Pierrot and L. Barbero	
Reykjafoss	2013-10-31	2013-11-08	North Atlantic	2715	Wanninkhof, R., D. Pierrot and L. Barbero	
Ronald H. Brown	2013-10-20	2013-10-30	Tropical Atlantic	4608	Wanninkhof, R., D. Pierrot and L. Barbero	doi:10.3334/CDIAC/OTG.VOS_RB_2013
Ronald H. Brown	2014-02-28	2014-03-13	Tropical Pacific	6052	Wanninkhof, R., D. Pierrot and L. Barbero	doi:10.3334/CDIAC/OTG.VOS_RB_2014
Santa Cruz	2014-01-17	2014-01-30	North Atlantic, Tropical Atlantic	5258	Lefèvre, N. and D. Diverrès	
Santa Cruz	2014-02-19	2014-02-28	North Atlantic, Tropical Atlantic	3251	Lefèvre, N. and D. Diverrès	
Simon Stevin	2014-08-20	2014-08-20	North Atlantic	31 827	Gkritzalis, T.	
Simon Stevin	2014-08-21	2014-08-21	North Atlantic	30 640	Gkritzalis, T.	
Simon Stevin	2014-08-22	2014-08-22	North Atlantic	5382	Gkritzalis, T.	
Simon Stevin	2014-08-25	2014-08-25	North Atlantic	508	Gkritzalis, T.	
Simon Stevin	2014-08-27	2014-08-27	North Atlantic	28 904	Gkritzalis, T.	
Simon Stevin	2014-08-28	2014-08-28	North Atlantic	15 148	Gkritzalis, T.	
Simon Stevin	2014-08-29	2014-08-29	North Atlantic	12 492	Gkritzalis, T.	
Simon Stevin	2014-09-01	2014-09-01	North Atlantic	21 372	Gkritzalis, T.	
Simon Stevin	2014-09-03	2014-09-03	North Atlantic	23069	Gkritzalis, T.	
Simon Stevin	2014-09-08	2014-09-08	North Atlantic	24 445	Gkritzalis, T.	
Simon Stevin	2014-10-22	2014-10-23	North Atlantic	28 397	Gkritzalis, T.	
Simon Stevin	2014-10-24	2014-10-24	North Atlantic	11 920	Gkritzalis, T.	
Skogafoss	2014-03-17	2014-04-11	North Atlantic	10 168	Wanninkhof, R., D. Pierrot and L. Barbero	doi:10.3334/CDIAC/OTG.VOS_SKO2014
Skogafoss	2014-05-10	2014-06-05	North Atlantic	11 010	Wanninkhof, R., D. Pierrot and L. Barbero	doi:10.3334/CDIAC/OTG.VOS_SKO2014

Table A1. Continued.

Vessel	Start date yyyy-mm-dd	End date yyyy-mm-dd	Regions	No. of samples	Principal Investigators	DOI (if available)/comment
Skogafoss	2014-06-07	2014-06-28	North Atlantic	6702	Wanninkhof, R., D. Pierrot and L. Barbero	doi:10.3334/CDIAC/OTG.VOS_SKO2014
Skogafoss	2014-06-29	2014-07-26	North Atlantic	7280	Wanninkhof, R., D. Pierrot and L. Barbero	doi:10.3334/CDIAC/OTG.VOS_SKO2014
Skogafoss	2014-07-27	2014-08-21	North Atlantic	5528	Wanninkhof, R., D. Pierrot and L. Barbero	doi:10.3334/CDIAC/OTG.VOS_SKO2014
Skogafoss	2014-08-22	2014-09-01	North Atlantic	3601	Wanninkhof, R., D. Pierrot and L. Barbero	doi:10.3334/CDIAC/OTG.VOS_SKO2014
Soyo-maru	2013-12-08	2013-12-19	North Pacific	10 583	Ichikawa, T. and T. Ono	
Soyo-maru	2014-02-10	2014-02-24	North Pacific	15 841	Ichikawa, T. and T. Ono	
Soyo-maru	2014-03-02	2014-03-09	North Pacific	9589	Ichikawa, T. and T. Ono	
Soyo-maru	2014-05-10	2014-05-18	North Pacific	9608	Ichikawa, T. and T. Ono	
Soyo-maru	2014-05-24	2014-06-19	North Pacific	29 872	Ichikawa, T. and T. Ono	
Soyo-maru	2014-08-22	2014-08-26	North Pacific	4162	Ichikawa, T. and T. Ono	
Soyo-maru	2014-01-24	2014-01-30	North Pacific, Tropical Pacific	8784	Ichikawa, T. and T. Ono	
Trans Future 5	2013-08-26	2013-08-27	North Pacific	58	Nakaoka, S. and Y. Nojiri	
Trans Future 5	2013-09-27	2013-09-27	North Pacific	63	Nakaoka, S. and Y. Nojiri	
Trans Future 5	2013-11-04	2013-11-05	North Pacific	58	Nakaoka, S. and Y. Nojiri	
Trans Future 5	2013-11-08	2013-11-09	North Pacific	52	Nakaoka, S. and Y. Nojiri	
Trans Future 5	2013-12-16	2013-12-16	North Pacific	56	Nakaoka, S. and Y. Nojiri	
Trans Future 5	2013-12-20	2013-12-20	North Pacific	56	Nakaoka, S. and Y. Nojiri	
Trans Future 5	2014-02-10	2014-02-10	North Pacific	77	Nakaoka, S. and Y. Nojiri	
Trans Future 5	2014-02-14	2014-02-15	North Pacific	41	Nakaoka, S. and Y. Nojiri	
Trans Future 5	2014-03-24	2014-03-25	North Pacific	63	Nakaoka, S. and Y. Nojiri	
Trans Future 5	2014-03-28	2014-03-29	North Pacific	61	Nakaoka, S. and Y. Nojiri	
Trans Future 5	2014-05-06	2014-05-07	North Pacific	73	Nakaoka, S. and Y. Nojiri	
Trans Future 5	2014-05-09	2014-05-09	North Pacific	59	Nakaoka, S. and Y. Nojiri	
Trans Future 5	2014-06-16	2014-06-17	North Pacific	70	Nakaoka, S. and Y. Nojiri	
Trans Future 5	2014-06-20	2014-06-20	North Pacific	61	Nakaoka, S. and Y. Nojiri	
Trans Future 5	2014-07-28	2014-07-29	North Pacific	71	Nakaoka, S. and Y. Nojiri	
Trans Future 5	2014-08-01	2014-08-01	North Pacific	50	Nakaoka, S. and Y. Nojiri	
Trans Future 5	2014-09-08	2014-09-08	North Pacific	55	Nakaoka, S. and Y. Nojiri	
Trans Future 5	2014-09-12	2014-09-12	North Pacific	54	Nakaoka, S. and Y. Nojiri	
Trans Future 5	2014-10-20	2014-10-21	North Pacific	53	Nakaoka, S. and Y. Nojiri	
Trans Future 5	2014-10-24	2014-10-24	North Pacific	55	Nakaoka, S. and Y. Nojiri	
Trans Future 5	2014-12-01	2014-12-01	North Pacific	52	Nakaoka, S. and Y. Nojiri	
Trans Future 5	2014-12-05	2014-12-05	North Pacific	53	Nakaoka, S. and Y. Nojiri	
Trans Future 5	2013-09-28	2013-10-09	North Pacific, Tropical Pacific	1118	Nakaoka, S. and Y. Nojiri	
Trans Future 5	2013-11-09	2013-11-18	North Pacific, Tropical Pacific	1104	Nakaoka, S. and Y. Nojiri	
Trans Future 5	2013-12-21	2014-01-02	North Pacific, Tropical Pacific	1168	Nakaoka, S. and Y. Nojiri	
Trans Future 5	2014-02-16	2014-02-25	North Pacific, Tropical Pacific	1122	Nakaoka, S. and Y. Nojiri	
Trans Future 5	2014-03-30	2014-04-09	North Pacific, Tropical Pacific	1121	Nakaoka, S. and Y. Nojiri	
Trans Future 5	2014-05-10	2014-05-19	North Pacific, Tropical Pacific	1159	Nakaoka, S. and Y. Nojiri	
Trans Future 5	2014-06-21	2014-07-02	North Pacific, Tropical Pacific	1124	Nakaoka, S. and Y. Nojiri	
Trans Future 5	2014-08-02	2014-08-11	North Pacific, Tropical Pacific	1142	Nakaoka, S. and Y. Nojiri	
Trans Future 5	2014-10-25	2014-11-04	North Pacific, Tropical Pacific	1086	Nakaoka, S. and Y. Nojiri	
Trans Future 5	2014-12-06	2014-12-15	North Pacific, Tropical Pacific	1104	Nakaoka, S. and Y. Nojiri	
Trans Future 5	2013-10-23	2013-11-03	North Pacific, Tropical Pacific, Southern Ocean	1432	Nakaoka, S. and Y. Nojiri	
Trans Future 5	2013-12-03	2013-12-15	North Pacific, Tropical Pacific, Southern Ocean	1434	Nakaoka, S. and Y. Nojiri	
Trans Future 5	2014-01-25	2014-02-07	North Pacific, Tropical Pacific, Southern Ocean	1558	Nakaoka, S. and Y. Nojiri	
Trans Future 5	2014-03-12	2014-03-23	North Pacific, Tropical Pacific, Southern Ocean	1451	Nakaoka, S. and Y. Nojiri	
Trans Future 5	2014-04-24	2014-05-05	North Pacific, Tropical Pacific, Southern Ocean	1381	Nakaoka, S. and Y. Nojiri	
Trans Future 5	2014-06-03	2014-06-15	North Pacific, Tropical Pacific, Southern Ocean	1456	Nakaoka, S. and Y. Nojiri	

Table A1. Continued.

Vessel	Start date yyyy-mm-dd	End date yyyy-mm-dd	Regions	No. of samples	Principal Investigators	DOI (if available)/comment
Trans Future 5	2014-07-16	2014-07-27	North Pacific, Tropical Pacific, Southern Ocean	1415	Nakaoka, S. and Y. Nojiri	
Trans Future 5	2014-08-27	2014-09-07	North Pacific, Tropical Pacific, Southern Ocean	1405	Nakaoka, S. and Y. Nojiri	
Trans Future 5	2014-10-06	2014-10-19	North Pacific, Tropical Pacific, Southern Ocean	1422	Nakaoka, S. and Y. Nojiri	
Trans Future 5	2014-11-18	2014-11-29	North Pacific, Tropical Pacific, Southern Ocean	809	Nakaoka, S. and Y. Nojiri	
Trans Future 5	2014-09-23	2014-10-05	Southern Ocean	196	Nakaoka, S. and Y. Nojiri	
Trans Future 5	2013-10-09	2013-10-21	Tropical Pacific, Southern Ocean	880	Nakaoka, S. and Y. Nojiri	
Trans Future 5	2013-11-19	2013-12-01	Tropical Pacific, Southern Ocean	921	Nakaoka, S. and Y. Nojiri	
Trans Future 5	2014-01-02	2014-01-17	Tropical Pacific, Southern Ocean	1000	Nakaoka, S. and Y. Nojiri	
Trans Future 5	2014-02-25	2014-03-10	Tropical Pacific, Southern Ocean	909	Nakaoka, S. and Y. Nojiri	
Trans Future 5	2014-04-10	2014-04-23	Tropical Pacific, Southern Ocean	941	Nakaoka, S. and Y. Nojiri	
Trans Future 5	2014-05-20	2014-06-01	Tropical Pacific, Southern Ocean	910	Nakaoka, S. and Y. Nojiri	
Trans Future 5	2014-07-02	2014-07-15	Tropical Pacific, Southern Ocean	1027	Nakaoka, S. and Y. Nojiri	
Trans Future 5	2014-08-12	2014-08-25	Tropical Pacific, Southern Ocean	1040	Nakaoka, S. and Y. Nojiri	
Trans Future 5	2014-11-05	2014-11-17	Tropical Pacific, Southern Ocean	853	Nakaoka, S. and Y. Nojiri	
Trans Future 5	2014-12-16	2014-12-30	Tropical Pacific, Southern Ocean	939	Nakaoka, S. and Y. Nojiri	
Wakataka-maru	2014-05-10	2014-05-20	North Pacific	9360	Kuwata, A. and K. Tadokoro	
Wakataka-maru	2014-06-05	2014-06-11	North Pacific	9025	Kuwata, A. and K. Tadokoro	
Walton Smith	2013-03-31	2013-04-18	North Atlantic, Tropical Atlantic	8392	Millero, F.	
Walton Smith	2013-04-19	2013-04-28	North Atlantic, Tropical Atlantic	4890	Millero, F.	
Walton Smith	2014-04-28	2014-05-25	North Atlantic, Tropical Atlantic	12 666	Millero, F.	
Walton Smith	2013-05-25	2013-05-27	Tropical Atlantic	898	Millero, F.	
Walton Smith	2013-06-13	2013-06-15	Tropical Atlantic	1214	Millero, F.	
Walton Smith	2013-06-20	2013-06-27	Tropical Atlantic	2883	Millero, F.	
Walton Smith	2013-07-06	2013-07-18	Tropical Atlantic	5529	Millero, F.	
Walton Smith	2013-08-13	2013-08-28	Tropical Atlantic	7900	Millero, F.	
Walton Smith	2013-10-08	2013-10-09	Tropical Atlantic	509	Millero, F.	
Walton Smith	2013-10-17	2013-10-18	Tropical Atlantic	707	Millero, F.	
Walton Smith	2013-12-20	2013-12-21	Tropical Atlantic	748	Millero, F.	
Walton Smith	2014-04-22	2014-04-22	Tropical Atlantic	214	Millero, F.	
Walton Smith	2014-04-23	2014-04-24	Tropical Atlantic	657	Millero, F.	
Walton Smith	2014-04-26	2014-04-26	Tropical Atlantic	155	Millero, F.	

Data availability

The data presented here are made available in the belief that their wide dissemination will lead to greater understanding and new scientific insights of how the carbon cycle works, how humans are altering it, and how we can mitigate the resulting human-driven climate change. The free availability of these data does not constitute permission for publication of the data. For research projects, if the data are essential to the work, or if an important result or conclusion depends on the data, co-authorship may need to be considered. Full contact details and information on how to cite the data are given at the top of each page in the accompanying database, and summarised in Table 2.

The accompanying database includes two Excel files organised in the following spreadsheets (accessible with the free viewer http://www.microsoft.com/en-us/download/details.aspx?id=10):

The file Global_Carbon_Budget_2015.xlsx includes

1. a summary;
2. the global carbon budget (1959–2014);
3. global CO_2 emissions from fossil fuels and cement production by fuel type, and the per-capita emissions (1959–2014);
4. CO_2 emissions from land-use change from the individual methods and models (1959–2014);
5. ocean CO_2 sink from the individual ocean models and data products (1959–2014);
6. terrestrial residual CO_2 sink from the DGVMs (1959–2014);
7. additional information on the carbon balance prior to 1959 (1750–2014).

The file National_Carbon_Emissions_2015.xlsx includes

1. a summary;
2. territorial country CO_2 emissions from fossil fuels and industry (1959–2014) from CDIAC, extended to 2014 using BP data;
3. territorial country CO_2 emissions from fossil fuels and industry (1959–2014) from CDIAC with UNFCCC data overwritten where available, extended to 2014 using BP data;
4. consumption country CO_2 emissions from fossil fuels and industry and emissions transfer from the international trade of goods and services (1990–2013) using CDIAC/UNFCCC data (worksheet 3 above) as reference;
5. emissions transfers (consumption minus territorial emissions; 1990–2013);
6. country definitions.

National emissions data are also available from the Global Carbon Atlas (http://globalcarbonatlas.org).

Acknowledgements. We thank all people and institutions who provided the data used in this carbon budget, as well as P. Cadule, C. Enright, J. Ghattas, G. Hurtt, L. Mercado, S. Shu, and S. Jones for support with the model simulations and data analysis, and F. Joos and S. Khatiwala for providing historical data. We thank E. Dlugokencky, who provided the atmospheric and oceanographic CO_2 measurements used here, and all those involved in collecting and providing oceanographic data CO_2 measurements used here, in particular for the ocean data for years 2013–2014 that are not included in SOCAT v3: M. Becker, A. Körtzinger, S. Alin, G. Lebon, D. Diverrès, R. Wanninkhof, M. Glockzin, I. Skjelvan, I. Brown, C. Sweeney, C. Lo Monaco, A. Omar, T. Johannessen, M. Hoppema, X. A. Padin, T. Ichikawa, A. Kuwata, and K. Tadokoro. We thank the institutions and funding agencies responsible for the collection and quality control of the data included in SOCAT, and the support of the International Ocean Carbon Coordination Project (IOCCP), the Surface Ocean Lower Atmosphere Study (SOLAS), and the Integrated Marine Biogeochemistry, Ecosystem Research programme (IMBER) and UK Natural Environment Research Council (NERC) projects including National Capability, Ocean Acidification, Greenhouse Gases and Shelf Seas Biogeochemistry. We thank W. Peters for CTE2015 model simulations, and all data providers to ObsPack GLOBALVIEWplus v1.0 for atmospheric CO_2 observations.

NERC provided funding to C. Le Quéré, R. Moriarty, and the GCP through their International Opportunities Fund specifically to support this publication (NE/103002X/1). G. P. Peters and R. M. Andrew were supported by the Norwegian Research Council (236296). J. G. Canadell was supported by the Australian Climate Change Science Programme. S. Sitch was supported by EU FP7 for funding through projects LUC4C (GA603542). R. J. Andres was supported by US Department of Energy, Office of Science, Biological and Environmental Research (BER) programmes under US Department of Energy contract DE-AC05-00OR22725. T. A. Boden was supported by US Department of Energy, Office of Science, Biological and Environmental Research (BER) programmes under US Department of Energy contract DE-AC05-00OR22725. J. I. House was supported by the Leverhulme foundation and the EU FP7 through project LUC4C (GA603542). P. Friedlingstein was supported by the EU FP7 for funding through projects LUC4C (GA603542) and EMBRACE (GA282672). A. Arneth was supported by the EU FP7 for funding through LUC4C (603542), and the Helmholtz foundation and its ATMO programme. D. C. E. Bakker was supported by the EU FP7 for funding through project CARBOCHANGE (284879), the UK Ocean Acidification Research Programme (NE/H017046/1; funded by the Natural Environment Research Council, the Department for Energy and Climate Change and the Department for Environment, Food and Rural Affairs). L. Barbero was supported by NOAA's Ocean Acidification Program and acknowledges

support for this work from the National Aeronautics and Space Administration (NASA) ROSES Carbon Cycle Science under NASA grant 13-CARBON13_2-0080. P. Ciais acknowledges support from the European Research Council through Synergy grant ERC-2013-SyG-610028 "IMBALANCE-P". M. Fader was supported by the EU FP7 for funding through project LUC4C (GA603542). J. Hauck was supported by the Helmholtz Postdoc Programme (Initiative and Networking Fund of the Helmholtz Association). R. A. Feely and A. J. Sutton were supported by the Climate Observation Division, Climate Program Office, NOAA, US Department of Commerce. A. K. Jain was supported by the US National Science Foundation (NSF AGS 12-43071) the US Department of Energy, Office of Science and BER programmes (DOE DE-SC0006706) and NASA LCLUC programme (NASA NNX14AD94G). E. Kato was supported by the ERTDF (S-10) from the Ministry of Environment, Japan. K. Klein Goldewijk was supported by the Dutch NWO VENI grant no. 863.14.022. S. K. Lauvset was supported by the project "Monitoring ocean acidification in Norwegian waters" from the Norwegian Ministry of Climate and Environment. V. Kitidis was supported by the EU FP7 for funding through project CARBOCHANGE (264879). C. Koven was supported by the Director, Office of Science, Office of Biological and Environmental Research of the US Department of Energy under contract no. DE-AC02-05CH11231 as part of their Regional and Global Climate Modeling Program. P. Landschützer was supported by GEOCarbon. I. T. van der Lann-Luijkx received financial support from OCW/NWO for ICOS-NL and computing time from NWO (SH-060-13). I. D. Lima was supported by the US National Science Foundation (NSF AGS-1048827). N. Metzl was supported by Institut National des Sciences de l'Univers (INSU) and Institut Paul Emile Victor (IPEV) for OISO cruises. D. R. Munro was supported by the US National Science Foundation (NSF PLR-1341647 and NSF AOAS-0944761). J. E. M. S. Nabel was supported by the German Research Foundation's Emmy Noether Programme (PO1751/1-1) and acknowledges Julia Pongratz and Kim Naudts for their contributions. Y. Nojiri and S. Nakaoka were supported by the Global Environment Research Account for National Institutes (1432) by the Ministry of Environment of Japan. A. Olsen appreciates support from the Norwegian Research Council (SNACS, 229752). F. F. Pérez were supported by BOCATS (CTM2013-41048-P) project co-founded by the Spanish government and the Fondo Europeo de Desarrollo Regional (FEDER). B. Pfeil was supported through the European Union's Horizon 2020 research and innovation programme AtlantOS under grant agreement no. 633211. D. Pierrot was supported by NOAA through the Climate Observation Division of the Climate Program Office. B. Poulter was supported by the EU FP7 for funding through GEOCarbon. G. Rehder was supported by BMBF (Bundesministerium für Bildung und Forschung) through project ICOS, grant no. 01LK1224D. U. Schuster was supported by NERC UKOARP (NE/H017046/1), NERC RAGANRoCC (NE/K002473/1), the European Space Agency (ESA) OceanFlux Evolution project, and EU FP7 CARBOCHANGE (264879). T. Steinhoff was supported by ICOS-D (BMBF FK 01LK1101C) and EU FP7 for funding through project CARBOCHANGE (264879). J. Schwinger was supported by the Research Council of Norway through project EVA (229771), and acknowledges the Norwegian Metacenter for Computational Science (NOTUR, project nn2980k), and the Norwegian Storage Infrastructure (NorStore, project ns2980k) for supercomputer time and storage resources. T. Takahashi was supported by grants from NOAA and the Comer Education and Science Foundation. B. Tilbrook was supported by the Australian Department of Environment and the Integrated Marine Observing System. B. D. Stocker was supported by the Swiss National Science Foundation and FP7 funding through project EMBRACE (282672). S. van Heuven was supported by the EU FP7 for funding through project CARBOCHANGE (264879). G. R. van der Werf was supported by the European Research Council (280061). A. Wiltshire was supported by the Joint UK DECC/Defra Met Office Hadley Centre Climate Programme (GA01101) and EU FP7 Funding through project LUC4C (603542). S. Zaehle was supported by the European Research Council (ERC) under the European Union's Horizon 2020 research and innovation programme (QUINCY; grant agreement no. 647204). ISAM (PI: Atul K. Jain) simulations were carried out at the National Energy Research Scientific Computing Center (NERSC), which is supported by the US DOE under contract DE-AC02-05CH11231. Contributions from the Scripps Institution of Oceanography were supported under DoE grant DE-SC0012167 and by Schmidt Philanthropies. This is NOAA-PMEL contribution number 4400.

Edited by: D. Carlson

References

Achard, F. and House, J. I.: Reporting Carbon losses from tropical deforestation with Pan-tropical biomass maps, Environ. Res. Lett., 10, 101002, 2015.

Achard, F., Beuchle, R., Mayaux, P., Stibig, H. J., Bodart, C., Brink, A., Carboni, S., Desclée, B., Donnay, F., and Eva, H.: Determination of tropical deforestation rates and related carbon losses from 1990 to 2010, Glob. Change Biol., 20, 2540–2554, 2014.

Andres, R. J., Fielding, D. J., Marland, G., Boden, T. A., Kumar, N., and Kearney, A. T.: Carbon dioxide emissions from fossil fuel use, 1751–1950, Tellus, 51, 759–765, 1999.

Andres, R. J., Boden, T. A., Bréon, F.-M., Ciais, P., Davis, S., Erickson, D., Gregg, J. S., Jacobson, A., Marland, G., Miller, J., Oda, T., Olivier, J. G. J., Raupach, M. R., Rayner, P., and Treanton, K.: A synthesis of carbon dioxide emissions from fossil-fuel combustion, Biogeosciences, 9, 1845–1871, doi:10.5194/bg-9-1845-2012, 2012.

Andres, R. J., Boden, T., and Higdon, D.: A new evaluation of the uncertainty associated with CDIAC estimates of fossil fuel carbon dioxide emission, Tellus B, 66, 23616, doi:10.3402/tellusb.v66.23616, 2014.

Andrew, R. M. and Peters, G. P.: A multi-region input-output table based on the Global Trade Analysis Project Database (GTAP-MRIO), Economic Systems Research, 25, 99–121, 2013.

Archer, D., Eby, M., Brovkin, V., Ridgwell, A., Cao, L., Mikolajewicz, U., Caldeira, K., Munhoven, G., Montenegro, A., and Tokos, K.: Atmospheric Lifetime of Fossil Fuel Carbon Dioxide, Annu. Rev. Earth Pl. Sc., 37, 117–134, 2009.

Arora, V. and Boer, G.: A parameterization of leaf phenology for the terrestrialecosystem component of climate models, Glob. Change Biol., 11, 39–59, 2005.

Assmann, K. M., Bentsen, M., Segschneider, J., and Heinze, C.: An isopycnic ocean carbon cycle model, Geosci. Model Dev., 3, 143–167, doi:10.5194/gmd-3-143-2010, 2010.

Atlas, R., Hoffman, R. N., Ardizzone, J., Leidner, S. M., Jusem, J. C., Smith, D. K., and Gombos, D.: A cross-calibrated, multiplatform ocean surface wind velocity product for meteorological and oceanographic applications, B. Amer. Meteorol. Soc., 92, 157–174, 2011.

Aumont, O. and Bopp, L.: Globalizing results from ocean in situ iron fertilization studies, Global Biogeochem. Cy., 20, GB2017, doi:10.1029/2005GB002591, 2006.

Baccini, A., Goetz, S. J., Walker, W. S., Laporte, N. T., Sun, M., Sulla-Menashe, D., Hackler, J., Beck, P. S. A., Dubayah, R., Friedl, M. A., Samanta, S., and Houghton, R. A.: Estimated carbon dioxide emissions from tropical deforestation improved by carbon-density maps, Nature Clim. Change, 2, 182–186, 2012.

Bakker, D. C. E., Pfeil, B., Smith, K., Hankin, S., Olsen, A., Alin, S. R., Cosca, C., Harasawa, S., Kozyr, A., Nojiri, Y., O'Brien, K. M., Schuster, U., Telszewski, M., Tilbrook, B., Wada, C., Akl, J., Barbero, L., Bates, N. R., Boutin, J., Bozec, Y., Cai, W.-J., Castle, R. D., Chavez, F. P., Chen, L., Chierici, M., Currie, K., de Baar, H. J. W., Evans, W., Feely, R. A., Fransson, A., Gao, Z., Hales, B., Hardman-Mountford, N. J., Hoppema, M., Huang, W.-J., Hunt, C. W., Huss, B., Ichikawa, T., Johannessen, T., Jones, E. M., Jones, S. D., Jutterström, S., Kitidis, V., Körtzinger, A., Landschützer, P., Lauvset, S. K., Lefèvre, N., Manke, A. B., Mathis, J. T., Merlivat, L., Metzl, N., Murata, A., Newberger, T., Omar, A. M., Ono, T., Park, G.-H., Paterson, K., Pierrot, D., Ríos, A. F., Sabine, C. L., Saito, S., Salisbury, J., Sarma, V. V. S. S., Schlitzer, R., Sieger, R., Skjelvan, I., Steinhoff, T., Sullivan, K. F., Sun, H., Sutton, A. J., Suzuki, T., Sweeney, C., Takahashi, T., Tjiputra, J., Tsurushima, N., van Heuven, S. M. A. C., Vandemark, D., Vlahos, P., Wallace, D. W. R., Wanninkhof, R., and Watson, A. J.: An update to the Surface Ocean CO_2 Atlas (SOCAT version 2), Earth Syst. Sci. Data, 6, 69–90, doi:10.5194/essd-6-69-2014, 2014.

Bakker, D. C. E., Pfeil, B., Smith, K., Harasawa, S., Landa, C., Nakaoka, S., Nojiri, Y., Metzl, N., O'Brien, K. M., Olsen, A., Schuster, U., Tilbrook, B., Wanninkhof, R., Alin, S. R., Barbero, L., Bates, N. R., Bianchi, A. A., Bonou, F., Boutin, J., Bozec, Y., Burger, E., Cai, W.-J., Castle, R. D., Chen, L., Chierici, M., Cosca, C., Currie, K., Evans, W., Featherstone, C., Feely, R. A., Fransson, A., Greenwood, N., Gregor, L., Hankin, S., Hardman-Mountford, N. J., Harlay, J., Hauck, J., Hoppema, M., Humphreys, M., Hunt, C. W., Ibánhez, J. S. P., Johannessen, T., Jones, S. D., Keeling, R., Kitidis, V., Körtzinger, A., Kozyr, A., Krasakopolou, E., Kuwata, A., Landschtzer, P., Lauvset, S. K., Lefèvre, N., Lo Monaco, C., Manke, A. B., Mathis, J. T., Merlivat, L., Monteiro, P., Munro, D., Murata, A., Newberger, T., Omar, A. M., Ono, T., Paterson, K., Pierrot, D., Robbins, L. L., Sabine, C. L., Saito, S., Salisbury, J., Schneider, B., Schlitzer, R., Sieger, R., Skjelvan, I., Steinhoff, T., Sullivan, K. F., Sutherland, S. C., Sutton, A. J., Sweeney, C., Tadokoro, K., Takahashi, T., Telszewski, M., van Heuven, S. M. A. C., Vandemark, D., Wada, C., Ward, B., and Watson, A. J.: A 58-year record of high quality data in version 3 of the Surface Ocean CO_2 Atlas (SOCAT), Earth Syst. Sci. Data Discuss., in preparation, 2015.

Ballantyne, A. P., Alden, C. B., Miller, J. B., Tans, P. P., and White, J. W. C.: Increase in observed net carbon dioxide uptake by land and oceans during the last 50 years, Nature, 488, 70–72, 2012.

Ballantyne, A. P., Andres, R., Houghton, R., Stocker, B. D., Wanninkhof, R., Anderegg, W., Cooper, L. A., DeGrandpre, M., Tans, P. P., Miller, J. B., Alden, C., and White, J. W. C.: Audit of the global carbon budget: estimate errors and their impact on uptake uncertainty, Biogeosciences, 12, 2565–2584, doi:10.5194/bg-12-2565-2015, 2015.

Bauer, J. E., Cai, W.-J., Raymond, P. A., Bianchi, T. S., Hopkinson, C. S., and Regnier, P. A. G.: The changing carbon cycle of the coastal ocean, Nature, 504, 61–70, 2013.

Best, M. J., Pryor, M., Clark, D. B., Rooney, G. G., Essery, R .L. H., Ménard, C. B., Edwards, J. M., Hendry, M. A., Porson, A., Gedney, N., Mercado, L. M., Sitch, S., Blyth, E., Boucher, O., Cox, P. M., Grimmond, C. S. B., and Harding, R. J.: The Joint UK Land Environment Simulator (JULES), model description – Part 1: Energy and water fluxes, Geosci. Model Dev., 4, 677–699, doi:10.5194/gmd-4-677-2011, 2011.

Biemans, H., Haddeland, I., Kabat, P., Ludwig, F., Hutjes, R. W. A., Heinke, J., von Bloh, W., and Gerten, D.: Impact of reservoirs on river discharge and irrigation water supply during the 20th century, Water Resour. Res., 47, W03509, doi:10.1029/2009WR008929, 2011.

Boden, T. A., Marland, G., and Andres, R. J.: Global, Regional, and National Fossil-Fuel CO_2 Emissions, Oak Ridge National Laboratory, US Department of Energy, Oak Ridge, Tenn., USA, 2013.

Boden, T. A., Marland, G., and Andres, R. J.: Global, Regional, and National Fossil-Fuel CO_2 Emissions, Oak Ridge National Laboratory, US Department of Energy, Oak Ridge, Tenn., USA, 2015.

Bondeau, A., Smith, P., Zaehle, S., Schaphoff, S., Lucht, W., Cramer, W., Gerten, D., Lotze-Campen, H., Müller, C., Reichstein, M., and Smith, B.: Modelling the role of agriculture for the 20th century global terrestrial carbon balance, Glob. Change Biol., 13, 1–28, 2007.

BP: Statistical Review of World Energy 2015, available at: http://www.bp.com/en/global/corporate/about-bp/energy-economics/statistical-review-of-world-energy.html, last access: 5 October 2015.

Bruno, M. and Joos, F.: Terrestrial carbon storage during the past 200 years: A monte carlo analysis of CO_2 data from ice core and atmospheric measurements, Global Biogeochem. Cy., 11, 111–124, 1997.

Buitenhuis, E. T., Rivkin, R. B., Sailley, S., and Le Quéré, C.: Biogeochemical fluxes through microzooplankton, Global Biogeochem. Cy., 24, Gb4015, doi:10.1029/2009gb003601, 2010.

Canadell, J., Ciais, P., Sabine, C., and Joos, F. (Eds.): REgional Carbon Cycle Assessment and Processes (RECCAP), Biogeosciences, http://www.biogeosciences.net/special_issue107.html, 2012–2013.

Canadell, J. G., Le Quéré, C., Raupach, M. R., Field, C. B., Buitenhuis, E. T., Ciais, P., Conway, T. J., Gillett, N. P., Houghton, R. A., and Marland, G.: Contributions to accelerating atmospheric CO_2 growth from economic activity, carbon intensity, and efficiency of natural sinks, P. Natl. Acad. Sci. USA, 104, 18866–18870, 2007.

Chevallier, F.: On the statistical optimality of CO_2 atmospheric inversions assimilating CO_2 column retrievals, Atmos. Chem. Phys., 15, 11133–11145, doi:10.5194/acp-15-11133-2015, 2015.

Chevallier, F., Fisher, M., Peylin, P., Serrar, S., Bousquet, P., Bréon, F.-M., Chédin, A., and Ciais, P.: Inferring CO_2 sources and sinks from satellite observations: Method and application to TOVS data, J. Geophys. Res., D24309, doi:10.1029/2005JD006390, 2005.

China Coal Industry Association: Economic performance of coal in the first half of 2015, available at: http://www.coalchina.org.cn/detail/15/07/30/00000027/content.html, last access: July 2015 (in Chinese).

China Coal Resource: Economic performance of China's coal industry in the first 8 months of the year, available at: http://www.sxcoal.com/coal/4237319/articlenew.html (last access: 16 September 2015), 2015 (in Chinese).

Ciais, P., Sabine, C., Govindasamy, B., Bopp, L., Brovkin, V., Canadell, J., Chhabra, A., DeFries, R., Galloway, J., Heimann, M., Jones, C., Le Quéré, C., Myneni, R., Piao, S., and Thornton, P.: Chapter 6: Carbon and Other Biogeochemical Cycles, in: Climate Change 2013 The Physical Science Basis, edited by: Stocker, T., Qin, D., and Platner, G.-K., Cambridge University Press, Cambridge, 2013.

Clark, D. B., Mercado, L. M., Sitch, S., Jones, C. D., Gedney, N., Best, M. J., Pryor, M., Rooney, G. G., Essery, R. L. H., Blyth, E., Boucher, O., Harding, R. J., Huntingford, C., and Cox, P. M.: The Joint UK Land Environment Simulator (JULES), model description – Part 2: Carbon fluxes and vegetation dynamics, Geosci. Model Dev., 4, 701–722, doi:10.5194/gmd-4-701-2011, 2011.

Danabasoglu, G., Yeager, S. G., Bailey, D., Behrens, E., Bentsen, M., Bi, D., Biastoch, A., Böning, C., Bozec, A., Canuto, V. M., Cassou, C., Chassignet, E., Coward, A. C., Danilov, S., Diansky, N., Drange, H., Farneti, R., Fernandez, E., Fogli, P. G., Forget, G., Fujii, Y., Griffies, S. M., Gusev, A., Heimbach, P., Howard, A., Jung, T., Kelley, M., Large, W.G., Leboissetier, A., Lu, J., Madec, G., Marsland, S.J., Masina, S., Navarra, A., Nurser, A. J. G., Pirani, A., Salas y Mélia, D., Samuels, B. L., Scheinert, M., Sidorenko, D., Treguier, A.-M., Tsujino, H., Uotila, P., Valcke, S., Voldoire, A., and Wangi, Q.: North Atlantic simulations in Coordinated Ocean-ice Reference Experiments phase II (CORE-II). Part I: Mean states, Ocean Model., 73, 76–107, 2014.

Davis, S. J. and Caldeira, K.: Consumption-based accounting of CO_2 emissions, P. Natl. Acad. Sci., 107, 5687–5692, 2010.

Davis, S. J., Peters, G. P., and Caldeira, K.: The supply chain of CO_2 emissions, P. Natl. Acad. Sci., 108, 18554–18559, 2011.

Denman, K. L., Brasseur, G., Chidthaisong, A., Ciais, P., Cox, P. M., Dickinson, R. E., Hauglustaine, D., Heinze, C., Holland, E., Jacob, D., Lohmann, U., Ramachandran, S., Leite da Silva Dias, P., Wofsy, S. C., and Zhang, X.: Couplings Between Changes in the Climate System and Biogeochemistry, Intergovernmental Panel on Climate Change, 978-0-521-70596-7, 499–587, 2007.

Dietzenbacher, E., Pei, J., and Yang, C.: Trade, production fragmentation, and China's carbon dioxide emissions, J. Environ. Econ. Manag., 2012, 88–101, 2012.

Dlugokencky, E. and Tans, P.: Trends in atmospheric carbon dioxide, National Oceanic & Atmospheric Administration, Earth System Research Laboratory (NOAA/ESRL), available at: http://www.esrl.noaa.gov/gmd/ccgg/trends, last access: 8 August 2014.

Dlugokencky, E. and Tans, P.: Trends in atmospheric carbon dioxide, National Oceanic & Atmospheric Administration, Earth System Research Laboratory (NOAA/ESRL), available at: http://www.esrl.noaa.gov/gmd/ccgg/trends, last access: 7 October 2015.

Doney, S. C., Lima, I., Feely, R. A., Glover, D. M., Lindsay, K., Mahowald, N., Moore, J. K., and Wanninkhof, R.: Mechanisms governing interannual variability in upper-ocean inorganic carbon system and air–sea CO_2 fluxes: Physical climate and atmospheric dust, Deep-Sea Res. Pt. II, 56, 640-655, 2009.

Durant, A. J., Le Quéré, C., Hope, C., and Friend, A. D.: Economic value of improved quantification in global sources and sinks of carbon dioxide, Philos. T. R. Soc. A, 269, 1967–1979, 2010.

Earles, J. M., Yeh, S., and Skog, K. E.: Timing of carbon emissions from global forest clearance, Nature Clim. Change, 2, 682–685, 2012.

El-Masri, B., Barman, R., Meiyappan, P., Song, Y., Liang, M., and Jain, A. K.: Carbon dynamics in the Amazonian Basin: Integration of eddy covariance and ecophysiological data with a land surface model, Agr. Forest Meteorol., 182–183, 156–167, 2013.

Erb, K.-H., Kastner, T., Luyssaert, S., Houghton, R. A., Kuemmerle, T., Olofsson, P., and Haberl, H.: Bias in the attribution of forest carbon sinks, Nature Clim. Change, 3, 854–856, 2013.

Etheridge, D. M., Steele, L. P., Langenfelds, R. L., and Francey, R. J.: Natural and anthropogenic changes in atmospheric CO_2 over the last 1000 years from air in Antarctic ice and firn, J. Geophys. Res., 101, 4115–4128, 1996.

Fader, M., Rost, S., Müller, C., Bondeau, A., and Gerten, D.: Virtual water content of temperate cereals and maize: Present and potential future patterns, J. Hydrol., 384, 218–231, 2010.

FAO: Global Forest Resource Assessment 2010, 378 pp., 2010.

FAOSTAT: Food and Agriculture Organization Statistics Division, available at: http://faostat.fao.org/2010 (last access: October 2012), 2010.

Federici, S., Tubiello, F. N., Salvatore, M., Jacobs, H., and Schmidhuber, J.: New estimates of CO_2 forest emissions and removals: 1990–2015, Forest Ecol. Manag., 352, 89–98, 2015.

Francey, R. J., Trudinger, C. M., van der Schoot, M., Law, R. M., Krummel, P. B., Langenfelds, R. L., Steele, L. P., Allison, C. E., Stavert, A. R., Andres, R. J., and Rodenbeck, C.: Reply to "Anthropogenic CO_2 emissions", Nature Clim. Change, 3, 604–604, 2013.

Friedlingstein, P., Andrew, R. M., Rogelj, J., Peters, G. P., Canadell, J. G., Knutti, R., Luderer, G., Raupach, M. R., Schaeffer, M., van Vuuren, D. P., and Le Quéré, C.: Persistent growth of CO_2 emissions and implications for reaching climate targets, Nat. Geosci., 7, 709–715, doi:10.1038/ngeo2248, 2014.

Friedlingstein, P., Houghton, R. A., Marland, G., Hackler, J., Boden, T. A., Conway, T. J., Canadell, J. G., Raupach, M. R., Ciais, P., and Le Quéré, C.: Update on CO_2 emissions, Nat. Geosci., 3, 811–812, 2010.

Friend, A. D.: Terrestrial Plant Production and Climate Change, J. Exp. Bot., 61, 1293–1309, 2010.

Gasser, T. and Ciais, P.: A theoretical framework for the net land-to-atmosphere CO_2 flux and its implications in the definition of "emissions from land-use change", Earth Syst. Dynam., 4, 171–186, doi:10.5194/esd-4-171-2013, 2013.

GCP: The Global Carbon Budget 2007, available at: http://lgmacweb.env.uea.ac.uk/lequere/co2/2007/carbon_budget_2007.htm (last access: November 2013), 2007.

General Administration of Customs of the People's Republic of China: China's major exports by quantity and RMB value, August 2015, available at: http://www.customs.gov.cn/publish/portal0/tab49666/info772246.htm, last access: October 2015 (in Chinese).

General Administration of Customs of the People's Republic of China: China's major imports by quantity and RMB value, August 2015, available at: http://www.customs.gov.cn/publish/portal0/tab49666/info772245.htm, last access: October 2015 (in Chinese).

Giglio, L., Randerson, J., and van der Werf, G.: Analysis of daily, monthly, and annual burned area using the fourth-generation global fire emissions database (GFED4), J. Geophys. Res.-Biogeo., 118, 317–328, doi:10.1002/jgrg.20042, 2013.

Gitz, V. and Ciais, P.: Amplifying effects of land-use change on future atmospheric CO_2 levels, Global Biogeochem. Cy., 17, 1024, doi:10.1029/2002GB001963, 2003.

Goll, D. S., Brovkin, V., Liski, J., Raddatz, T., Thum, T., and Todd-Brown, K. E. O.: Strong dependence of CO_2 emissions from anthropogenic land cover change on initial land cover and soil carbon parametrization, Global Biogeochem. Cy., 29, 1511–1523, doi:10.1002/2014GB004988, 2015.

Green, F. and Stern, N.: China's "new normal": structural change, better growth, and peak emissions, Policy report, Centre for Climate Change Economics and Policy (CCCEP), University of Leeds, 2015.

Gregg, J. S., Andres, R. J., and Marland, G.: China: Emissions pattern of the world leader in CO_2 emissions from fossil fuel consumption and cement production, Geophys. Res. Lett., 35, L08806, doi:10.1029/2007GL032887, 2008.

Hansen, M., Potapov, P., and Moore, R.: High-resolution global maps of 21st century forest cover change, Science, 342, 850–853, 2013.

Hansis, E., Davis, S. J., and Pongratz, J.: Relevance of methodological choices for accounting of land use change carbon fluxes, Global Biogeochem. Cy., 29, 1230–1246, 2015.

Harris, I., Jones, P. D., Osborn, T. J., and Lister, D. H.: Updated high-resolution grids of monthly climatic observations – the CRU TS3.10 Dataset, Int. J. Climatol., 34, 623–642, 2015.

Harris, N., Brown, S., and Hagen, S. C.: Baseline map of carbon emissions from deforestation in tropical regions, Science, 336, 1573–1576, 2012.

Hauck, J., Völker, C., Wang, T., Hoppema, M., Losch, M., and Wolf-Gladrow, D. A.: Seasonally different carbon flux changes in the Southern Ocean in response to the southern annular mode, Global Biogeochem. Cy., 27, 1236–1245, 2013.

Hertwich, E. G. and Peters, G. P.: Carbon Footprint of Nations: A Global, Trade-Linked Analysis, Environ. Sci. Technol., 43, 6414–6420, 2009.

Houghton, R. A.: Revised estimates of the annual net flux of carbon to the atmosphere from changes in land use and land management 1850–2000, Tellus B, 55, 378–390, 2003.

Houghton, R. A., House, J. I., Pongratz, J., van der Werf, G. R., DeFries, R. S., Hansen, M. C., Le Quéré, C., and Ramankutty, N.: Carbon emissions from land use and land-cover change, Biogeosciences, 9, 5125–5142, doi:10.5194/bg-9-5125-2012, 2012.

Hourdin, F., Musat, I., Bony, S., Braconnot, P., Codron, F., Dufresne, J.-L., Fairhead, L., Filiberti, M.-A., Freidlingstein, P., Grandpeix, J.-Y., Krinner, G., LeVan, P., Li, Z.-X., and Lott, F.: The LMDZ4 general circulation model: climate performance and sensitivity to parametrized physics with emphasis on tropical convection, Clim. Dynam., 27, 787–813, 2006.

Hurtt, G. C., Chini, L. P., Frolking, S., Betts, R. A., Feddema, J., Fischer, G., Fisk, J. P., Hibbard, K., Houghton, R. A., Janetos, A., Jones, C. D., Kindermann, G., Kinoshita, T., Klein Goldewijk, K., Riahi, K., Shevliakova, E., Smith, S., Stehfest, E., Thomson, A., Thornton, P., van Vuuren, D. P., and Wang, Y. P.: Harmonization of land-use scenarios for the period 1500–2100: 600 years of global gridded annual land-use transitions, wood harvest, and resulting secondary lands, Climatic Change, 109, 117–161, 2011.

IEA/OECD: CO_2 emissions from fuel combustion highlights, Paris, International Energy Agency, 2014.

Ilyina, T., Six, K., Segschneider, J., Maier-Reimer, E., Li, H., and Núñez-Riboni, I.: The global ocean biogeochemistry model HAMOCC: Model architecture and performance as component of the MPI-Earth System Model in different CMIP5 experimental realizations, Journal of Advances in Modeling Earth Systems, 5, 287–315, 2013.

IMF: World Economic Outlook of the International Monetary Fund, available at: http://www.imf.org/external/ns/cs.aspx?id=_29, last access: 9 October 2015.

Inomata, S. and Owen, A.: COMPARATIVE EVALUATION OF MRIO DATABASES, Economic Systems Research, 26, 239–244, 2014.

Ito, A. and Inatomi, M.: Use of a process-based model for assessing the methane budgets of global terrestrial ecosystems and evaluation of uncertainty, Biogeosciences, 9, 759–773, doi:10.5194/bg-9-759-2012, 2012.

Jackson, R. B., Canadell, J. G., Le Quéré, C., Andrew, R. M., Korsbakken, J. I., Peters, G. P., and Nakicenovic, N.: Reaching Peak Emissions, Nature Clim. Change, doi:10.1038/nclimate2892, online first, 2015.

Jacobson, A. R., Mikaloff Fletcher, S. E., Gruber, N., Sarmiento, J. L., and Gloor, M.: A joint atmosphere-ocean inversion for surface fluxes of carbon dioxide: 1. Methods and global-scale fluxes, Global Biogeochem. Cy., 21, GB1019, doi:10.1029/2005GB002556, 2007.

Jain, A. K., West, T., Yang, X., and Post, W.: Assessing the Impact of Changes in Climate and CO_2 on Potential Carbon Sequestration in Agricultural Soils, Geophys. Res. Lett., 32, L19711, doi:10.1029/2005GL023922, 2005.

Jain, A. K., Meiyappan, P., Song, Y., and House, J. I.: CO_2 Emissions from Land-Use Change Affected More by Nitrogen Cycle, than by the Choice of Land Cover Data, Glob. Change Biol., 9, 2893–2906, 2013.

Joos, F. and Spahni, R.: Rates of change in natural and anthropogenic radiative forcing over the past 20,000 years, P. Natl. Acad. Sci., 105, 1425–1430, 2008.

Karstensen, J., Peters, G. P., and Andrew, R. M.: Uncertainty in temperature response of current consumption-based emissions estimates, Earth Syst. Dynam., 6, 287–309, doi:10.5194/esd-6-287-2015, 2015.

Kato, E., Kinoshita, T., Ito, A., Kawamiya, M., and Yamagata, Y.: Evaluation of spatially explicit emission scenario of land-use

change and biomass burning using a process-based biogeochemical model, Journal of Land Use Science, 8, 104–122, 2013.

Keeling, C. D., Bacastow, R. B., Bainbridge, A. E., Ekdhal, C. A., Guenther, P. R., and Waterman, L. S.: Atmospheric carbon dioxide variations at Mauna Loa Observatory, Hawaii, Tellus, 28, 538–551, 1976.

Keeling, R. F., Manning, A. C., and Dubey, M. K.: The atmospheric signature of carbon capture and storage, Philos. T. R. Soc. A, 369, 2113–2132, 2011.

Khatiwala, S., Primeau, F., and Hall, T.: Reconstruction of the history of anthropogenic CO_2 concentrations in the ocean, Nature, 462, 346–350, 2009.

Khatiwala, S., Tanhua, T., Mikaloff Fletcher, S., Gerber, M., Doney, S. C., Graven, H. D., Gruber, N., McKinley, G. A., Murata, A., Ríos, A. F., and Sabine, C. L.: Global ocean storage of anthropogenic carbon, Biogeosciences, 10, 2169–2191, doi:10.5194/bg-10-2169-2013, 2013.

Kirschke, S., Bousquet, P., Ciais, P., Saunois, M., Canadell, J. G., Dlugokencky, E. J., Bergamaschi, P., Bergmann, D., Blake, D. R., Bruhwiler, L., Cameron Smith, P., Castaldi, S., Chevallier, F., Feng, L., Fraser, A., Heimann, M., Hodson, E. L., Houweling, S., Josse, B., Fraser, P. J., Krummel, P. B., Lamarque, J., Langenfelds, R. L., Le Quéré, C., Naik, V., O'Doherty, S., Palmer, P. I., Pison, I., Plummer, D., Poulter, B., Prinn, R. G., Rigby, M., Ringeval, B., Santini, M., Schmidt, M., Shindell, D. T., Simpson, I. J., Spahni, R., Steele, L. P., Strode, S. A., Sudo, K., Szopa, S., van der Werf, G. R., Voulgarakis, A., van Weele, M., Weiss, R. F., Williams, J. E., and Zeng, G.: Three decades of global methane sources and sinks, Nat. Geosci., 6, 813–823, 2013.

Klein Goldewijk, K., Beusen, A., van Drecht, G., and de Vos, M.: The HYDE 3.1 spatially explicit database of human-induced global land-use change over the past 12,000 years, Global Ecol. Biogeogr., 20, 73–86, 2011.

Krinner, G., Viovy, N., de Noblet, N., Ogée, J., Friedlingstein, P., Ciais, P., Sitch, S., Polcher, J., and Prentice, I. C.: A dynamic global vegetation model for studies of the coupled atmosphere-biosphere system, Global Biogeochem. Cy., 19, 1–33, 2005.

Lamarque, J.-F., Bond, T. C., Eyring, V., Granier, C., Heil, A., Klimont, Z., Lee, D., Liousse, C., Mieville, A., Owen, B., Schultz, M. G., Shindell, D., Smith, S. J., Stehfest, E., Van Aardenne, J., Cooper, O. R., Kainuma, M., Mahowald, N., McConnell, J. R., Naik, V., Riahi, K., and van Vuuren, D. P.: Historical (1850–2000) gridded anthropogenic and biomass burning emissions of reactive gases and aerosols: methodology and application, Atmos. Chem. Phys., 10, 7017–7039, doi:10.5194/acp-10-7017-2010, 2010.

Landschützer, P., Gruber, N., Bakker, D. C. E., and Schuster, U.: Recent variability of the global ocean carbon sink, Global Biogeochem. Cy., 28, 927–949, doi:10.1002/2014GB004853, 2014.

Landschützer, P., Gruber, N., Haumann, F. A., Rödenbeck, C., Bakker, D. C. E., van Heuven, S., Hoppema, M., Metzl, N., Sweeney, C., Takahashi, T., Tilbrook, B., and Wanninkhof, R.: The reinvigoration of the Southern Ocean carbon sink, Science, 349, 1221–1224, 2015.

Le Quéré, C.: Closing the global budget for CO_2, Global Change, 74, 28–31, 2009.

Le Quéré, C., Raupach, M. R., Canadell, J. G., Marland, G., Bopp, L., Ciais, P., Conway, T. J., Doney, S. C., Feely, R. A., Foster, P., Friedlingstein, P., Gurney, K., Houghton, R. A., House, J. I., Huntingford, C., Levy, P. E., Lomas, M. R., Majkut, J., Metzl, N., Ometto, J. P., Peters, G. P., Prentice, I. C., Randerson, J. T., Running, S. W., Sarmiento, J. L., Schuster, U., Sitch, S., Takahashi, T., Viovy, N., van der Werf, G. R., and Woodward, F. I.: Trends in the sources and sinks of carbon dioxide, Nat. Geosci., 2, 831–836, 2009.

Le Quéré, C., Andres, R. J., Boden, T., Conway, T., Houghton, R. A., House, J. I., Marland, G., Peters, G. P., van der Werf, G. R., Ahlström, A., Andrew, R. M., Bopp, L., Canadell, J. G., Ciais, P., Doney, S. C., Enright, C., Friedlingstein, P., Huntingford, C., Jain, A. K., Jourdain, C., Kato, E., Keeling, R. F., Klein Goldewijk, K., Levis, S., Levy, P., Lomas, M., Poulter, B., Raupach, M. R., Schwinger, J., Sitch, S., Stocker, B. D., Viovy, N., Zaehle, S., and Zeng, N.: The global carbon budget 1959–2011, Earth Syst. Sci. Data, 5, 165–185, doi:10.5194/essd-5-165-2013, 2013.

Le Quéré, C., Peters, G. P., Andres, R. J., Andrew, R. M., Boden, T. A., Ciais, P., Friedlingstein, P., Houghton, R. A., Marland, G., Moriarty, R., Sitch, S., Tans, P., Arneth, A., Arvanitis, A., Bakker, D. C. E., Bopp, L., Canadell, J. G., Chini, L. P., Doney, S. C., Harper, A., Harris, I., House, J. I., Jain, A. K., Jones, S. D., Kato, E., Keeling, R. F., Klein Goldewijk, K., Körtzinger, A., Koven, C., Lefèvre, N., Maignan, F., Omar, A., Ono, T., Park, G.-H., Pfeil, B., Poulter, B., Raupach, M. R., Regnier, P., Rödenbeck, C., Saito, S., Schwinger, J., Segschneider, J., Stocker, B. D., Takahashi, T., Tilbrook, B., van Heuven, S., Viovy, N., Wanninkhof, R., Wiltshire, A., and Zaehle, S.: Global carbon budget 2013, Earth Syst. Sci. Data, 6, 235–263, doi:10.5194/essd-6-235-2014, 2014.

Le Quéré, C., Moriarty, R., Andrew, R. M., Peters, G. P., Ciais, P., Friedlingstein, P., Jones, S. D., Sitch, S., Tans, P., Arneth, A., Boden, T. A., Bopp, L., Bozec, Y., Canadell, J. G., Chini, L. P., Chevallier, F., Cosca, C. E., Harris, I., Hoppema, M., Houghton, R. A., House, J. I., Jain, A. K., Johannessen, T., Kato, E., Keeling, R. F., Kitidis, V., Klein Goldewijk, K., Koven, C., Landa, C. S., Landschützer, P., Lenton, A., Lima, I. D., Marland, G., Mathis, J. T., Metzl, N., Nojiri, Y., Olsen, A., Ono, T., Peng, S., Peters, W., Pfeil, B., Poulter, B., Raupach, M. R., Regnier, P., Rödenbeck, C., Saito, S., Salisbury, J. E., Schuster, U., Schwinger, J., Séférian, R., Segschneider, J., Steinhoff, T., Stocker, B. D., Sutton, A. J., Takahashi, T., Tilbrook, B., van der Werf, G. R., Viovy, N., Wang, Y.-P., Wanninkhof, R., Wiltshire, A., and Zeng, N.: Global carbon budget 2014, Earth Syst. Sci. Data, 7, 47–85, doi:10.5194/essd-7-47-2015, 2015.

Liu, Z., Guan, D., Wei, W., Davis, S. J., Ciais, P., Bai, J., Peng, S., Zhang, Q., Hubacek, K., Marland, G., Andres, R. J., Crawford-Brown, D., Lin, J., Zhao, H., Hong, C., Boden, T. A., Feng, K., Peters, G. P., Xi, F., Liu, J., Li, Y., Zhao, Y., Zeng, N., and He, K.: Reduced carbon emission estimates from fossil fuel combustion and cement production in China, Nature, 524, 335–338, 2015.

MacDicken, K. G.: Global Forest Resources Assessment 2015: What, why and how?, Forest Ecol.Manage., 352, 3–8, 2015.

Manning, A. C. and Keeling, R. F.: Global oceanic and land biotic carbon sinks from the Scripps atmospheric oxygen flask sampling network, Tellus B, 58, 95–116, 2006.

Marland, G.: Uncertainties in accounting for CO_2 from fossil fuels, J. Ind. Ecol., 12, 136–139, 2008.

Marland, G., Andres, R. J., Blasing, T. J., Boden, T. A., Broniak, C. T., Gregg, J. S., Losey, L. M., and Treanton, K.: Energy, industry and waste management activities: An introduction to CO_2 emis-

sions from fossil fuels, in: A report by the US Climate Change Science Program and the Subcommittee on Global Change Research, in: The First State of the Carbon Cycle Report (SOCCR): The North American Carbon Budget and Implications for the Global Carbon Cycle, edited by: King, A. W., Dilling, L., Zimmerman, G. P., Fairman, D. M., Houghton, R. A., Marland, G., Rose, A. Z., and Wilbanks, T. J., Asheville, NC, 2007.

Marland, G., Hamal, K., and Jonas, M.: How Uncertain Are Estimates of CO_2 Emissions?, J. Ind. Ecol., 13, 4–7, 2009.

Masarie, K. A. and Tans, P. P.: Extension and integratino of atmospheric carbon dioxide data into a globally consistent measurement record, J. Geophys. Res.-Atmos., 100, 11593–11610, 1995.

McNeil, B. I., Matear, R. J., Key, R. M., Bullister, J. L., and Sarmiento, J. L.: Anthropogenic CO_2 uptake by the ocean based on the global chlorofluorocarbon data set, Science, 299, 235–239, 2003.

Mikaloff Fletcher, S. E., Gruber, N., Jacobson, A. R., Doney, S. C., Dutkiewicz, S., Gerber, M., Follows, M., Joos, F., Lindsay, K., Menemenlis, D., Mouchet, A., Müller, S. A., and Sarmiento, J. L.: Inverse estimates of anthropogenic CO_2 uptake, transport, and storage by the oceans, Global Biogeochem. Cy., 20, GB2002, doi:10.1029/2005GB002530, 2006.

Moran, D. and Wood, R.: CONVERGENCE BETWEEN THE EORA, WIOD, EXIOBASE, AND OPENEU'S CONSUMPTION-BASED CARBON ACCOUNTS, Economic Systems Research, 26, 245–261, 2014.

Myhre, G., Alterskjær, K., and Lowe, D.: A fast method for updating global fossil fuel carbon dioxide emissions, Environ. Res. Lett., 4, 034012, doi:10.1088/1748-9326/4/3/034012, 2009.

Narayanan, B., Aguiar, A., and McDougall, R.: Global Trade, Assistance, and Production: The GTAP 9 Data Base, available at: www.gtap.agecon.purdue.edu/databases/v9/default.asp, last access: September 2015.

National Bureau of Statistics of China: China Energy Statistical Yearbook 2014, China Statistics Press, Beijing, 2015a.

National Bureau of Statistics of China: Industrial Production Operation in August 2015, available at: http://www.stats.gov.cn/english/PressRelease/201509/t20150915_1245026.html, last access: September 2015b.

National Energy Administration: Conference on energy trends for the first half of 2015, available at: http://www.nea.gov.cn/2015-07/27/c_134450600.htm, last access: July 2015.

NOAA/ESRL: NOAA/ESRL calculation of global means, available at: http://www.esrl.noaa.gov/gmd/ccgg/about/global_means.html, last access: 7 October 2015a.

NOAA/ESRL: Multi-laboratory compilation of atmospheric carbon dioxide data for the period 1968–2014, obspack_co2_1_GLOBALVIEWplus_v1.0_2015-07-30, Project, C. G. A. D. I., 2015b.

Oke, P. R., Griffin, D. A., Schiller, A., Matear, R. J., Fiedler, R., Mansbridge, J., Lenton, A., Cahill, M., Chamberlain, M. A., and Ridgway, K.: Evaluation of a near-global eddy-resolving ocean model, Geosci. Model Dev., 6, 591–615, doi:10.5194/gmd-6-591-2013, 2013.

Oleson, K., Lawrence, D., Bonan, G., Drewniak, B., Huang, M., Koven, C., Levis, S., Li, F., Riley, W., Subin, Z., Swenson, S., Thornton, P., Bozbiyik, A., Fisher, R., Heald, C., Kluzek, E., Lamarque, J., Lawrence, P., Leung, L., Lipscomb, W., Muszala, S., Ricciuto, D., Sacks, W., Tang, J., and Yang, Z.: Technical Description of version 4.5 of the Community Land Model (CLM), NCAR, 2013.

Peters, G. P. and Hertwich, E. G.: Post-Kyoto Greenhouse Gas Inventories: Production versus Consumption, Climatic Change, 86, 51–66, 2008.

Peters, G. P., Andrew, R., and Lennos, J.: Constructing a multi-regional input-output table using the GTAP database, Economic Systems Research, 23, 131–152, 2011a.

Peters, G. P., Minx, J. C., Weber, C. L., and Edenhofer, O.: Growth in emission transfers via international trade from 1990 to 2008, P. Natl. Acad. Sci. USA, 108, 8903–8908, 2011b.

Peters, G. P., Davis, S. J., and Andrew, R.: A synthesis of carbon in international trade, Biogeosciences, 9, 3247–3276, doi:10.5194/bg-9-3247-2012, 2012a.

Peters, G. P., Marland, G., Le Quéré, C., Boden, T. A., Canadell, J. G., and Raupach, M. R.: Correspondence: Rapid growth in CO_2 emissions after the 2008–2009 global financial crisis, Nature Clim. Change, 2, 2–4, 2012b.

Peters, G. P., Andrew, R. M., Boden, T., Canadell, J. G., Ciais, P., Le Quéré, C., Marland, G., Raupach, M. R., and Wilson, C.: The challenge to keep global warming below 2 °C, Nature Clim. Change, 3, 4–6, 2013.

Peters, W., Krol, M. C., van der Werf, G. R., Houweling, S., Jones, C. D., Hughes, J., Schaefer, K., Masarie, K. A., Jacobson, A. R., Miller, J. B., Cho, C. H., Ramonet, M., Schmidt, M., Ciattaglia, L., Apadula, F., Heltai, D., Meinhardt, F., Di Sarra, A. G., Piacentino, S., Sferlazzo, D., Aalto, T., Hatakka, J., Ström, J., Haszpra, L., Meijer, H. A. J., Van Der Laan, S., Neubert, R. E. M., Jordan, A., Rodó, X., Morguí, J.-A., Vermeulen, A. T., Popa, E., Rozanski, K., Zimnoch, M., Manning, A. C., Leuenberger, M., Uglietti, C., Dolman, A. J., Ciais, P., Heimann, M., and Tans, P. P.: Seven years of recent European net terrestrial carbon dioxide exchange constrained by atmospheric observations, Glob. Change Biol., 16, 1317–1337, 2010.

Pfeil, B., Olsen, A., Bakker, D. C. E., Hankin, S., Koyuk, H., Kozyr, A., Malczyk, J., Manke, A., Metzl, N., Sabine, C. L., Akl, J., Alin, S. R., Bates, N., Bellerby, R. G. J., Borges, A., Boutin, J., Brown, P. J., Cai, W.-J., Chavez, F. P., Chen, A., Cosca, C., Fassbender, A. J., Feely, R. A., González-Dávila, M., Goyet, C., Hales, B., Hardman-Mountford, N., Heinze, C., Hood, M., Hoppema, M., Hunt, C. W., Hydes, D., Ishii, M., Johannessen, T., Jones, S. D., Key, R. M., Körtzinger, A., Landschützer, P., Lauvset, S. K., Lefèvre, N., Lenton, A., Lourantou, A., Merlivat, L., Midorikawa, T., Mintrop, L., Miyazaki, C., Murata, A., Nakadate, A., Nakano, Y., Nakaoka, S., Nojiri, Y., Omar, A. M., Padin, X. A., Park, G.-H., Paterson, K., Perez, F. F., Pierrot, D., Poisson, A., Ríos, A. F., Santana-Casiano, J. M., Salisbury, J., Sarma, V. V. S. S., Schlitzer, R., Schneider, B., Schuster, U., Sieger, R., Skjelvan, I., Steinhoff, T., Suzuki, T., Takahashi, T., Tedesco, K., Telszewski, M., Thomas, H., Tilbrook, B., Tjiputra, J., Vandemark, D., Veness, T., Wanninkhof, R., Watson, A. J., Weiss, R., Wong, C. S., and Yoshikawa-Inoue, H.: A uniform, quality controlled Surface Ocean CO_2 Atlas (SOCAT), Earth Syst. Sci. Data, 5, 125–143, doi:10.5194/essd-5-125-2013, 2013.

Pongratz, J., Reick, C. H., Raddatz, T., and Claussen, M.: Effects of anthropogenic land cover change on the carbon cycle of the last millennium, Global Biogeochem. Cy., 23, Gb4001, doi:10.1029/2009gb003488, 2009.

Pongratz, J., Reick, C. H., Houghton, R. A., and House, J. I.: Terminology as a key uncertainty in net land use and land cover change carbon flux estimates, Earth Syst. Dynam., 5, 177–195, doi:10.5194/esd-5-177-2014, 2014.

Poulter, B., Frank, D., Ciais, P., Myneni, R. B., Andela, N., Bi, J., Broquet, G., Canadell, J. G., Chevallier, F., Liu, Y. Y., Running, S. W., Sitch, S., and van der Werf, G. R.: Contribution of semi-arid ecosystems to interannual variability of the global carbon cycle, Nature, 509, 600–603, 2014.

Prather, M. J., Holmes, C. D., and Hsu, J.: Reactive greenhouse gas scenarios: Systematic exploration of uncertainties and the role of atmospheric chemistry, Geophys. Res. Lett., 39, L09803, doi:10.1029/2012GL051440, 2012.

Prentice, I. C., Farquhar, G. D., Fasham, M. J. R., Goulden, M. L., Heimann, M., Jaramillo, V. J., Kheshgi, H. S., Le Quéré, C., Scholes, R. J., and Wallace, D. W. R.: The Carbon Cycle and Atmospheric Carbon Dioxide, in: Climate Change 2001: The Scientific Basis. Contribution of Working Group I to the Third Assessment Report of the Intergovernmental Panel on Climate Change, edited by: Houghton, J. T., Ding, Y., Griggs, D. J., Noguer, M., van der Linden, P. J., Dai, X., Maskell, K., and Johnson, C. A., Cambridge University Press, Cambridge, United Kingdom and New York, NY, USA, 2001.

Randerson, J., Chen, Y., van der Werf, G. R., Rogers, B. M., and Morton, D. C.: Global burned area and biomass burning emissions from small fires, J. Geophys. Res.-Biogeo., 117, G04012, doi:10.1029/2012JG002128, 2012.

Raupach, M. R., Marland, G., Ciais, P., Le Quéré, C., Canadell, J. G., Klepper, G., and Field, C. B.: Global and regional drivers of accelerating CO_2 emissions, P. Natl. Acad. Sci. USA, 104, 10288–10293, 2007.

Regnier, P., Friedlingstein, P., Ciais, P., Mackenzie, F. T., Gruber, N., Janssens, I. A., Laruelle, G. G., Lauerwald, R., Luyssaert, S., Andersson, A. J., Arndt, S., Arnosti, C., Borges, A. V., Dale, A. W., Gallego-Sala, A., Goddéris, Y., Goossens, N., Hartmann, J., Heinze, C., Ilyina, T., Joos, F., La Rowe, D. E., Leifeld, J., Meysman, F. J. R., Munhoven, G., Raymond, P. A., Spahni, R., Suntharalingam, P., and Thullner M.: Anthropogenic perturbation of the carbon fluxes from land to ocean, Nat. Geosci., 6, 597–607, 2013.

Reick, C. H., Raddatz, T., Brovkin, V., and Gayler, V.: The representation of natural and anthropogenic land cover change in MPI-ESM, Journal of Advances in Modeling Earth Systems, 5, 459–482, 2013.

Rhein, M., Rintoul, S. R., Aoki, S., Campos, E., Chambers, D., Feely, R. A., Gulev, S., Johnson, G. C., Josey, S. A., Kostianoy, A., Mauritzen, C., Roemmich, D., Talley, L. D., and Wang, F.: Chapter 3: Observations: Ocean, in: Climate Change 2013 The Physical Science Basis, Cambridge University Press, Cambridge, United Kingdom, 2013.

Rödenbeck, C.: Estimating CO_2 sources and sinks from atmospheric mixing ratio measurements using a global inversion of atmospheric transport, Max Planck Institute, MPI-BGC, 2005.

Rödenbeck, C., Houweling, S., Gloor, M., and Heimann, M.: CO_2 flux history 1982–2001 inferred from atmospheric data using a global inversion of atmospheric transport, Atmos. Chem. Phys., 3, 1919–1964, doi:10.5194/acp-3-1919-2003, 2003.

Rödenbeck, C., Keeling, R. F., Bakker, D. C. E., Metzl, N., Olsen, A., Sabine, C., and Heimann, M.: Global surface-ocean pCO_2 and sea-air CO_2 flux variability from an observation-driven ocean mixed-layer scheme, Ocean Sci., 9, 193–216, doi:10.5194/os-9-193-2013, 2013.

Rödenbeck, C., Bakker, D. C. E., Metzl, N., Olsen, A., Sabine, C., Cassar, N., Reum, F., Keeling, R. F., and Heimann, M.: Interannual sea-air CO_2 flux variability from an observation-driven ocean mixed-layer scheme, Biogeosciences, 11, 4599–4613, doi:10.5194/bg-11-4599-2014, 2014.

Rödenbeck, C., Bakker, D. C. E., Gruber, N., Iida, Y., Jacobson, A. R., Jones, S., Landschützer, P., Metzl, N., Nakaoka, S., Olsen, A., Park, G.-H., Peylin, P., Rodgers, K. B., Sasse, T. P., Schuster, U., Shutler, J. D., Valsala, V., Wanninkhof, R., and Zeng, J.: Data-based estimates of the ocean carbon sink variability – first results of the Surface Ocean pCO_2 Mapping intercomparison (SOCOM), Biogeosciences Discuss., 12, 14049–14104, doi:10.5194/bgd-12-14049-2015, 2015.

Rost, S., Gerten, D., Bondeau, A., Lucht, W., Rohwer, J., and Schaphoff, S.: Agricultural green and blue water consumption and its influence on the global water system, Water Resour. Res., W09405, doi:10.1029/2007WR006331, 2008.

Rypdal, K., Paciomik, N., Eggleston, S., Goodwin, J., Irving, W., Penman, J., and Woodfield, M.: Chapter 1 Introduction to the 2006 Guidelines, in: 2006 IPCC Guidelines for National Greenhouse Gas Inventories, edited by: Eggleston, S., Buendia, L., Miwa, K., Ngara, T., and Tanabe, K., Institute for Global Environmental Strategies (IGES), Hayama, Kanagawa, Japan, 2006.

Saatchi, S. S., Harris, N. L., and Brown, S.: Benchmark map of forest carbon stocks in tropical regions across three continents, P. Natl. Acad. Sci., 108, 9899–9904, 2011.

Schaphoff, S., Heyder, U., Ostberg, S., Gerten, D., Heinke, J., and Lucht, W.: Contribution of permafrost soils to the global carbon budget., Environ. Res. Lett., 8, 014026, doi:10.1088/1748-9326/8/1/014026, 2013.

Schimel, D., Alves, D., Enting, I., Heimann, M., Joos, F., Raynaud, D., Wigley, T., Prater, M., Derwent, R., Ehhalt, D., Fraser, P., Sanhueza, E., Zhou, X., Jonas, P., Charlson, R., Rodhe, H., Sadasivan, S., Shine, K. P., Fouquart, Y., Ramaswamy, V., Solomon, S., Srinivasan, J., Albritton, D., Derwent, R., Isaksen, I., Lal, M., and Wuebbles, D.: Radiative Forcing of Climate Change, in: Climate Change 1995 The Science of Climate Change. Contribution of Working Group I to the Second Assessment Report of the Intergovernmental Panel on Climate Change, edited by: Houghton, J. T., Meira Rilho, L. G., Callander, B. A., Harris, N., Kattenberg, A., and Maskell, K., Cambridge University Press, Cambridge, United Kingdom and New York, NY, USA, 1995.

Scripps: The Keeling Curve, available at: http://keelingcurve.ucsd.edu/, last access: 7 November 2013.

Séférian, R., Bopp, L., Gehlen, M., Orr, J., Ethé, C., Cadule, P., Aumont, O., Salas y Mélia, D., Voldoire, A., and Madec, G.: Skill assessment of three earth system models with common marine biogeochemistry, Clim. Dynam., 40, 2549–2573, 2013.

Shevliakova, E., Pacala, S., Malyshev, S., Hurtt, G., Milly, P., Caspersen, J., Sentman, L., Fisk, J., Wirth, C., and Crevoisier, C.: Carbon cycling under 300 years of land use change: Importance of the secondary vegetation sink, Global Biogeochem. Cy., 23, GB2022, doi:10.1029/2007GB003176, 2009.

Sitch, S., Smith, B., Prentice, I. C., Arneth, A., Bondeau, A., Cramer, W., Kaplan, J. O., Levis, S., Lucht, W., Sykes, M. T., Thonicke, K., and Venevsky, S.: Evaluation of ecosystem dynamics, plant geography and terrestrial carbon cycling in the LPJ dynamic global vegetation model, Glob. Change Biol., 9, 161–185, 2003.

Sitch, S., Friedlingstein, P., Gruber, N., Jones, S. D., Murray-Tortarolo, G., Ahlström, A., Doney, S. C., Graven, H., Heinze, C., Huntingford, C., Levis, S., Levy, P. E., Lomas, M., Poulter, B., Viovy, N., Zaehle, S., Zeng, N., Arneth, A., Bonan, G., Bopp, L., Canadell, J. G., Chevallier, F., Ciais, P., Ellis, R., Gloor, M., Peylin, P., Piao, S. L., Le Quéré, C., Smith, B., Zhu, Z., and Myneni, R.: Recent trends and drivers of regional sources and sinks of carbon dioxide, Biogeosciences, 12, 653–679, doi:10.5194/bg-12-653-2015, 2015.

Smith, B., Wårlind, D., Arneth, A., Hickler, T., Leadley, P., Siltberg, J., and Zaehle, S.: Implications of incorporating N cycling and N limitations on primary production in an individual-based dynamic vegetation model, Biogeosciences, 11, 2027–2054, doi:10.5194/bg-11-2027-2014, 2014.

Smith, P., Bustamante, M., Clark, H., Dong, H., Elsiddig, E. A., Haberl, H., Harper, R., House, J. I., Jafari, M., Masera, O., Mbow, C., Ravindranath, N. H., Rice, C. W., Robledo Abad, C., Romanovskaya, A., Sperling, F., and Tubiello, F. N.: Agriculture, Forestry and Other Land Use (AFOLU), in: Chapter 11 in Climate Change 2014: Mitigation of Climate Change. Contribution of Working Group III to the Fifth Assessment Report of the Intergovernmental Panel on Climate Change, edited by: Edenhofer, O., Pichs-Madruga, R., Sokona, Y., Farahani, E., Kadner, S., Seyboth, K., Adler, A., Baum, I., Brunner, S., Eickemeier, P., Kriemann, B., Savolainen, J., Schlömer, S., von Stechow, C., Zwickel, T., and Minx, J. C., Cambridge University Press, Cambridge, United Kingdom and New York, NY, USA, 2014.

Stephens, B. B., Gurney, K. R., Tans, P. P., Sweeney, C., Peters, W., Bruhwiler, L., Ciais, P., Ramonet, M., Bousquet, P., Nakazawa, T., Aoki, S., Machida, T., Inoue, G., Vinnichenko, N., Lloyd, J., Jordan, A., Heimann, M., Shibistova, O., Langenfelds, R. L., Steele, L. P., Francey, R. J., and Denning, A. S.: Weak Northern and Strong Tropical Land Carbon Uptake from Vertical Profiles of Atmospheric CO_2, Science, 316, 1732–1735, 2007.

Stocker, T., Qin, D., and Platner, G.-K.: Climate Change 2013 The Physical Science Basis, Cambridge University Press, Cambridge, United Kingdom, 2013.

Sweeney, C., Gloor, E., Jacobson, A. R., Key, R. M., McKinley, G., Sarmiento, J. L., and Wanninkhof, R.: Constraining global air-sea gas exchange for CO_2 with recent bomb ^{14}C measurements, Global Biogeochem. Cy., 21, GB2015, doi:10.1029/2006GB002784, 2007.

Tans, P. and Keeling, R. F.: Trends in atmospheric carbon dioxide, National Oceanic & Atmospheric Administration, Earth System Research Laboratory (NOAA/ESRL) & Scripps Institution of Oceanography, available at: http://www.esrl.noaa.gov/gmd/ccgg/trends/ and http://scrippsco2.ucsd.edu/, last access: 8 August 2014.

Tjiputra, J. F., Roelandt, C., Bentsen, M., Lawrence, D. M., Lorentzen, T., Schwinger, J., Seland, Ø., and Heinze, C.: Evaluation of the carbon cycle components in the Norwegian Earth System Model (NorESM), Geosci. Model Dev., 6, 301–325, doi:10.5194/gmd-6-301-2013, 2013.

Tubiello, F. N., Salvatore, M., Ferrara, A. F., House, J., Federici, S., Rossi, S., Biancalani, R., Condor Golec, R. D., Jacobs, H., Flammini, A., Prosperi, P., Cardenas-Galindo, P., Schmidhuber, J., Sanz Sanchez, M. J., Srivastava, N., and Smith, P.: The contribution of agriculture, forestry and other land use activities to global warming 1990–2012, Glob. Change Biol., 21, 2655–2660, doi:10.1111/gcb.12865, 2015.

Tyukavina, A., Baccini, A., Hansen, M. C., Potapov, P. V., Stehman, S. V., Houghton, R. A., Krylov, A. M., Turubanova, S., and Goetz, S. J.: Aboveground carbon loss in natural and managed tropical forests from 2000 to 2012, Environ. Res. Lett., 10, 074002, doi:10.1088/1748-9326/10/7/074002, 2015.

UN: United Nations Statistics Division: Energy Statistics, United Nations Statistics Division: Energy Statistics, available at: http://unstats.un.org/unsd/energy/ (last access: October 2015), 2014a.

UN: United Nations Statistics Division: Industry Statistics, United Nations Statistics Division: Industry Statistics, available at: http://unstats.un.org/unsd/industry/default.asp (last access: October 2015), 2014b.

UN: United Nations Statistics Division: National Accounts Main Aggregates Database, United Nations Statistics Division: National Accounts Main Aggregates Database, available at: http://unstats.un.org/unsd/snaama/Introduction.asp (last access: February 2015), 2014c.

UNFCCC: GHG Data – UNFCCC, available at: http://unfccc.int/ghg_data/ghg_data_unfccc/time_series_annex_i/items/3814.php, last access: May 2015.

USGS: Mineral Commodities Summaries: Cement, USGS, 2015.

van der Werf, G. R., Dempewolf, J., Trigg, S. N., Randerson, J. T., Kasibhatla, P., Giglio, L., Murdiyarso, D., Peters, W., Morton, D. C., Collatz, G. J., Dolman, A. J., and DeFries, R. S.: Climate regulation of fire emissions and deforestation in equatorial Asia, P. Natl. Acad. Sci., 15, 20350–20355, 2008.

van der Werf, G. R., Randerson, J. T., Giglio, L., Collatz, G. J., Mu, M., Kasibhatla, P. S., Morton, D. C., DeFries, R. S., Jin, Y., and van Leeuwen, T. T.: Global fire emissions and the contribution of deforestation, savanna, forest, agricultural, and peat fires (1997–2009), Atmos. Chem. Phys., 10, 11707–11735, doi:10.5194/acp-10-11707-2010, 2010.

van Minnen, J. G., Goldewijk, K. K., Stehfest, E., Eickhout, B., van Drecht, G., and Leemans, R.: The importance of three centuries of land-use change for the global and regional terrestrial carbon cycle, Climatic Change, 97, 123–144, 2009.

van Oss, H. G.: Cement, US Geological Survey, June, 2013.

van Oss, H. G.: Cement, US Geological Survey, 2015.

Waha, K., van Bussel, L. G. J., Müller, C., and Bondeau, A.: Climate-driven simulation of global crop sowing dates, Global Ecol. Biogeogr., 12, 247–259, 2012.

Wanninkhof, R., Park, G.-H., Takahashi, T., Sweeney, C., Feely, R., Nojiri, Y., Gruber, N., Doney, S. C., McKinley, G. A., Lenton, A., Le Quéré, C., Heinze, C., Schwinger, J., Graven, H., and Khatiwala, S.: Global ocean carbon uptake: magnitude, variability and trends, Biogeosciences, 10, 1983–2000, doi:10.5194/bg-10-1983-2013, 2013.

Watson, R. T., Rodhe, H., Oeschger, H., and Siegenthaler, U.: Greenhouse Gases and Aerosols, in: Climate Change: The IPCC Scientific Assessment. Intergovernmental Panel on Climate Change (IPCC), edited by: Houghton, J. T., Jenkins, G.

J., and Ephraums, J. J., Cambridge University Press, Cambridge, United Kingdom, 1990.

Zaehle, S., Friend, A. D., Friedlingstein, P., Dentener, F., Peylin, P., and Schulz, M.: Carbon and Nitrogen Cycle Dynamics in the O-CN Land Surface Model: 2. Role of the Nitrogen Cycle in the Historical Terrestrial Carbon Balance, Global Biogeochem. Cy., 24, GB1006, doi:10.1029/2009GB003522, 2010.

Zaehle, S., Ciais, P., Friend, A. D., and Prieur, V.: Carbon benefits of anthropogenic reactive nitrogen offset by nitrous oxide emissions, Nat. Geosci., 4, 601–605, 2011.